

# **Investigation on jute fibres and their composites based on polypropylene and epoxy matrices**

Der Fakultät Maschinenwesen  
der  
Technischen Universität Dresden  
zur

Erlangung des akademischen Grades  
Doktoringenieur (Dr.-Ing.)

angenommene Dissertation

M.Sc. Doan, Thi Thu Loan  
geboren am 14.08.1971 in Danang/Vietnam

Tag der Einreichung : 06.12.2005

Tag der Verteidigung : 19.05.2006

Gutachter: Prof. Dr.-Ing. habil. Dipl. -Wirt. -Ing. C. Cherif  
Prof. Dr.-Ing. habil. Dr. h. c. A. Bledzki  
Priv.-Doz. Dr.-Ing. habil. E. Mäder

Vorsitzender der Promotionskommission:

Prof. Dr.-Ing. habil. W. Hufenbach

## Acknowledgements

Firstly, I would like to say thank to my supervisor, Dr. Edith Mäder. for her guidance and valuable suggestions during the last years and for being always supportive, kind and understanding.

I am also specially thankful to Dr. Hanna Brodowsky for many helpful suggestions about this thesis. She is always ready to help with a smile.

I would like to express my sincere thanks to Shang-Lin Gao for generously sharing his knowledge in evaluating the experimental data and AFM measurements.

I would like to thank Dr. Konrad Gliesche and Mrs. Helga Kirsten for instructing me about making composite samples by Vacuum Assisted Resin Transfer Moulding method and for making the stitched jute samples.

I thank Dr. Rüdiger Häßler, Mrs. Christina Rothe and Mrs. Sabine Görner for TG and DMA measurements.

I am grateful to Mrs. Rosemarie Plonka for her helpful and kindness concerning my experiment.

I would like to convey my sincere thanks to Mr. Jianwen Liu for his helpful discussions and for fibre tensile test as well as SEM measurements.

I am grateful to Mr. Werner Ehrentraut for helping my experiments.

I would like to thank Mrs. Uta Reuter for mechanical tests, Mrs. Gudrun Adam for FTIR measurement and Mrs. Pusch for the fibre tensile tests.

I would like to thank Mr. Andreas Scholze, Mr. Petra Treppe for composite processing and Mr. Jürgen Schade, Mrs. Ruth Preisker, Mrs. Steffi Preßler for other tests.

I would like to thank all colleagues for their kind helpfulness.

I am grateful to my family, my friends and my students, who have been a great source of strength all through this work during the time far from home.

Finally, I would like to thank the Vietnamese government and the Institute of Polymer Research Dresden for the financial support of this work.

## Table of contents

<b>List of figures</b>	<b>IV</b>
<b>List of tables</b>	<b>VII</b>
<b>Symbols and Abbreviations</b>	<b>VIII</b>
<b>1. Introduction</b>	<b>1</b>
<b>2. Objective</b>	<b>8</b>
<b>3. Jute fibre composites and their constituents</b>	<b>11</b>
3.1. Jute fibre	11
3.2. Polypropylenes	14
3.3. Epoxy Resins	15
3.4. Modifications and composite processing	18
3.4.1. Natural fibre/polymer matrix interphase	18
3.4.2. Theoretical perspectives of modifications	19
3.4.2.1. Matrix modification	19
3.4.2.2. Fibre modification	19
3.4.3. Composite processing	23
3.4.3.1. Jute/polypropylene composites	23
3.4.3.2. Jute/epoxy composites	27
<b>4. State-of-the-art and tools of investigation</b>	<b>32</b>
4.1. Fibre	32
4.1.1. Single fibre tensile test	32
4.1.2. Wetting measurement	33
4.1.3. Thermal analysis	37
4.1.4. Atomic Force Microscopy (AFM)	38
4.1.5. Scanning Electron Microscopy (SEM)	40
4.2. Model composites	41
4.2.1. Micro-mechanical analysis	41
4.2.2. Pull-out test	41
4.2.3. Analysis of fracture surfaces (Fractography)	45
4.2.4. Aging of micro-composites	45

4.3. Composites	46
4.3.1. Fibre length and content	46
4.3.1.1. Fibre length distribution	46
4.3.1.2. Fibre content	47
4.3.2. Static mechanical properties	47
4.3.2.1. Tensile test	47
4.3.2.2. Bending test	49
4.3.2.3. Impact test	50
4.3.3. Aging behaviour	50
4.3.3.1. Model for the moisture diffusion process	50
4.3.3.2. Determination of diffusion constant	51
4.3.4. Dynamic Mechanical Thermal Analysis	54
<b>5. Results and discussion</b>	<b>56</b>
5.1. Jute fibres	56
5.1.1. Fibre mechanical properties	56
5.1.2. Mechanical properties of treated fibre	60
5.1.2.1. Alkaline treatment	60
5.1.2.2. Silane treatment	61
5.1.3. Wetting of the fibres	62
5.1.4. Moisture absorption	65
5.1.5. Thermal behaviour	67
5.2. Micro-composites	69
5.2.1. Micro-mechanical behaviour	69
5.2.1.1. Untreated jute fibre composites	69
5.2.1.2. Treated matrix composites	69
5.2.1.3. Treated fibre composites	71
5.2.2. Morphology of the fibre fracture surfaces	75
5.2.2.1. Influences of matrix modifications	75
5.2.2.2. Influences of fibre modifications	77
5.3. Jute/PP composites	81
5.3.1. Fibre length	82
5.3.2. Mechanical properties	84
5.3.3. SEM	88

5.3.4. Thermal analysis	90
5.3.4.1. Effect of the atmosphere of measurement	90
5.3.4.2. Effect of modifier	92
5.3.4.3. Effect of fibre content	92
5.3.5. Dynamic mechanical analysis	94
5.3.6. Moisture absorption behaviour	96
5.3.7. Influence of moisture absorption on the tensile strength and interfacial adhesion strength of the composites	97
5.3.8. Influence of moisture absorption on the dynamic mechanical behaviour	100
5.4. Jute/epoxy composites	101
5.4.1. Mechanical properties	101
5.4.1.1. Alkaline fibre treatment	101
5.4.1.2. Coupling agent and Sizing	102
5.4.1.3. Combination of fibre alkali treatment with the coupling agent and the sizing	104
5.4.2. SEM	106
5.4.3. Dynamic mechanical analysis	108
5.4.4. Water absorption	110
<b>6. Summary</b>	<b>112</b>
6.1. Fibres	112
6.2. Jute/polypropylene composites	113
6.3. Jute/epoxy composites	114
<b>7. References</b>	<b>116</b>

## List of Figures

1	Classification of natural fibres which can be used as reinforcement or fillers	1
2	Interaction between natural and industrial cycles	3
3	North American market demand of natural fibre composites 2000	4
4	Use of natural fibre (except cotton and wood) for composites in the German automotive industry 1996-2003	4
5	Plant fibre applications in the current Mercedes-Benz R-class	5
6	Overview of the work plan/main chapters of the thesis	10
7	Harvest of jute plants	11
8	Scheme of jute fibre structure	12
9	Structure of cellulose as it occurs in a plant cell wall	13
10	Chemical structure of isotactic polypropylene	14
11	Chemical structure of a typical epoxy	15
12	Schematic representation of cured epoxy resin	16
13	Model of fibre matrix interphase	18
14	Hypothetical structure of MAHgPP coupling agent and jute fibre at the interface	19
15	Hydrolysis and bonding formation at the interface of the jute fibre and epoxy matrix	22
16	Schematic diagram of (A) screw configuration and (B) extrusion procedure used for jute/PP compounding	25
17	Schematic diagram of an injection moulding machine	26
18	Schematic arrangement of jute/epoxy composite processing by VARTM tool	29
19	Processing cycle of jute/epoxy composite by VARTM	30
20	Stitched jute fibre samples used as single layer in VARTM-processing	31
21	Force balance between the fibre, vapour and liquid during Wilhemy	34
22	Scheme of the tensiometer K 14	36
23	Principle of detection of oscillating cantilever	38
24	Micromechanical tests: (a) fragmentation, (b) microindentation, (c) pull-out	41
25	A typical plot of pull-out force versus displacement	42
26	Schematic of single fibre pull-out test equipment	44
27	Weibull plot of fracture probability as a function of jute fibre tensile strength for different gauge lengths	57
28	Schematic of a technical fibre	57
29	Variations of jute fibre tensile strength as a function of gauge length	58
30	Variations of jute fibre tensile strength as a function of fibre cross-section area of (A) J1, (B) J2 and (C) J3	59
31	Weight loss (%) of jute fibre at different conditions of alkali treatment	60
32	Fibre tensile strength calculated by Weibull statistics for differently	61
33	Influences of difference fibre treatments on fibre tensile strength calculated	62
34	Force vs. immersion depth for jute fibre (J3) in water	63
35	Diagram to estimate the fibre surface energy	64
36	Surface free energy, polar and dispersive components of untreated and treated fibre	65
37	Moisture absorption of jute fibres as a function of exposure time at 95%	66
38	Saturated moisture content values of untreated and treated fibres	67
39	TG and DTG curves of treated and untreated jute fibre (J3)	68
40	Typical force-displacement curves for pull-out test of PP and EP matrix composites	70
41	Apparent interfacial shear strength in jute/PP systems	71
42	Apparent interfacial shear strength in jute/epoxy systems	72

43	Apparent IFSS as a function of (A) fibre diameter and (B) embedded length	73
44	Apparent IFSS as a function of (A) fibre diameter and (B) embedded length	73
45	Apparent IFSS as a function of (A) fibre diameter and (B) embedded length	74
46	Apparent IFSS as a function of (A) fibre diameter and (B) embedded length	74
47	Apparent IFSS as a function of (A) fibre diameter and (B) embedded length	75
48	Three-dimensional AFM topographical images of fracture surfaces of pulled-out jute fibres from unmodified and modified polypropylene composites (size: $2 \times 2 \mu\text{m}$ )	76
49	Comparison of image mean roughness ( $R_a$ ) and maximum height roughness ( $R_{\text{max}}$ ) of the fibre after pull-out test from PP1 and PP2 matrices with and without modifier	76
50	Schematic model of (A) unmodified and (B) modified PP matrix composites	77
51	Three-dimensional AFM topographical images of unmodified and modified fibre surfaces (A) before and (B) after pull-out test	78
52	SEM photographs of the jute fibre with different modifications (A) untreated_J3,	79
53	Comparison of (A) image mean roughness and (B) maximum height roughness of the treated and untreated fibres before and after pull-out test from epoxy matrix	79
54	Schematic model of untreated and treated fibre surfaces of (A) before and (B) after pullout tests	80
55	Influences of three kinds of MAHgPP on tensile strength of jute/PP1 composites with fibre content of 19.78 vol%	81
56	Influences of three kinds of MAHgPP on impact toughness of jute/PP1 composites with fibre content of 19.78 vol%	82
57	Cumulated probability of fibre length in J1/PP1 + 2wt% Ex composites with different fibre content	83
58	Cumulated probability of fibre length/diameter ratios in J1/PP1 + 2 wt% Ex composite plate with fibre content of 19.78 vol%. A histogram of the frequency of length/diameter ratio is shown in the bar graphs.	83
59	Comparing average fibre lengths of PP1 and PP2 composites with MAHgPP, using both SIS and SCAN methods	84
60	Influences of interfacial adhesion on the mechanical properties of jute/PP composites. Experimental data of tensile strength as a function of the fibre volume content	86
61	Influences of interfacial adhesion on the mechanical properties of jute/PP composites. Experimental data of tensile modulus as a function of the fibre volume content	87
62	Charpy impact toughness as a function of the fibre volume content	87
63	Fracture surface of J1/PP1 composite broken in tensile test	88
64	Fracture surface of J1/PP1 + 2 wt% Ex composite broken in tensile test	89
65	Fracture surface of J1/PP2 composite broken in tensile test	89
66	Fracture surface of J1/PP2 + 2 wt% Ex composite broken in tensile test	90
67	DTG curves of (A) jute, (B) PP1 and (C) jute/PP1 composite 19.78 vol% fibre	91
68	TGA curves of (A) jute, (B) PP1 and (C) jute/PP1 composite 19.78 vol % fibre	92
69	Thermogravimetric curves of J1/PP1 composites with and without Ex modifier under nitrogen atmosphere at a fibre content of 19.78 vol%	93
70	Thermogravimetric curves of jute/PP1 + 2 wt% MAHgPP composites (C) under the nitrogen (I) and the air (II) with different fibre contents: 9.39 vol. % (1), 19.78 vol. % (2) and 31.34 vol.% (3)	93
71	Temperature dependence of storage modulus of PP1 and modified jute/PP1 composites at different fibre contents	95
72	Temperature dependence of loss modulus and tan delta of PP1 and modified	95

	jute/PP1 composites at different fibre contents	
73	Moisture absorption behaviour of jute/PP1 composites at 95 %RH	96
74	Influence of humidity aging on tensile strength of neat PP polymer and composites based on (A) PP1 and (B) PP2, (filled symbols) with and (empty symbols) without Ex	98
75	Influence of humidity aging on interfacial adhesion strength of neat PP polymer and composites based on (A) PP1 and (B) PP2	99
76	Comparison of storage modulus of modified PP1 composites	100
77	Glass-transition temperature of modified PP composites before and after aging at different fibre contents	101
78	Influence of the NaOH fibre treatment on the transverse tensile modulus and strength of unidirectional jute/epoxy composites	102
79	Influence of the fibre sizings on the transverse tensile modulus and strength of unidirectional jute/epoxy composites	103
80	Influence of the fibre sizings on the transverse bending modulus and strength of unidirectional jute/epoxy composites	104
81	Influence of the fibre treatments on the transverse tensile modulus and strength of unidirectional jute/epoxy composites (insert: optical microscopy image of a failure surface after transverse tensile test indicating the failure in weak regions at the interface)	105
82	Influence of the fibre treatment on the transverse bending modulus and strength of unidirectional jute/epoxy composites (insert: optical microscopy image of a polished cross section indicating the fibre/matrix distribution)	105
83	SEM photographs of (A) fracture surfaces and (B) fibre surface after tensile test of unidirectional jute fibre epoxy composites	107
84	Storage modulus curves for epoxy sample and unidirectional jute/epoxy composites with and without fibre treatments as a function of temperature at a frequency of 1 Hz	108
85	Tan $\delta$ curves for epoxy sample and unidirectional jute/epoxy composites with and without treatments versus temperature	108
86	Water absorption behaviour of epoxy plate and unidirectional jute/epoxy composite with and without treatments	111
87	The diffusion coefficient of epoxy plate and unidirectional jute/epoxy composite	111



## List of Tables

1	Properties of jute fibre in comparison with other fibres	2
2	Typical composition of jute fibre	13
3	Some properties of the used jute fibres	14
4	Polypropylene properties	15
5	Parameters of the used epoxy systems	17
6	Properties of three kinds of coupling agents	23
7	Sizing formulations	28
8	Functions and materials of the items in VARTM	30
9	Surface tensions of model liquids and dispersive/polar parts	36
10	Tensile strength of jute fibres (J1)	56
11	Advancing contact angle of untreated and treated jute fibre (J3)	63
12	Effect of matrix and fibre treatments on apparent interfacial shear strength	70
13	Average fibre length, diameter, and length/diameter ratio derived from compound granules and plates with 19.78 vol% fibre.	82
14	The calculated critical fibre length and fibre orientation factor	85
15	Equilibrium water content ( $M_{\infty}$ ) and the moisture diffusion coefficient (D)	97

## Symbols and Abbreviations

AFM	Atomic force microscopy
APS	3-Aminopropyl-triethoxysilane
MAHgPP	Maleic anhydride grafted polypropylene
D	Moisture diffusion coefficient
DTG	Differential Thermal Gravimetry
E'	Storage modulus
E''	Loss modulus
EP1	Resin Bakelite EPR L 20 + hardener Bakelite EPH 960
EP2	Resin Bakelite EPR L 20 + hardener Bakelite EPH 161
Ex	Exxelor PO 1020 MAHgPP
PO	Polybond 3200 MAHgPP
TP	TPPP 8012 MAHgPP
M <sub>∞</sub>	Equilibrium water content
J1	Jute from Spinnerij Blancquaert NV (Lokeren, Belgium)
J2	Jute from Vietnam
J3	Jute from Schilgen GmbH
NaOH	Sodium hydroxide
PP	Polypropylene
PP1	HD 120 M polypropylene
PP2	Purell 570 U polypropylene
R <sub>a</sub>	Mean roughness
R <sub>max</sub>	Maximum height roughness
RH	Relative humidity
ROM	Rule of mixture
SEM	Scanning Electron Microscopy
SCAN	Image Scan Multi program
SIS	AnalySIS Software program
T <sub>g</sub>	glass transition temperature
TG	Thermal gravimetry
$\tau_{app}$	Apparent interfacial shear strength
$\tau_f$	Post-debonding friction stress
$\tau_w$	Interfacial adhesion strength after aging

$\tan \delta$	Loss factor
UD	Unidirectional
VARTM	Vacuum Assisted Resin Transfer Moulding
XB	Epoxy dispersion XB 3791
Y96693	Phenylaminopropyl-trimethoxy-silane

## 1. Introduction

Natural fibres already have been used the first time 3000 years ago in composite systems in the ancient Egypt, where straw and clay were mixed together to build walls. Over the last decade, polymer composites reinforced with natural fibres have received ever increasing attention, both from the academic world and from various industries. There is a wide variety of different natural fibres which can be applied as reinforcement or fillers. An organigram with a classification of the various fibres is presented in Fig. 1.

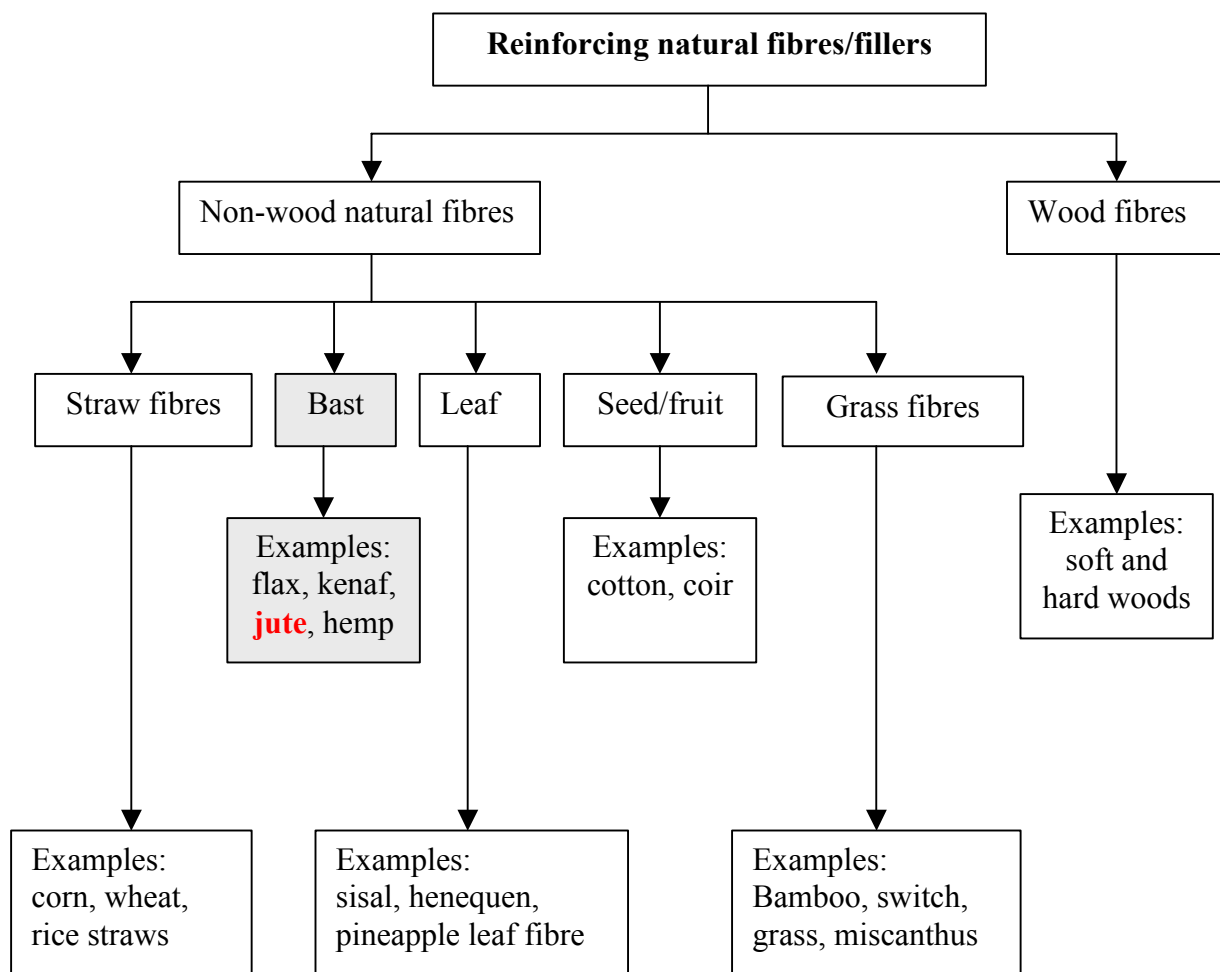


Fig. 1. Classification of natural fibres which can be used as reinforcement or fillers in polymers [1]

The most important types of natural fibres used in composite materials are flax, hemp, jute, kenaf, and sisal due to their properties and availability. Jute is an important bast fibre with a number of advantages. Jute has high specific properties, low density, less abrasive behaviour to the processing equipment, good dimensional stability and harmlessness. Jute textile is a low cost eco-friendly product and is abundantly available, easy to transport and has superior drapability

and moisture retention capacity. It is widely being used as a natural choice for plant mulching and rural road pavement construction. The biodegradable and low priced jute products merge with the soil after using providing nourishment to the soil. Being made of cellulose, on combustion, jute does not generate toxic gases.

Due to jute's low density combined with relatively stiff and strong behaviour, the specific properties of jute fibre can compare to those of glass and some other fibres (Table 1)

Table 1. Properties of jute fibre in comparison with other fibres

<b>Fibre</b>	<b>Density (g/cm<sup>3</sup>)</b>	<b>Tensile Strength (MPa)</b>	<b>Young's Modulus (GPa)</b>	<b>Elongation At break (%)</b>	<b>Specific Tensile Strength (MPa/ g.cm<sup>-3</sup>)</b>	<b>Specific Young's Modulus (GPa/g.cm<sup>-3</sup>)</b>
Jute	1.3-1.45	393-773	13-26.5	1.16-1.5	286-562	9-19
Flax	1.5	345-1100	27.6	2.7-3.2	230-773	18
Ramie	1.5	400-938	61.4-128	1.2-3.8	267-625	41-85
Sisal	1.45	468-640	9.4-22.0	3-7	323-441	6-15
Coir	1.15	131-175	4-6	15-40	114-152	3-5
E-glass	2.5	2000-3500	70	2.5	800-1400	28
S-glass	2.5	4570	86	2.8	1828	34

The natural fibres can be used to reinforce both thermosetting and thermoplastic matrices. Thermosetting resins, such as epoxy, polyester, polyurethane, phenolic, etc. are commonly used today in natural fibre composites, in which composites requiring higher performance applications. They provide sufficient mechanical properties, in particular stiffness and strength, at acceptably low price levels. Compared to compounds based on thermoplastic polymers, thermoset compounds have a superior thermal stability and lower water absorption. However, in the case of the demand for improved recycling and in combination with new long fibre reinforced thermoplastic (LFT) processing, thermoplastic polymers have been expected to substitute the thermoset polymers.

Considering the ecological aspects of material selection, replacing synthetic fibres by natural ones is only a first step. Restricting the emission of green house effect causing gases such as CO<sub>2</sub> into the atmosphere and an increasing awareness of the finiteness of fossil energy resources are leading to developing new materials that are entirely based on renewable resources.

Fig. 2 shows the industrial and natural life cycles of a product made from renewable resources. Because the CO<sub>2</sub> emission produced by EMBED-incineration [2] at the end of the technical cycle

is compensated through photosynthesis during growth, the total CO<sub>2</sub> balance is zero and the emissions thus do not contribute to the greenhouse effect.

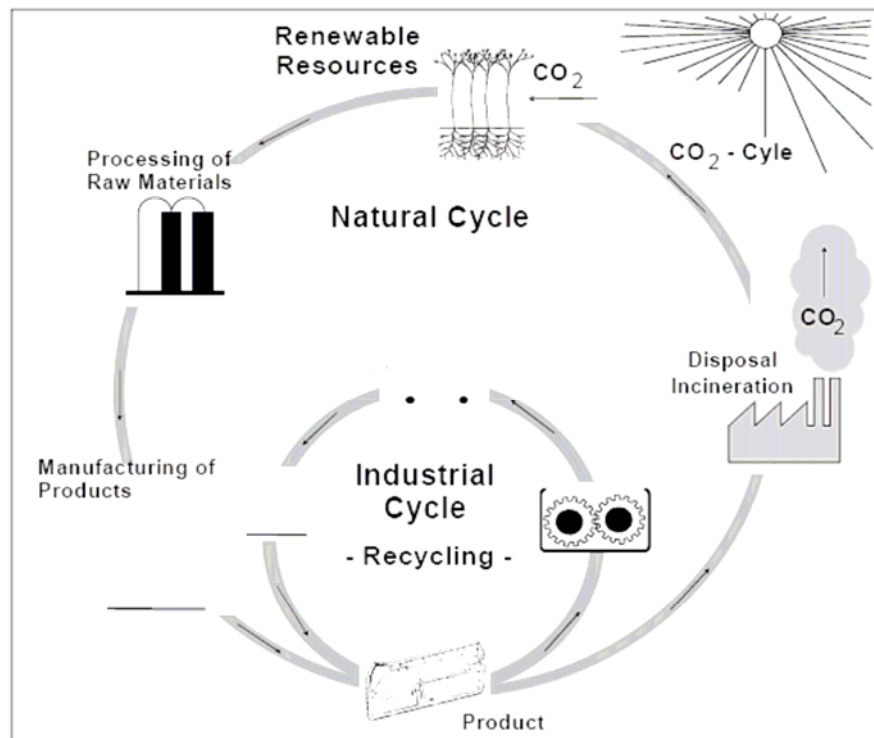


Fig. 2. Interaction between natural and industrial cycles [2]

The natural fibre composites can be very cost effective material for following applications:

- Building and construction industry: panels for partition and false ceiling, partition boards, wall, floor, window and door frames, roof tiles, mobile or pre-fabricated buildings which can be used in times of natural calamities such as floods, cyclones, earthquakes, etc.
- Storage devices: post-boxes, grain storage silos, bio-gas containers, etc.
- Furniture: chair, table, shower, bath units, etc.
- Electric devices: electrical appliances, pipes, etc.
- Everyday applications: lampshades, suitcases, helmets, etc.
- Transportation: automobile and railway coach interior, boat, etc.
- Toys

The Asian markets have been using natural fibres for many years. For example, jute is a common reinforcement in India. The major market for natural fibres in the year 2000 is in building applications (Fig. 3), whereas other applications have been growing at an increasing rate, especially in the automotive industry [3]. For instance, from 1996 till 2003, the use of natural fibres in composites of the German automotive industry increased from 4,000 tons to 18,000 tons

per year. From 1996 till 2002, an almost linear increase of used quantities with yearly growth rates between 10 and 20% can be seen in Fig. 4 [4].

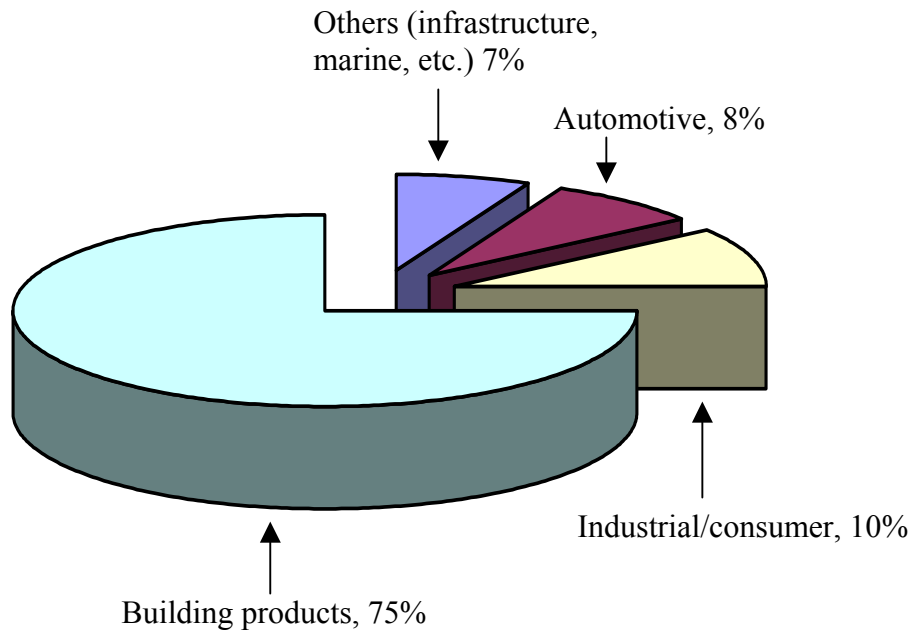


Fig. 3. North American market demand of natural fibre composites 2000 [5]

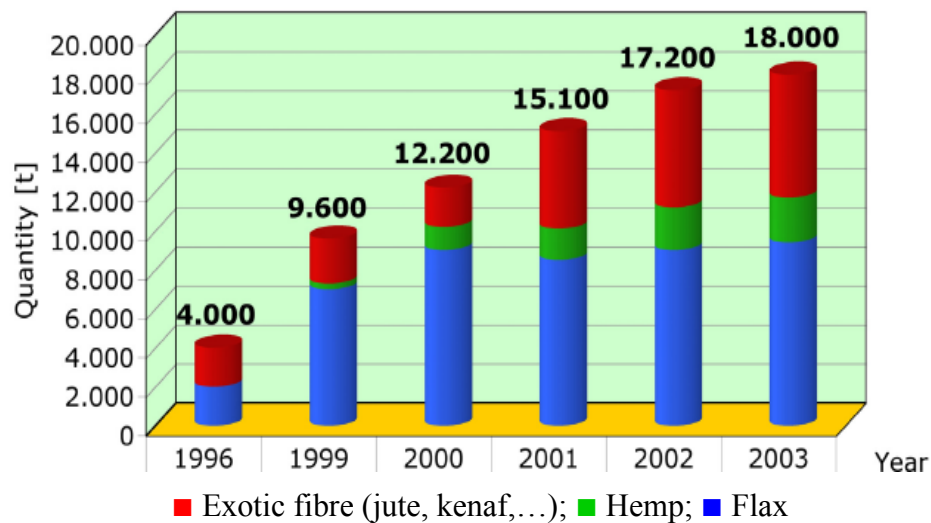


Fig. 4. Use of natural fibre (except cotton and wood) for composites in the German automotive industry 1996-2003

The reasons for the application of natural fibres in the automotive industry include [6, 7]:

- Low density: which may lead to a weight reduction of 10 to 30%.
- Acceptable mechanical properties, good acoustic properties.
- Favourable processing properties, for instance low wear on tools, etc.

- Options for new production technologies and materials.
- Favourable accident performance, high stability, less splintering.
- Favourable ecobalance for part production.
- Favourable ecobalance during vehicle operation due to weight savings.
- Occupational health benefits compared to glass fibres during production.
- No off-gassing of toxic compounds (in contrast to phenol resin bonded wood and recycled cotton fibre parts).
- Reduced fogging behaviour.
- Price advantages both for the fibres and the applied technologies.

Applications of natural fibre reinforcement for automotive parts are shown in Fig. 5.

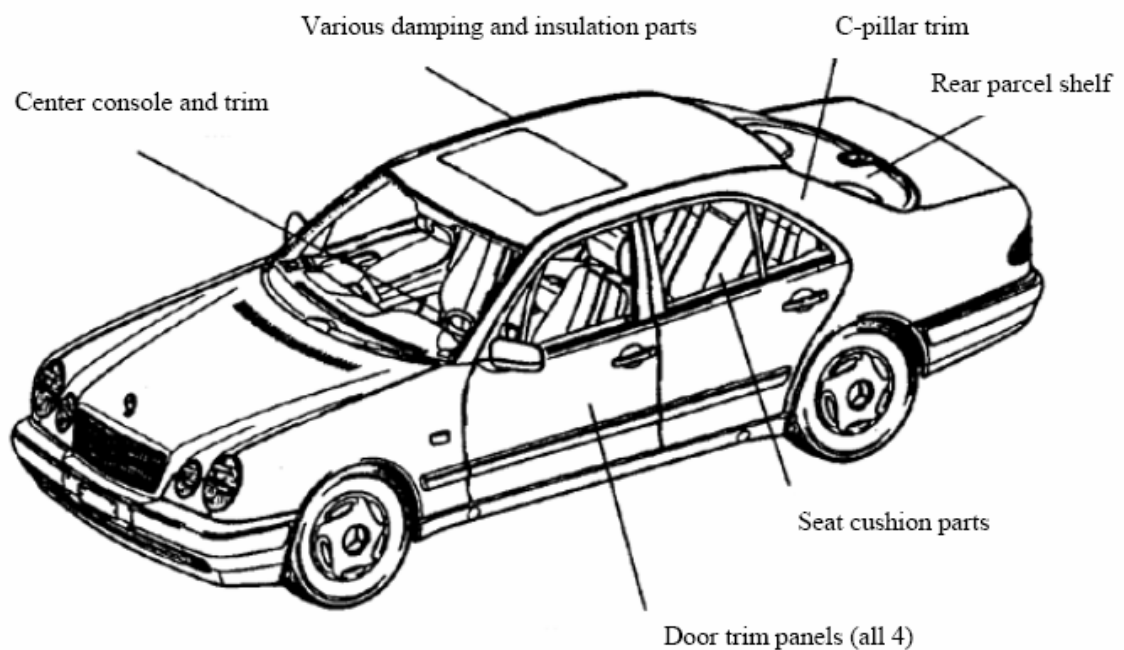


Fig. 5. Plant fibre applications in the current Mercedes-Benz R-class [2]

Besides the advantages mentioned above, the natural fibre composites possess also some disadvantages. The main disadvantage is the poor compatibility between a hydrophobic polymer matrix and the hydrophilic fibres. This leads to the formation of weak interfaces, which result in poor mechanical properties of the composites. Other important disadvantages of the natural fibre composites are the high sensitivity of natural fibres towards water and the relatively poor thermal stability. Water absorption on composites is an issue to be considered since the water absorbed by the fibres in the composite could lead to swelling and dimensional instability and to a loss of



mechanical properties due to the degradation of the fibres and the interface between the fibre and matrix [8, 9, 10, 11, 12, 13].

Therefore, to improve the adhesion between the matrix and the fibres, a third component, called compatibiliser, has to be used for matrix modification or the fibres have to be surface modified prior to the preparation of the composites [14, 15, 16]. Several studies have shown the influence of various types of chemical modifications on the performance of natural fibres and fibre reinforced composites. The different surface chemical modifications of natural fibres such as alkali treatment, silane treatment, isocyanate treatment, latex coating, permanganate treatment, acetylation, monomer grafting under UV radiation, etc. have achieved various levels of success in improving fibre strength and fibre/matrix adhesion in natural fibre composites.

For the composites based on thermoplastic matrices such as polypropylene, polyethylene, etc., the coupling agent maleic anhydride grafted polypropylene (MAHgPP), as a matrix modifier, has been found to be the most efficient in improving interfacial adhesion of natural fibres and a PP matrix [15,17, 18, 19, 20, 21]. Kamaker et al. [22, 23, 24] reported that using 3wt% MAHgPP (type G-3002, with an average molecular weight of 40,000 and containing 6 wt% of maleic anhydride, from Eastman Chemical products, Kingston, TN) as coupling agent in Jute/PP composite increases composite mechanical properties. The tensile strength is doubled from 29.82 MPa to 59.13 MPa and the bending strength increases from 49.97 MPa to 87.66 MPa in composite with 50 wt% fibre content. Similarly, Gassan et al. [25, 26] showed that the tensile, flexural and dynamic strength increase up to 50% but impact energy decreases due to the lower energy absorption in the interface of jute/PP composite when jute fibres are treated by 0.1wt% MAHgPP solution in toluene for 5min at 100°C. In a comparable system, the tensile strength increases from 40 MPa to 69 MPa for a viscose/PP composite using 6 wt% Exxelor PO1015 as a coupling agent [27]. Snijder et al. [28] showed that, also for polystyrene (PS) reinforced with flax fibres, addition of a compatibiliser (Styrene Maleic Anhydride (SMA) copolymer in this case) increases the flexural strength, but the increase here is much smaller, from 58 MPa to about 66 MPa.

For the composites based on thermoset matrices such as epoxy, polyester, phenol formaldehyde, etc., alkali treatment of natural fibres is one of the most common treatments of the natural fibres [29, 30] as it improves the interfacial adhesion between the fibre and matrix [31, 32, 33, 34]. Gassan and Bledzki reported that treating the fibre surface by NaOH 26 wt% for 20 minutes at 20°C improves the mechanical properties of unidirectional jute/epoxy composite up to 60% compared to untreated fibre composite, at a fibre content of 40 vol% [35]. Prasad et al. studied the alkali treatment of coir fibre by NaOH 5% for 72-96 hours at 28°C. An improvement of the

tensile strength and Young's modulus of the fibre by 10-15% and 40%, respectively, was observed. The alkali treatment of the coir fibre improved the flexural strength of the polyester resin composites by 40% [36]. Thais et al. showed an increasing shear strength from 2.6 to 6.9 MPa in the case of fibre surface treatment by NaOH 2% for 1 hour at room temperature of sisal/polyester composites [37]. Ray et al. used a solution of NaOH 5% to treat the jute fibre for 0, 2, 4, 6 and 8 hours at 30°C. For the vinyl ester resin composites reinforced by 35 wt% jute fibre treated for 4 h, an improvement of 20% for the flexural strength, of 23% for the flexural modulus and of 19% for the laminar shear strength was observed [29].

Using silane coupling agents was found to be effective in modifying the natural fibre-matrix interface [38, 39, 40, 41]. Gassan and Bledzki investigated the influence of silane coupling agent on the performance of jute-epoxy composite. A treatment of jute fibre by epoxy functional- $\gamma$ -glycidoxypolytrimethoxy-silane (A-187 from Osi-Specialtis GmbH, Germany) solution in alcoholic with the concentration of 2% for 24 hours at 23°C was found to increase by approximately 30% of the static characteristic values of the composites compared to unmodified composites at standard humidity [42]. Yan et al. showed the influence of fibre surface treatment on the performance of the sisal textile reinforced vinyl ester composites [43]. Sisal fibre was treated by 3-aminopropyltriethoxy silane and  $\gamma$ -methacryloxypropyl trimethoxy silane solution in acetone with a concentration of 6% for 24 hours. Only marginal improvement by 3% and 14% of the tensile strength and tensile modulus of the composites, respectively, was obtained in the case of fibre surface treatment. The flexural strength and modulus of the silaned fibre composites increased by 15% and 30%, respectively compared to untreated composites. However, the fibre surface treatment by silane did not affect the impact energy. Mäder and Gliesche investigated epoxy composites and found out that there was a reduction in the flexural strength and an increase by about 20% in flexural modulus of the flax composites, if an aqueous  $\gamma$ -aminopropyl triethoxy silane solution of 3% was used for treating the fibre surface at 80°C. That did not result, however, any remarkable increase in flexural strength and resulted an increase by about 20% for the flexural modulus of the ramie composites [44].

## 2. Objective

The objective of the investigation is to improve the performance of jute/polypropylene and jute/epoxy composites. The effect of the matrix or fibre surface treatment on the composites performance depends on the type of matrix. For a non-polar polymer matrix, the adhesion occurs through van der Waals interaction only, therefore, a matrix modification is necessary to improve the adhesion strength. For a polar polymer matrix, adhesion is sensitive to fibre surface treatments.

In this study, jute fibre will be used to reinforce two matrix systems, exemplarily polypropylene and epoxy. Polypropylene is a non-polar matrix, therefore it has a poor adhesion towards polar jute fibre. To improve the interfacial adhesion between polypropylene thermoplastic matrix and jute fibre, a matrix modification by grafted polypropylene will be selected.

On the other hand, in order to reduce the hydrophilic behaviour of jute fibre as well as the composite and improve the adhesion with the thermoset epoxy matrix, fibre surface treatment will be used for epoxy composite system.

Based on a critical literature review, the objective of this thesis comprises the following main tasks:

- **Jute/polypropylene composites**
  - comparing three kinds of maleic anhydride grafted polypropylene and finding out the optimal one for matrix modification of the polypropylene composite systems.
  - finding out how matrix modification based on maleic anhydride grafted polypropylene (MAHgPP) affects the interfacial adhesion and mechanical properties of jute/polypropylene composites.
  - composite testing by both micro-mechanical methods and mechanical composite testing will be used to evaluate the introduced properties changes in two kinds of polypropylenes PP1 (low melt flow rate) and PP2 (high melt flow rate) matrixes.
  - study of interfacial fracture morphology by atomic force microscopy (AFM).
  - analysis of fibre length/diameter distribution will be also used to assess the specific behaviour of jute fibres in PP-composites.
  - investigating the thermal behaviour of jute fibre, polypropylene resin and composites in two atmospheres, namely nitrogen and air.
  - examine the moisture diffusion process and dynamic mechanical behaviour of jute/PP composites under the influences of the modifier and fibre content.
  - investigation of aged specimens by dynamic mechanical analysis.

- examine the influence of the humidity aging on the mechanical properties of the micro-and macro-composites.

- **Jute/epoxy composites**

- investigating the influence of fibre surface treatments by alkali, organosilane, epoxy dispersions and the combinations of the treatments on both micro- and macro-mechanical behaviour of the epoxy composites.

- aromatic silane, which has been not commonly used so far, will be investigated in comparison with aliphatic silane.

- a combination of the silanes and aqueous epoxy dispersion as film former, which has also not been applied for the natural fibre treatment, will be performed and compared in order to find out the optimal fibre treatment.

- the influence of the fibre surface treatment on the dynamic mechanical behaviour and water absorption behaviour of the epoxy composites will be investigated.

- investigation of the influence of fibre surface treatments, surface roughness, wetting behaviour, tensile strength and thermal properties of the fibre.

Fig. 6 shows an overview of the work plan containing the main chapters of matrix/fibre modification and the approaches used to investigate fibre/matrix modification, interface/adhesion strength, processing and composite performance.

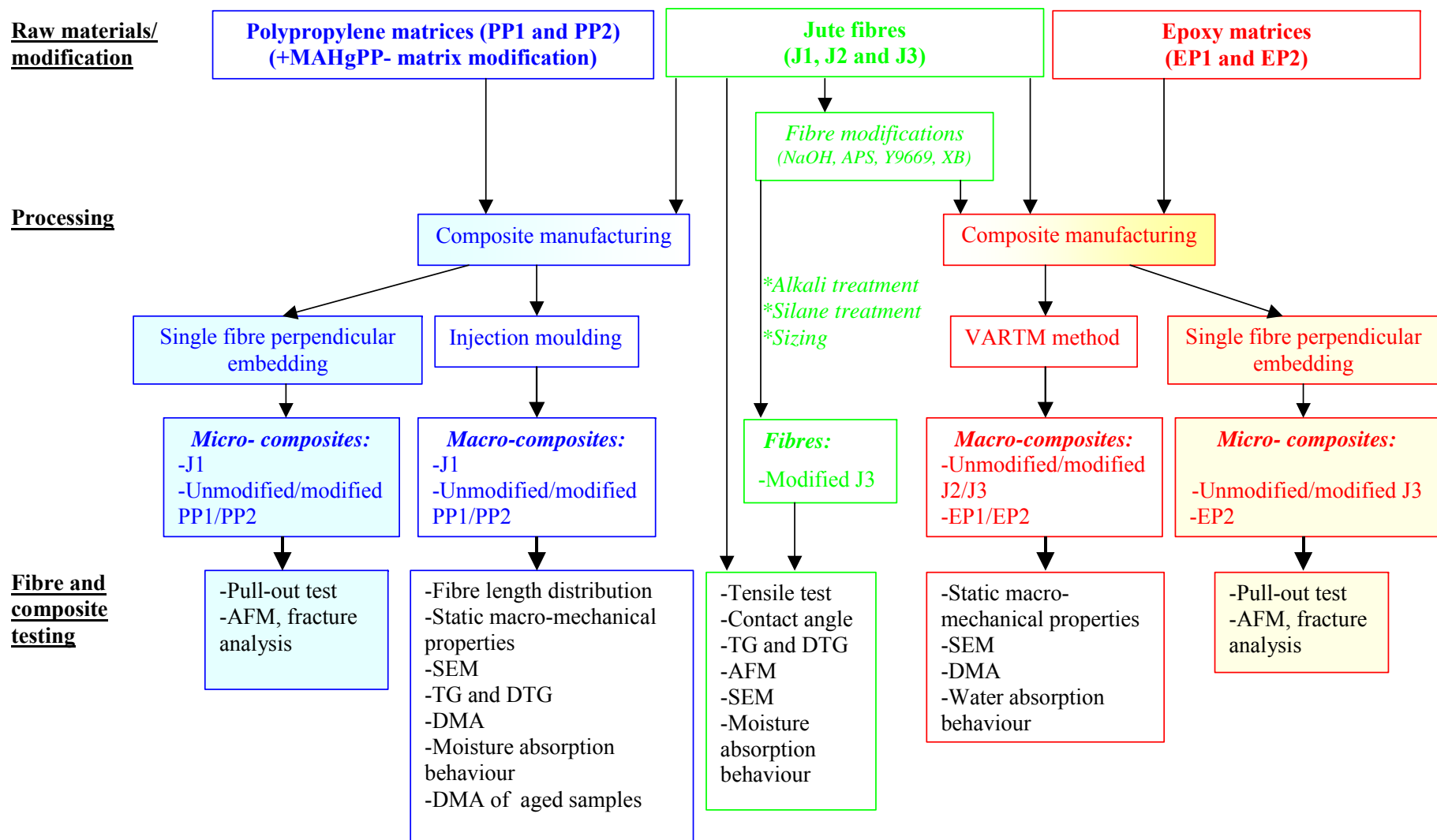


Fig. 6. Overview of the work plan/main chapters of the thesis

### 3. Jute fibre composites and their constituents

#### 3.1. Jute fibre

Jute fibre is obtained from two herbaceous annual plants, white *Corchorus capsularis* (white jute) originating from Asia and *Corchorus olitorius* (Tossa jute) originating from Africa. Next to cotton, it is the second most common natural fibre, cultivated in the world and extensively grown in Bangladesh, China, India, Indonesia, Brazil...[45].

The jute plant (Fig. 7) grows six to ten feet in height and has no branches. The stem of the jute plant is covered with thick bark, which contains the fibres. In two or three month time, the plants grow up and then are cut, tied up in bundles and kept under water for several days for fermentation. Thus, the stems rot and the fibres from the bark become loose. Then the cultivators pull off the fibres from the bark, wash very carefully and dry them in the sun.



Fig. 7. Harvest of jute plants

Jute is multicelled in structure (Fig. 8). The cell wall of a fibre is made up of a number of layers: the so-called primary wall (the first layer deposited during cell development) and the secondary wall (S), which again is made up of the three layers ( $S_1$ ,  $S_2$  and  $S_3$ ). As in all lignocellulosic fibres, these layers mainly contain cellulose, hemicellulose and lignin in varying amounts. The individual fibres are bonded together by a lignin-rich region known as the middle lamella. Cellulose attains highest concentration in the  $S_2$  layer (about 50%) and lignin is most

concentrated in the middle lamella (about 90%) which, in principle, is free of cellulose. The  $S_2$  layer is usually by far the thickest layer and dominates the properties of the fibres [46].

Cellulose, a primary component of the fibre, is a linear condensation polymer consisting of D-anhydro-glucopyranose units joined together by  $\beta$ -1, 4-glucosidic bonds [47]. The long chains of cellulose are linked together in bundles called micro-fibrils (Fig. 9).

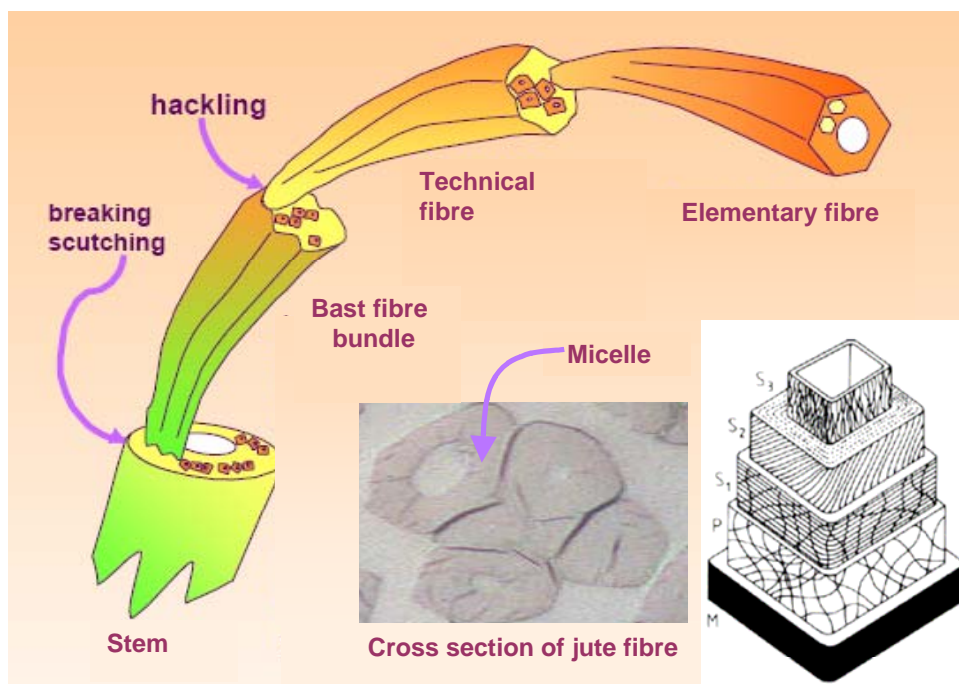


Fig. 8. Scheme of jute fibre structure [48]

Hemicelluloses are also found in all plant fibres. Hemicelluloses are polysaccharides bonded together in relatively short, branching chains. They are intimately associated with the cellulose microfibrils, embedding the cellulose in a matrix. Hemicelluloses are very hydrophilic and have lower molecular masses than both cellulose and lignin. The degree of polymerization (DP) is about 50 – 200. The two main types of hemicelluloses are xylans and glucomannans.

Lignin is a randomly branched polyphenol, made up of phenyl propane ( $C_9$ ) units. It is the most complex polymer among naturally occurring high-molecular-weight materials [49] with an amorphous structure. Of the three main constituents in fibres, lignin is expected to be the one with least affinity for water. Another important feature of lignin is that it is thermoplastic (i.e., at temperatures around  $90^\circ\text{C}$  it starts to soften and at temperatures around  $170^\circ\text{C}$  it starts to flow) [46].

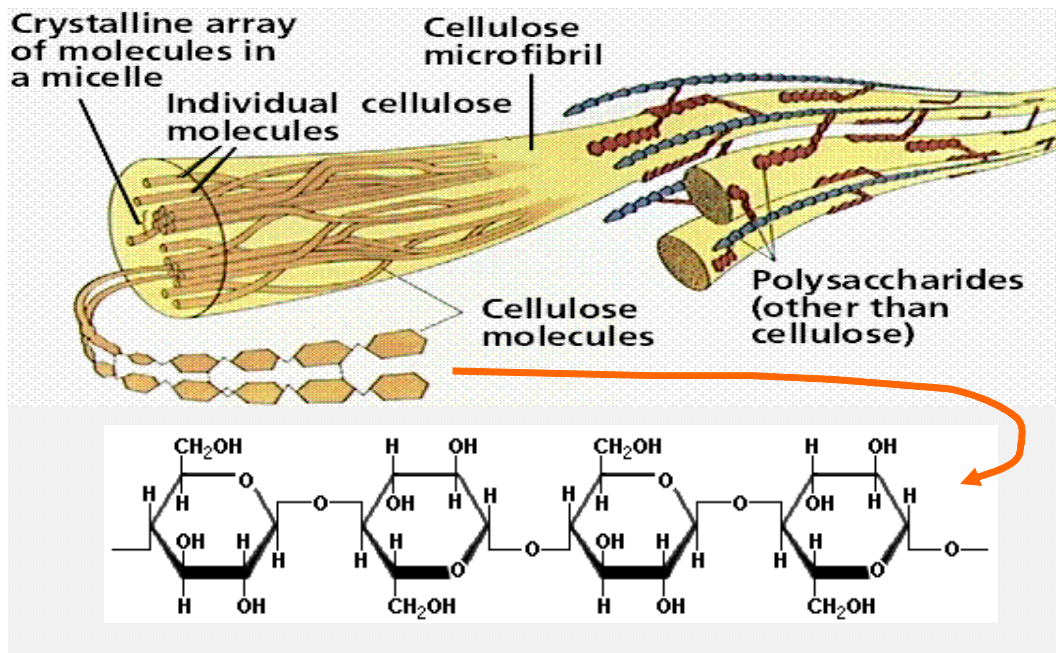


Fig. 9. Structure of cellulose as it occurs in a plant cell wall [50].

The jute fibre is polygonal or oval in cross section with a lumen as shown in Fig. 8. The structure of the jute fibre is influenced by climatic conditions, age and the fermentation process, which influence also the chemical composition [14] (Table 2).

Table 2. Typical composition of jute fibre [51]

Substances	Weight percent (%)
Cellulose	61-71.5
Hemicellulose	13.6-20.40
Pectin	0.2
Lignin	12-13
Moisture content	12.6
Wax	0.5

The jute fibre possesses moderately high specific strength and stiffness. Therefore, it is suitable as reinforcement in a polymeric resin matrix. However, it exhibits considerable variation in diameter along with the length of individual filaments. The properties of the fibre depend on factors such as size, maturity and processing methods adopted for the extraction of the fibre. Properties such as density, electrical resistivity, ultimate tensile strength and initial modulus are related to the internal structure and chemical composition of fibre [52, 53].



Three types of jute fibres were used for the present research, J1, J2 and J3, which were obtained from Spinnerij Blancquaert NV (Lokeren, Belgium), Vietnam (commercially available) and Schilgen GmbH, respectively. Some properties of the jute fibres were shown in Table 3.

Table 3. Some properties of the used jute fibres

<b>Fibre</b>	<b>Fineness of yarn (tex)</b>	<b>Twist (turn/m)</b>	<b>Tensile strength (cN/dtex)</b>
J1	1100	110	4.16
J2	480	300	4.31
J3	390	290	4.65

### 3.2. Polypropylenes

Polypropylene is a polymer which combines versatility with a low price. It is a vinyl polymer and can be made with different tacticities. Polypropylene is commonly made from the monomer propylene by a Ziegler-Natta polymerization, the result is an isotactic polymer, in which all the methyl groups are on the same side of the chain (Fig. 10).

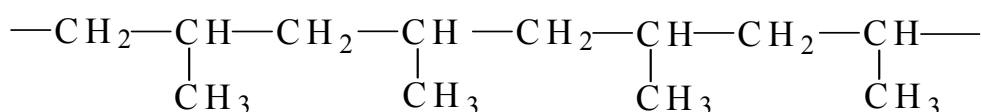


Fig. 10. Chemical structure of isotactic polypropylene

Isotactic polypropylene has good mechanical properties as well as low density. It is a non-polar material. The crystallinity is about 60 - 70% [54]. The crystalline isotactic polypropylene is insoluble in all common solvents at room temperature, it starts swelling and is finally dissolved by specific solvents only at temperatures generally higher than 100°C. Its tensile strength, surface hardness and stiffness are higher than that of polyethylene [54].

In our work, two kinds of polypropylenes PP1 and PP2 were used as the matrices. PP1 was supplied by Borealis A/S as commercial grade HD 120 M and PP2 was provided by Basell (Frankfurt, Germany) as commercial grade Purell 570 U. Some properties are shown in Table 4.

Table 4. Polypropylene properties

Properties	HD 120 M (PP1)	Purell 570 U (PP2)
Density at 23°C (g/cm <sup>3</sup> )	0.908	0.910
Melt Flow Rate (g/10 min) (230°C/2.16kg)	8	92
M <sub>w</sub> (10 <sup>3</sup> g / mol)	290	145
Melting Point (°C)	180	170

### 3.3. Epoxy Resins

The large family of epoxy resins contains some of the highest performance resins available at this time. The generic term epoxy resins describes a class of thermosetting resins prepared by the ring-opening polymerization of compounds containing an average of more than one epoxy group per molecule [55]. Epoxy resins (Fig. 11) traditionally are made by reacting epichlorohydrin with bis-phenol A, which are linear polymers that cross-link, forming thermosetting resins basically by the reaction with the hardeners.

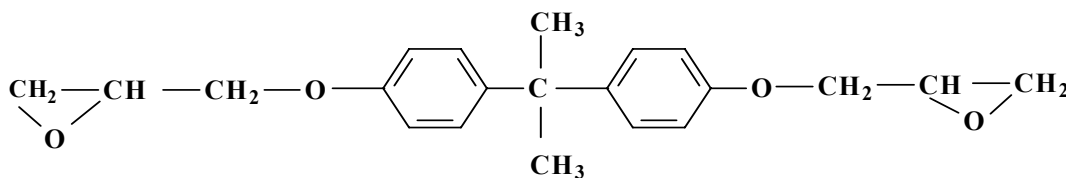


Fig. 11. Chemical structure of a typical epoxy

The curing agent for the epoxy resins usually is amine. No volatile by-products are generated during the curing process. During curing, epoxy resins can undergo three basic reactions:

1. Epoxy groups are rearranged and form direct linkages between themselves.
2. Aromatic and aliphatic hydroxyls link up to the epoxy groups.
3. Cross-linking takes place with the curing agent through various radical groups.

The result is a complex three-dimensional molecular structure which is illustrated in Fig. 12.

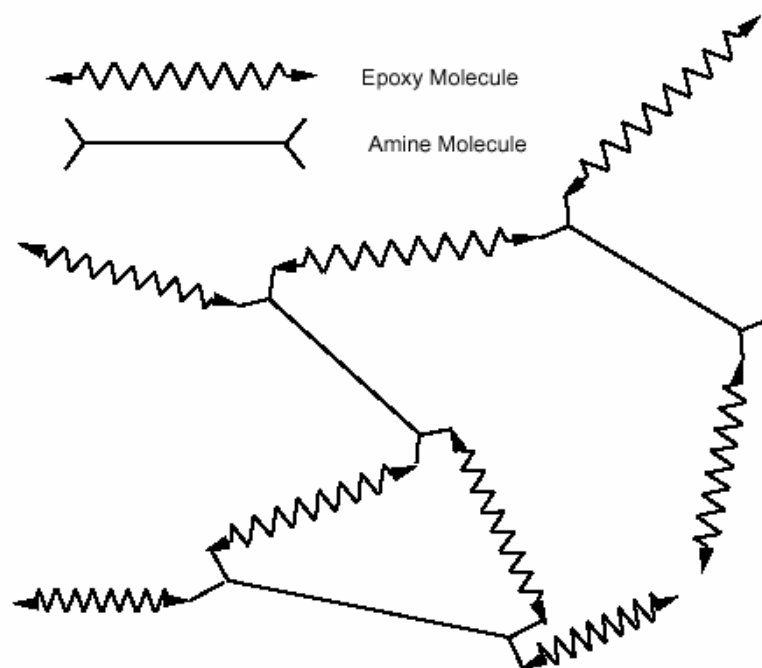


Fig. 12. Schematic representation of cured epoxy resin

The advantages of epoxy resins are low polymerization shrinkages, excellent mechanical strength, good electrical properties and chemical resistance. The epoxy molecule also contains two ring groups at its centre which are able to absorb both mechanical and thermal stresses better than linear groups and therefore give the epoxy resin very good stiffness, toughness and heat resistance. The primary disadvantages of the epoxy resins are that they require long curing times and, in general, their mold release characteristics are poor.

The epoxy resins are characterized by their high adhesive strengths. This property is attributed to the polarity of aliphatic hydroxyl groups and ether groups that exist in both the initial resin and cured system. The polarity associated with these groups promotes electromagnetic bonding forces between epoxy molecules and the substrate.

In this study, systems of epoxy (EP1 and EP2) from Bakelite AG company were used. The resin parameters and formulations are displayed in Table 5.

Table 5. Parameters of the used epoxy systems

Epoxy systems	Chemical Compositions	Ratio (wt.)	Viscosity at 25°C (mPa*s)	Density at 20°C (g/cm <sup>3</sup> )
<b>EP1:</b> * Resin Bakelite EPR L 20	-Bisphenol-A-epichlorhydrin resin (>50%) -Epoxide derivatives (<50%)	100	900-1000	1.14-1.16
* Hardener Bakelite EPH 960	-2,2'-dimethyl-4,4'-methylene bis (cyclohexylamine)	34	142	0.95
<b>EP2:</b> *Resin Bakelite EPR L 20	-Bisphenol-A-epichlorhydrin resin (>50%) -Bisphenol-F-epichlorhydrin resin (<25%) -Epoxide derivatives (<25%)	100	750-1050	1.14-1.16
*Hardener Bakelite EPH 161	Aminoethyl-3,5,5-trimethyl cyclohexamin	25	150-250	0.98

### 3.4. Modifications and composite processing

#### 3.4.1. Natural fibre/polymer matrix interphase

Fibre reinforced composite materials are composed of fibres and matrix material that bind and protect the fibres (A composite material is one in which two or more materials that are different (structure, properties) are combined to form a single structure with identifiable interfaces at multi-scales to achieve properties that are superior to those of its constituents.). The fibres are usually the load bearing members, while the polymeric matrix provides transverse integrity and transfers the load onto the fibres.

Besides of the properties of two main components of fibre and matrix, the fibre/matrix interphase also plays a crucial role for the load transfer. It is not a distinct phase, as the interphase does not have a clear boundary. This region exists between bulk fibre and bulk matrix and may contain several different layers as in the case of sizing (Fig. 13).

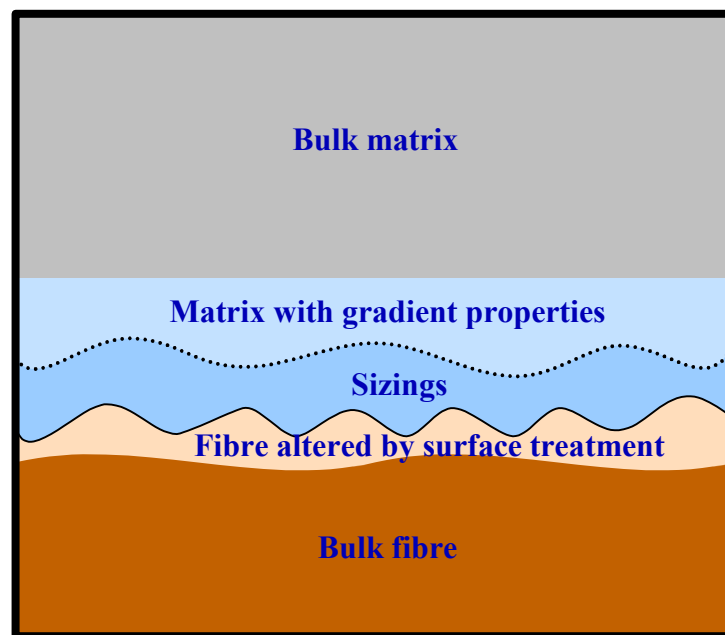


Fig. 13. Model of fibre matrix interphase

An interphase that is softer than the surrounding polymer would result in lower overall stiffness and strength, but greater resistance to fracture. On the other hand, an interphase that is stiffer than the surrounding polymer would give the composite less fracture resistance but make it very strong and stiff. The nature of the interphase varies with the specific composite system [56]. Therefore, in order to design an optimal composite system, it is important to characterize the interphase region, including its size, adhesion to the fibre and to the matrix and mechanical behaviour [57].

### 3.4.2. Theoretical perspectives of modifications

#### 3.4.2.1. Matrix modification

The adhesion is poor at the interface between jute fibre and non-polar polymer matrix, which is provided only by van der Waals forces due to the lack of reactive groups in the molecule of the polymers. In this study, matrix modification was carried out by using MAHgPP to improve the adhesion of the jute fibre and polypropylene matrix. The coupling agent is able to act as a compatibiliser for polar natural fibre and non-polar polymer matrix systems. A hypothetical model of the interface between MAHgPP with hydroxyl groups of jute fibre is shown in Fig. 14. The interfacial interaction mechanisms can be understood from this model, in which likely both chemical (ester bond) and physical interactions (hydrogen bond) should be formed between the hydroxyl groups of cellulose fibre and the maleic anhydride group of the coupling agent. The PP chain of MAHgPP diffuses into the PP matrix through interchain entanglements. These cause better adhesion between the fibre and the matrix.

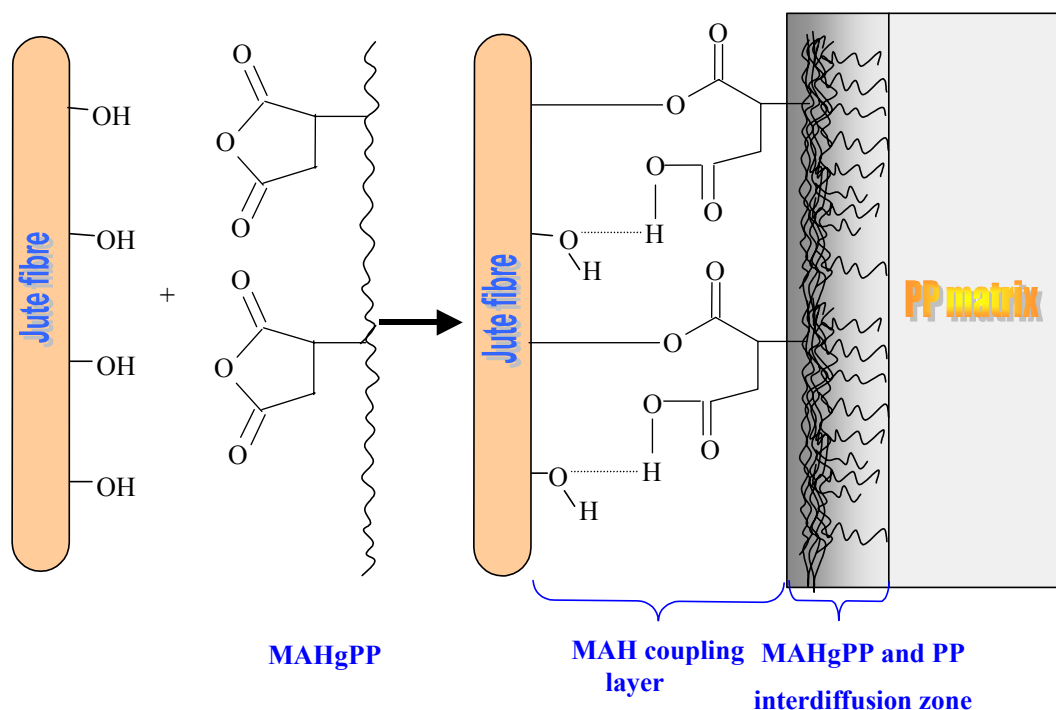


Fig. 14. Hypothetical structure of MAHgPP coupling agent and jute fibre at the interface

#### 3.4.2.2. Fibre modification

An interphase can be formed in composites with thermosetting epoxy matrix due to preferential adsorption of resin components onto the surface of the fibres, resulting in a gradient of cure and mechanical properties [58, 57]. The fibre surface treatment before introducing the matrix

material can modify the interphase region and alter the adhesion between the fibre and the matrix.

- ***NaOH treatment***

The alkali treatment can cause an increase of the fibre surface free energy. The adsorption of the epoxy resin on the jute fibre surface increases, which is a prerequisite condition for creating the interphases [59]. Moreover, the alkali treatment can make the fibre surface become 'clean' due to removal of waxes, hemicellulose, pectin and part of lignin. The removal of these substances enhances the surface roughness. Therefore, the mechanical interlocking at the interface could be improved.

- ***Silane coupling agent and film former***

A coupling agent is typically a small molecule that reacts with the fibre surfaces, which improves the degree of cross-linking in the interface region and offers a perfect chemical bonding with the matrix material. Coupling agents are most commonly used with glass fibres but also provide benefit in the use of natural fibres. They are a family of chemicals characterised by being organo-metallic, in most cases organo-silicon compounds, and possessing dual or multiple functionality. Each metal or silicon atom has attached to it one or more groups which can react with the fibre surface resulting either in the removal of –OH groups or the formation of hydrogen bonds, and one or more groups which, at least in the case of thermosetting resins, can co-react with the polymer during its polymerisation. A chemical bridge is thus formed between fibre surface and polymer. Of coupling agents, silane is commonly used. They were found to be effective in modifying the interface of natural fibre and polymer matrix [57].

Both aliphatic and aromatic silanes were used in this study. The silanes  $\text{RSi}(\text{OR}')_3$  are organo-silicon compounds and possess multiple functionality. With the hydrolyzable alkoxy groups ( $\text{OR}'$ ), silane can be hydrolyzed and becomes silanetriol ( $\text{RSi}(\text{OH})_3$ ), which is absorbed and condensed on the jute fibre surface. A hydrogen bond as well as a covalent bond can be formed between the fibre and silane. On the other hand, the organo functional group (R) causes the reaction as well as interdiffusion with the polymer matrix. Depending on the type of moiety R, there could be a co-polymerisation, and/or the formation of an interpenetrating network. Silane was also studied in combination with polymeric epoxy film formers. The reactions between fibre and matrix in the presence of coupling agents or film formers and also the hydrolysis of the silane were proposed as seen in Fig. 15. In this model, the coupling agent reacted with the fibre surface and with other silane molecules to form a covalently bound network possessing amine functionalities on the fibre surface. These pendent amines were able to react with epoxy rings in

the epoxy matrix and epoxy from the film former as well. Addition of coupling agent resulted in an interphase region covalent bond to both the fibre and the matrix [57].

The current view of the function of coupling agents is a little more complex. Since coupling agents are almost invariably used in aqueous systems, and since they polymerise under these conditions, several layers of coupling agent could react with and/or be adsorbed onto the fibre surface, and adequate number co-react with the resin, this gives rise to an 'interphase' layer possessing intermediate mechanical properties between the fibre and the polymer. This interphase of intermediate properties is believed to be a prerequisite for the successful reinforcement of the thermosetting, and appears to be the major contributor to efficient stress transfer between the fibre and the polymer.

For coupling agents to be effective in creating a stress-relieving boundary layer between the fibre and the polymer, the following conditions seem to have to apply:

- the boundary region must be firmly bonded to the fibre.
- the bulk polymer must efficiently wet the boundary layer in order to prevent voids from forming.
- the boundary layer must function to maintain contact of the fibre surface to the coupling agent interphase [60].

The purpose of using film former is firstly to bind the filaments together and give the strand specific handling characteristics and, secondly, to protect the filaments and the strand from damage during the various textile and other operations which have to be carried out. However, the new film formers have provided improved compatibility and increased wet-out times in polyester and epoxy resins. In the case where these film former are themselves polyester or epoxides, they have been formulated to be soluble or dispersible in water [61].



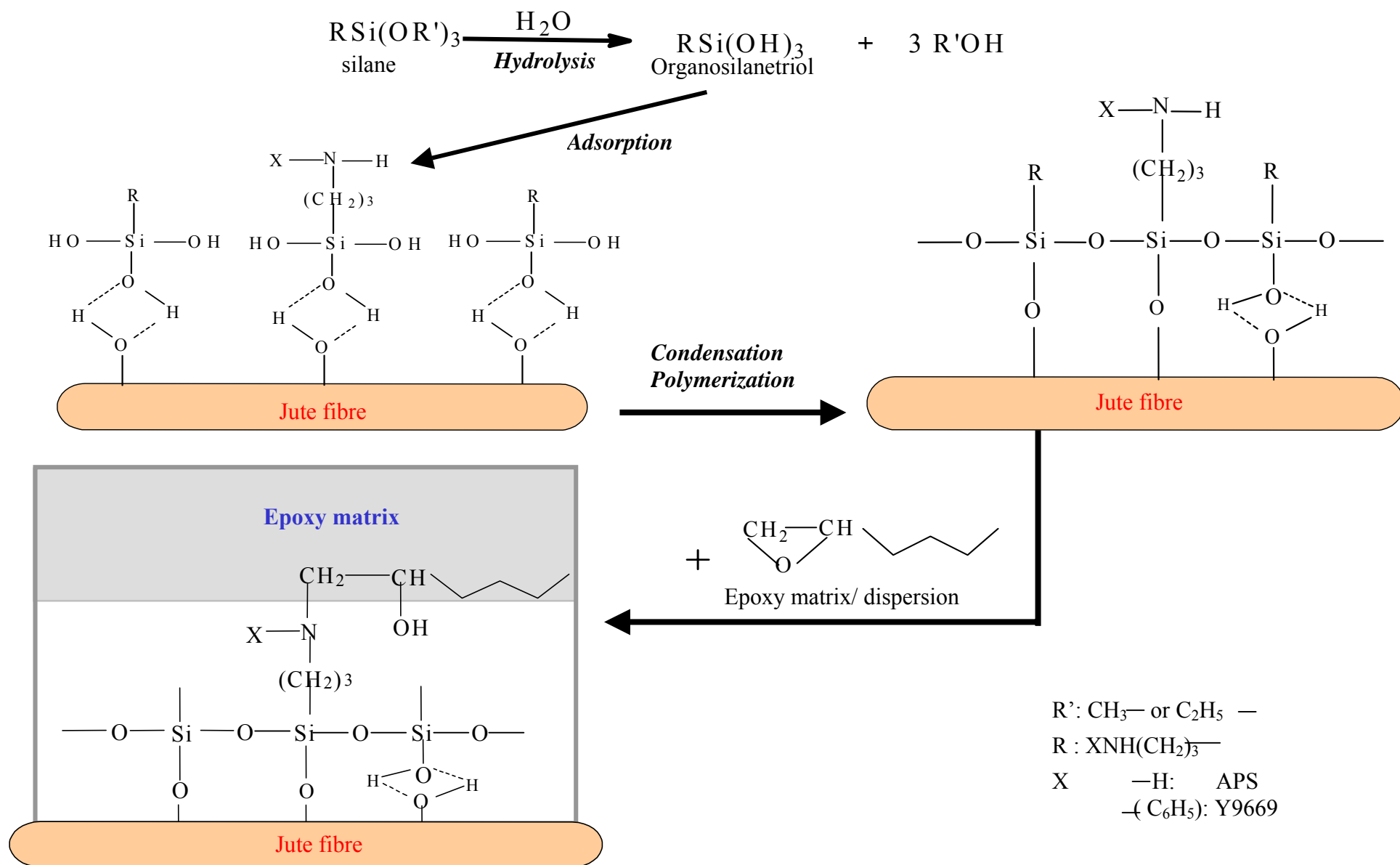


Fig. 15. Hydrolysis and bonding formation at the interface of the jute fibre and epoxy matrix

### 3.4.3. Composite processing

#### 3.4.3.1. Jute/polypropylene composites

For jute/polypropylene composite systems, the specimens were prepared by two steps: compounding and then injection moulding. The materials consist of jute yarn from Spinnerij Blancquaert NV (Lokeren, Belgium) (J1) and polypropylene (PP1 and PP2). Other components include as coupling agents maleic anhydride grafted polypropylenes (MAHgPP). Three kinds of MAHgPP were used for pre-investigation. Their properties are shown in Table 6 in terms of densities, melt flow rate (MFR), melting points, prices and maleic anhydride graft level of MAHgPP.

Table 6. Properties of three kinds of coupling agents

Properties	Coupling Agents		
	Exxelor PO 1020	Polybond 3200	TPPP 8012
Density at 23°C (g/cm <sup>3</sup> )	0.9	0.91	-
Melt Flow Rate (g/10 min) (190°C/1.2kg)	125	110	80
Melting Point (°C)	160	160-170	-
Maleic anhydride graft level (wt%)	0.5-1	1	1
Price (EUR)/kg	4.5-5.0	5.16	3.1

The commercial grade Exxelor PO 1020 (Exxon Mobil Corp., USA) was selected based on a comparison with two other commercial MAHgPP grades [62] and used for investigation in detail (cf. section 5.3).

- **Matrix modification and compounding**

Compounding means mixing polymer, fibres and possible additives in a molten state to form a homogeneous compound. The compounding is commonly carried out by extrusion, which is the most common manufacturing method for thermoplastic products in high volumes, such as plastic pipes, films, sheets, profiles and cables coating. A conventional extruder consists of one (single screw extruder -SSE) or two rotating screws (twin screw extruder -TSE) placed inside a heated barrel. In this study, the materials were compounded by a co-rotating twin-screw extruder ZSK 30 (Werner & Pfleiderer, Stuttgart, Germany). Polypropylene and MAHgPP (in the case of matrix modification) in granule form flow from the extruder hopper, which is placed on top of the extruder, into the screw throat from where the screw will convey the materials into the

extruder. The material is melted at the suitable temperature shown in Fig. 16 A. The fibre was dosed in the melted stage of the matrices in order to prevent extended fibre damage (Fig. 16 B). At the end of the screw, the materials are continuously pushed into and through a tempered die attached to the extruder. The extruded strands were cooled by immersion in a water bath and then pelletized and dried.

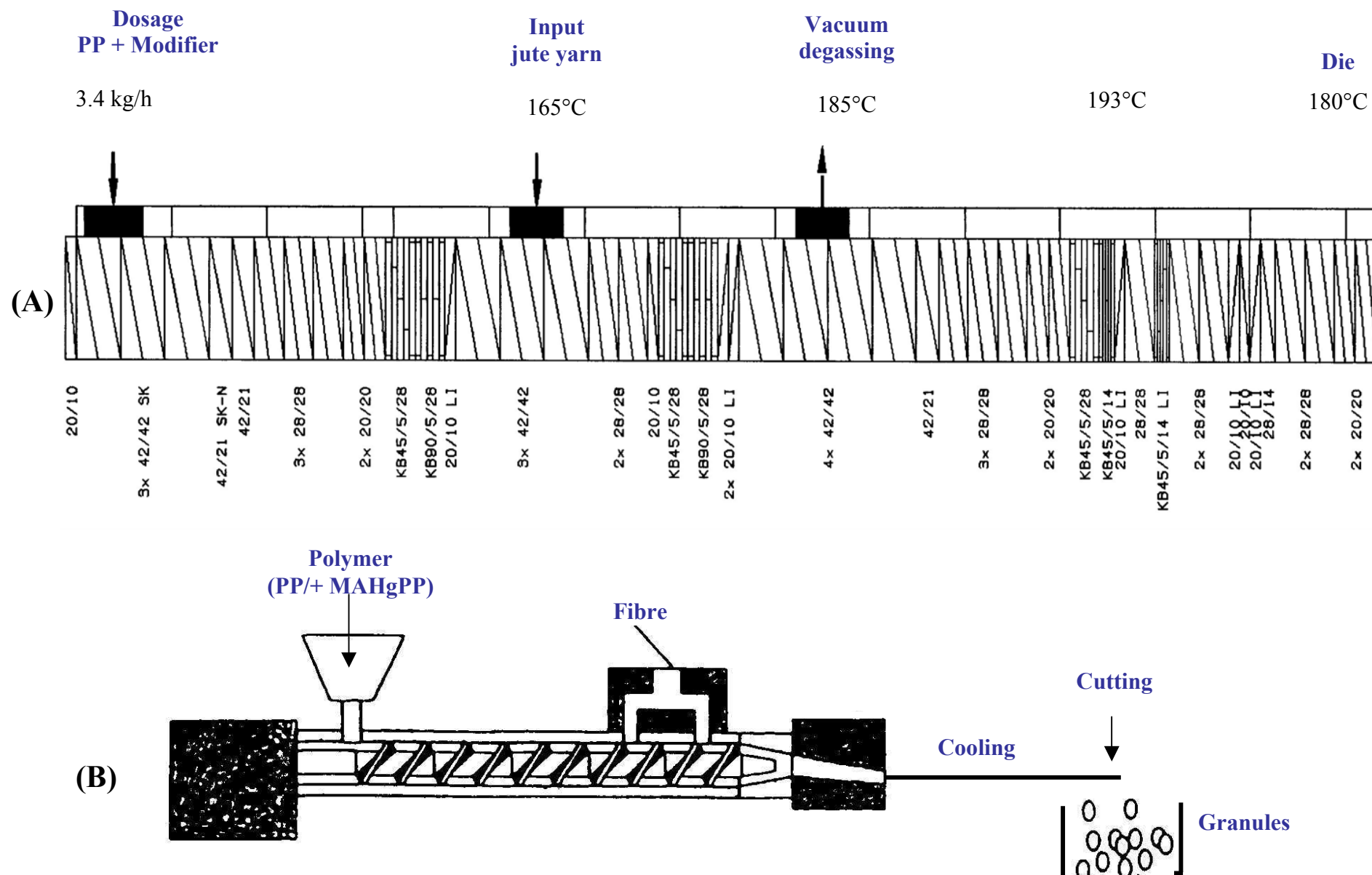


Fig. 16 Schematic diagram of (A) screw configuration and (B) extrusion procedure used for jute/PP compounding

- **Injection moulding**

Injection moulding is a widely used technology in the thermoplastics industry, especially in large series short cycle time production. It is useful when the products have complex geometries, and cost prohibitive to machine or when producing large series. With this process, many parts can be made at the same time, out of the same mould [63].

Pelletized compounds were dried in an oven for 4 hours at 100°C before injection moulding into the specimens for the measurements. The dog-bone shaped specimens ( $160 \times 10 \times 4$  mm, according to DIN 53455, specimen No. 3, ISO 527.2) and plates ( $80 \times 80 \times 2$  mm) were made on the injectionmoulding machine Ergotech 100 (Demag Ergotech Wiehe GmbH). In this process, melted (plasticized) composite is injected (forced) into a mould cavity or cavities, where it is held under pressure and cooled until it can be removed in a solid state. The schematic diagram of an injection moulding machine is displayed in Fig. 17. During processing there are three basic operations taking place: (1) heating up the composite in the injection or plasticizing unit so that it will flow under pressure, (2) allowing the polymer melt to solidify in the mould, and (3) opening the mould to eject the moulded product.

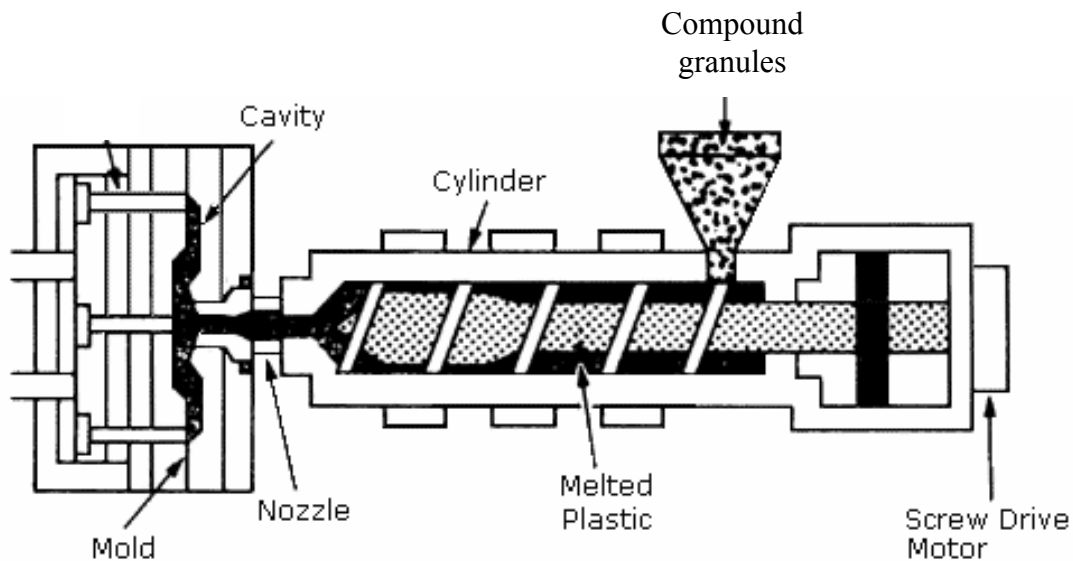


Fig. 17 Schematic diagram of an injection moulding machine

Injection moulding is a high-volume process and widely used by the toy, appliance, automotive and also aerospace industries.

#### 3.4.3.2. *Jute/epoxy composites*

In order to modify the properties of fibre and then the composites, alkali and some chemical treatments were investigated. Before these treatments, the fibre had to be de-waxed to remove the weaving size including potato starch and waxes [42].

- ***De-waxing***

The fibres were de-waxed in a mixture of Ethanol and Toluene with the ratios of 100:50, at 50°C for 2 days. Subsequently, the fibres were washed with pure water, and then dried. The de-waxed fibres were used for alkali treatment and other chemical modifications.

- ***Alkali treatment***

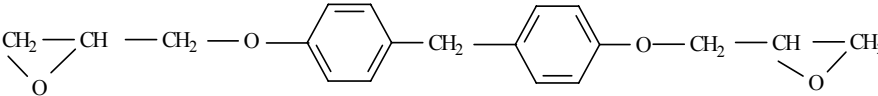
Alkali treatment of the fibre was performed by immersing them in NaOH solution at different concentrations and times. Then the fibres were washed thoroughly in pure water, neutralised with diluted acetic acid to remove the final alkali, then rinsed again with pure water and dried in an oven at 80°C for 4 h under vacuum.

- ***Silane coupling agent and film formers***

Coupling agents and film formers were prepared as in Table 7. The silanes were hydrolyzed in half the final amount of water at the pH necessary for the stability of the silane used and stirred for 45 min. In the case of the combination of silane and epoxy dispersion (film former), the epoxy dispersion was diluted and added. If necessary, the pH of the silane solution is adjusted by using acetic acid. Finally, the remaining water was added.

The jute fibres were immersed in the above solutions for 1 hour. Next, the mixtures were drained out with the assistance of the crush (or press) machine. Then the fibres were dried in an oven at 80°C for 4 hours and subsequently at 100°C for 30 min under vacuum.

Table 7. Sizing formulations

Modifiers	Formulas	Preparing solutions
3- Aminopropyl-triethoxy-silane 1% in water ( <i>APS</i> ).	$\text{H}_2\text{NCH}_2\text{CH}_2\text{CH}_2\text{Si}(\text{OC}_2\text{H}_5)_3$	Auto-catalytic hydrolysis for 45 min, no pH adjustment.
3-Phenyl-aminopropyl-trimethoxy-silane 1% in water ( <i>Y9669</i> ).	$\text{C}_6\text{H}_5\text{NHCH}_2\text{CH}_2\text{CH}_2\text{Si}(\text{OCH}_3)_3$	Adjustment pH= 2.9 by acetic acid, hydrolysis for 45 min.
3-Aminopropyl-triethoxy-silane (1%) + Epoxy dispersion XB 3791 (1.5%) in water ( <i>APS</i> + <i>XB</i> ).	 + $\text{H}_2\text{NCH}_2\text{CH}_2\text{CH}_2\text{Si}(\text{OC}_2\text{H}_5)_3$ or $\text{C}_6\text{H}_5\text{NHCH}_2\text{CH}_2\text{CH}_2\text{Si}(\text{OCH}_3)_3$	Firstly hydrolysis of <i>APS</i> , then adjustment pH= 4-5 by acetic acid. Next, <i>XB</i> was diluted by distilled water and added. The mixture was mixed well.
3-Phenyl-aminopropyl-trimethoxy-silane (1%) + Epoxy dispersion XB 3791 (1.5%) in water ( <i>Y9669</i> + <i>XB</i> ).	$\text{H}_2\text{NCH}_2\text{CH}_2\text{CH}_2\text{Si}(\text{OC}_2\text{H}_5)_3$ or $\text{C}_6\text{H}_5\text{NHCH}_2\text{CH}_2\text{CH}_2\text{Si}(\text{OCH}_3)_3$	First hydrolysis of <i>Y9669</i> , then adjustment pH= 4-5. Next, <i>XB</i> was diluted by distilled water and added. Then mixture was mixed well.

- ***Vacuum Assisted Resin Transfer Moulding (VARTM) of jute/epoxy resin composites***

The use of VARTM process in the manufacturing of high performance composite materials has been greatly recognized as one of the most important processes. The advantage of this technique is that it is possible to manufacture very large products with high mechanical properties. It also allows producing fibre contents in the range of 70% by weight and creates a void-free laminate. This process has brought lightweight, superior laminates to the average mould shop as well as to aerospace and high-tech fabricators [64]. Dry jute in unidirectional (UD) stitched form by a frame (J2 and J3) was put in the mould, in several layers. A scheme and details of the items are displayed in Fig. 18 and Table 8

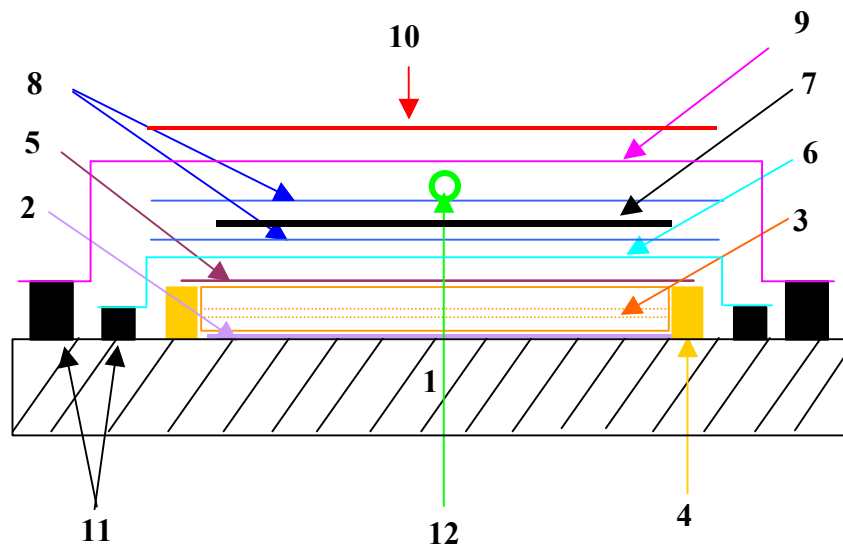


Fig. 18 Schematic arrangement of jute/epoxy composite processing by VARTM tool

After the tool is packed, a flexible bag is sealed around the perimeter and vacuum is applied which compacts the dry material, driving out the excess air. Resin is injected under vacuum, through the dry jute. The pressure during injection was 1 bar. Veins and capillaries are used to distribute the resin to the entire part [64]. After infusion at 50°C, the resin is allowed to cure at higher temperature (80°C). The temperature regime during processing is shown in Fig. 19. For post-cure, the composite samples then were dried in the oven at 80°C for 4 hours.



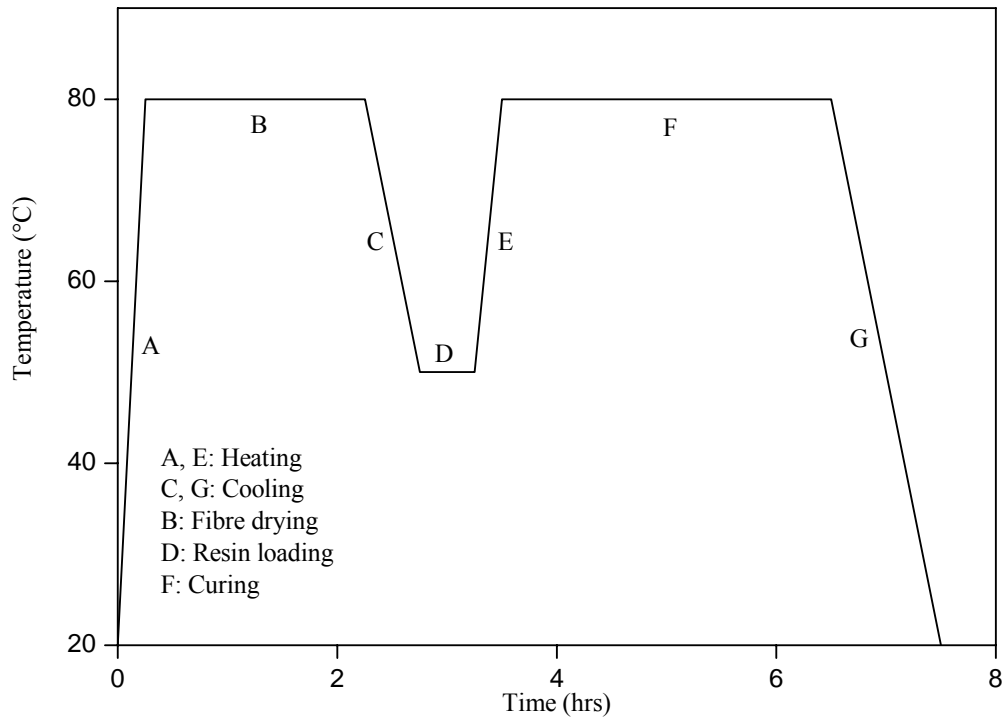


Fig. 19. Processing cycle of jute/epoxy composite by VARTM

Table 8. Functions and materials of the items in VARTM

No	Items	Functions	Materials
1	Tool	Mould	Steel
2	Release film	Release composite from tool	Wax/PVA solution
3	Laminate	Product	Fibre + resin
	Dam	Limit lateral flow of resin	Rubber
5	Peel ply	Provide surface texture and easy to peel	Nylon fabric
6	Bleeder ply	Remove the air and remain resin	Coated fabric
7	Metal plate	Heat distribution assistance and for a flat plane	Steel
8	Breather ply	Distribute vacuum over part area	Fleece
9	Vacuum bag	Envelope part and tool for vacuum	Nylons, silicone
10	Heating plate	Heating	Rubber with heating
11	Sealant tape	Make airtight	Rubber
12	Vacuum line	Make vacuum	Teflon

However, due to the disorientation of the jute yarns in stitched fibre sample (Fig. 20 A) due to the conditions of impregnation and the high torsion of the jute yarn, a homogeneous fibre-matrix distribution was limited. In order to reduce the disorientation of the jute yarn, a specific single layer consisting of stitched parts (Fig. 20 B) was used to prepare the VARTM-specimens and the properties of the composite specimens were tested in transverse direction.

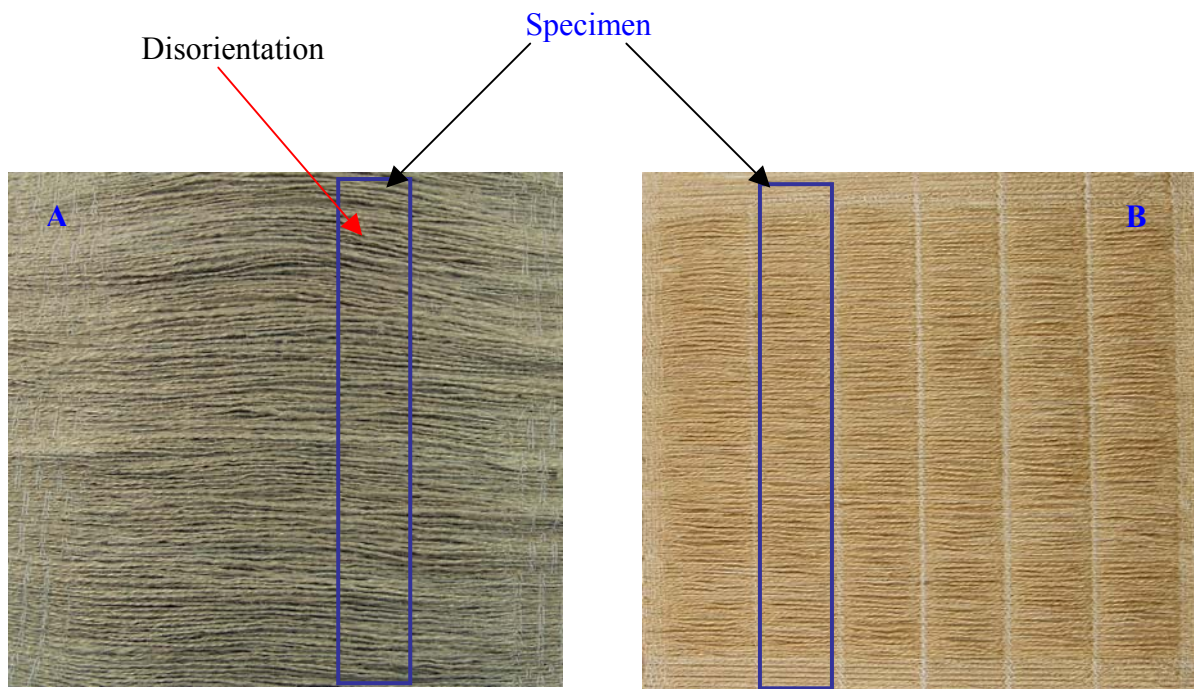


Fig. 20. Stitched jute fibre samples used as single layer in VARTM-processing

## 4. State-of-the-art and tools of investigation

### 4.1. Fibre

#### 4.1.1. Single fibre tensile test

The mechanical strength of the fibre is important for the reinforcing ability of the fibres in the composites [52]. The tensile strength of the filaments is derived from force-displacement curves. The influences of the fibre modifications on the fibre tensile properties were investigated by Mishra et al. A decrease in the tensile properties of the sisal fibre was observed after chemical modifications of the fibre. However, in the case of grafting the fibre tensile strengths increased compared to the untreated fibre [30]. NaOH treatments of the sisal fibre were found to decrease the fibre tensile strength [65, 66].

Within the present work, the tensile tests were performed in accordance with EN ISO 53812 and ASTM D 1577. The measurement is conducted in accordance with EN ISO 5079 using the Fafegraph ME testing device (Fa. Textechno) equipped with a 10 N force cell after determining the fineness of each selected fibre using a vibration approach in a Vibromat testing equipment (Fa. Textechno). Assuming a circular cross-section, a relation between the resonance frequency  $\nu$  and the fineness  $T_t$  at known pre-load  $F_v$  and gauge length  $L$  is defined as

$$T_t = \frac{F_v}{4 \cdot \nu^2 \cdot L^2} \quad (\text{Eq. 1})$$

The tensile test is conducted with a cross velocity of 0.5 mm/min using a gauge length of 5 - 20 mm, at 65 % RH and 20 °C temperature. The results of 50 single fibre tests are evaluated in terms of maximum force, elongation at break, and tensile modulus at an elongation between 0.5 and 1%, although the force-displacement curves reveal a Hookian behaviour. Special care was taken during preparation of the testing filaments to avoid the introduction of additional flaws.

The properties of fibre reinforced composites are dependent not only on the mean strength of the fibre but also the distribution of the fibre strength [67]. Therefore, in order to define the fibre strength distribution, the fibre strength data was analysed according to Weibull distribution. The Weibull probability distribution is a mathematical description of data, which can be used to evaluate many type of 'weakest link' experimental of data [66]. The statistical variability of the tensile strength of brittle materials is commonly described by following Weibull statistic analysis:

$$P = 1 - \exp\left[-\frac{V}{V_0} \left(\frac{\sigma}{\sigma_0}\right)^m\right] \quad (\text{Eq. 2})$$

$$V = SL_f \quad (\text{Eq. 3})$$

$P$ : the cumulative probability of failure ( $P=i/(n+1)$ ) at the tensile stress  $\sigma$ .

$V$ ,  $V_0$ ,  $S$ ,  $L_f$ : tested volume, scaling constant, mean cross-sectional area and fibre length, respectively.

$m$ : the Weibull shape factor (or modulus, slope of the distribution) describes the variability of the strength, a low value of  $m$  indicates high variability.

$\sigma_0$ : the scale factor (or characteristic strength) of fractured fibres indicates the stress at which the probability of failure of a unit length is 0.623 ( $1-\exp(-1)$ ).

The Weibull distribution expression can be rearranged as the following equation:

$$\ln \ln \left[ \frac{1}{1-P} \right] = m \ln \sigma - m \ln \sigma_0 + \ln L \quad (\text{Eq. 4})$$

The slope of the straight line ( $m$ ) is obtained from the plot  $\ln \ln[1/(1-P)]$  versus  $\ln \sigma$  and  $\sigma_0$  can be deduced from the intercept with the x-axis [68].

Fracture statistics are said to be correlated with the effects of gauge length and diameter variation. Hence, beside of studying the influence of fibre treatments on the fibre tensile strength, the effects of gauge length and fibre cross-section were also focused. The results were displayed and discussed in detail in section 5.1.1.

#### 4.1.2. Wetting measurement

The adhesion between the reinforcing fibre and the matrix in composite materials plays an important role in the final mechanical properties of the material. The wetting of the fibre is necessary for adhesion to occur.

The wetting measurement can be investigated using the Wilhelmy balance technique, in which wetting force on the fibre is measured as the fibre is immersed in or withdrawn from a liquid of known surface tension  $\gamma_{lv}$ . From this test, the contact angle  $\theta$ , which is the quantitative measure of liquid-solid interactions made up by a liquid played against a circular fibre of diameter  $d$ , can be determined from measurement of a wetting force,  $F$ , using the Wilhelmy equation [69, 70, 71, 72]:

$$F = \pi d \gamma_{lv} \cos \theta \quad (\text{Eq. 5})$$

From the Fig.21, contact angle  $\theta$  has a relation to the surface energies by the Young's equation:

$$\cos \theta = (\gamma_{sv} - \gamma_{sl}) / \gamma_{lv} \quad (\text{Eq. 6})$$

$\gamma_{sv}$ : Effective boundary tension of the solid-vapour interface (or solid/vapour interfacial energy).

For the fibre, subscript s (solid) represents the fibre.

$\gamma_{sl}$ : Effective boundary tension of the solid-liquid interface (or solid/liquid interfacial energy).

$\gamma_{lv}$ : Liquid surface tension.

There are three cases:

In the first case of  $\theta = 0$ , the fibre is said to be ‘wet out’ by the liquid. In the view of Young’s equation, this case is favoured by high  $\gamma_{sv}$  and low  $\gamma_{sl}$ . That means the fibre has high surface energy and the liquid has low surface tension. For the second case  $0^\circ < \theta < 90^\circ$ , the liquid is said to wet the fibre, but not completely. In the third case,  $90^\circ < \theta < 180^\circ$ , the liquid is said not to wet the fibre. This situation is favoured by low surface energy fibre  $\gamma_{sv}$  and high surface tension liquid  $\gamma_{sl}$ .

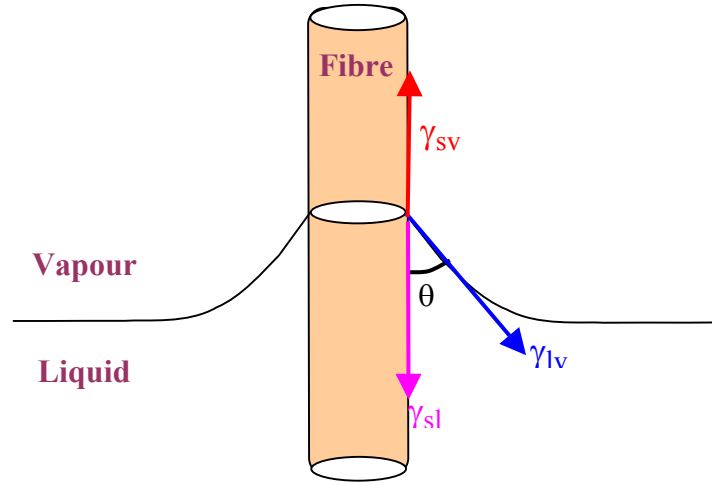


Fig.21. Force balance between the fibre, vapour and liquid during Wilhelmy wetting measurement

The work of adhesion is defined by

$$W_a = \gamma_{lv}(1 + \cos \theta) = \gamma_{lv} + \gamma_{sv} - \gamma_{ls} \quad (\text{Eq. 7})$$

Assumably, the total surface free energy across an interface ( $\gamma^T$ ) is split into two components: the non-polar or dispersive interaction ( $\gamma^d$ ) and the polar interactions ( $\gamma^p$ ).

$$\gamma^T = \gamma^d + \gamma^p \quad (\text{Eq. 8})$$

with

$$\alpha^2 = \gamma^d \quad (\text{Eq. 9})$$

and

$$\beta^2 = \gamma^p \quad (\text{Eq. 10})$$

$$\gamma_{sv} = \gamma_{sv}^d + \gamma_{sv}^p = \alpha_{sv}^2 + \beta_{sv}^2 \quad (\text{Eq. 11})$$

The following equation is obtained:

$$W_a / 2\alpha_{lv} = \alpha_{sv} + \beta_{sv} (\beta_{lv} / \alpha_{lv}) \quad (\text{Eq. 12})$$

$$\text{Where } W_a = \gamma_{lv} (1 + \cos \theta) \quad (\text{Eq. 13})$$

The contact angle  $\theta$  is measured for a range of liquids, for which  $\gamma_{lv}$ ,  $\gamma_{lv}^d$ ,  $\gamma_{lv}^p$  are known. By fitting a line to  $(W_a / 2\alpha_{lv})$  plotted versus  $(\beta_{lv} / \alpha_{lv})$ ,  $\alpha_{sv}$  and  $\beta_{sv}$  are estimated. The squares of these values give the dispersive part ( $\gamma_{sv}^d$ ) and the polar one ( $\gamma_{sv}^p$ ) of fibre surface energy. The sum of these components is the total fibre surface energy.

Besides, the surface polarity, the roughness of the fibre surface also contributes to fibre wettability.

Measurements of surface energies can lead to a prediction of the compatibility of the reinforcement fibres and the polymer matrix. Often the interface can be engineered by modification of the fibre surface chemistry to optimize the adhesion between fibre and matrix. This can be controlled by surface energy analysis [73].

The surface energy of rayon, cotton and wood fibres with different treatments such as heat treatment and acetylation was investigated by Liu et al. using contact angle analysis. The surface energy of acetylated wood fibres was 40% higher than that of fibre treated by heat. The acetylation of the fibres results in an increase of the surface energy [74]. Dynamic contact angle measurement and the capillary method were used by Gassan et al. for investigating the influences of fibre treatments on the polarity of the jute fibre surface. The results from the dynamic contact angle measurement showed an increase of the polar part of the fibre surface energy by corona treatment. Moreover, an increase of the polarity of the fibre surface was observed by silane treatment ( $\gamma$ -glycidoxypopyl trimethoxy silane) using the capillary rise method [75]. Using the dynamic contact angle method, the polarity of the surface of dew retted hackled long flax was characterized. It decreased with the fibre surface treatments including propyltrimethoxysilane, phenylisocyanate and maleic acid anhydride modified polypropylene [76]. Fibre treatments by maleic anhydride, maleic anhydride polypropylene copolymer and vinyl trimethoxy silane were also studied by Cantero et al. Using dynamic contact angle and capillary rise methods, the results showed decreasing polar component of the surface energy of the flax fibre and pulps [77].

For the present study, the wetting behaviour of the jute fibre was characterized, according to the dynamic contact angle method, using a Krüss K14 tensiometer. The liquids used for the

measurement are shown in Table 9. One end of a single fibre was attached to the hook of an electro balance by an adhesive tape as shown in Fig. 22. The sensitivity of the microbalance is  $\pm 0.1\mu\text{g}$ . The other end of the fibre was immersed into a liquid filling the glass container mounted on the movable table (elevator). While the elevator was moved, the balance recorded the weight of the fibre as a function of the position of liquid on the fibre surface. The final depth of immersion of the fibre in liquid was 1mm. The measurements were carried out at a rate of 1mm/min and at ambient temperature. Ten measurements were done in each case. From the test, the force versus position loop was recorded and the force was converted to the contact angle using the Wilhelmy equation. The surface energy of the fibre was then calculated and compared with the different fibre surface treatments, which are mentioned in section 5.1.3.

Table 9. Surface tensions of model liquids and dispersive/polar parts

<b>Liquids</b>	<b>Surface tension (mJ/m<sup>2</sup>)</b>	<b>Dispersive part (mJ/m<sup>2</sup>)</b>	<b>Polar part (mJ/m<sup>2</sup>)</b>
$\alpha$ -Bromo-naphtalene	44.6	44.6	0
Toluen	28.4	26.1	2.3
1,5 –Pentadiol	43.3	27.6	15.7
Water	72.8	21.8	51

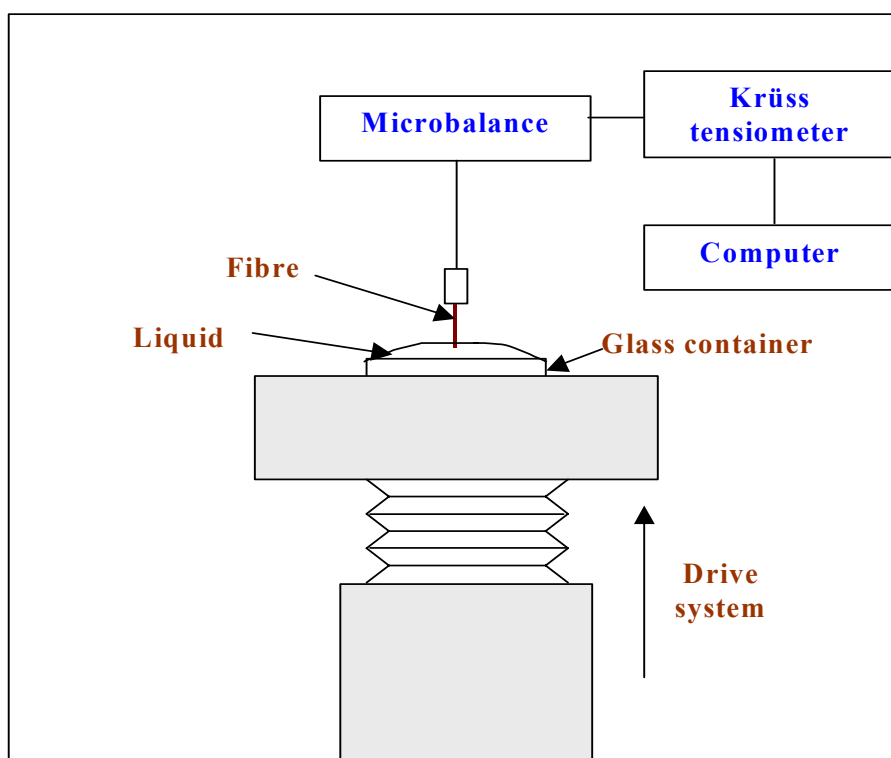


Fig. 22. Scheme of the tensiometer K 14

#### 4.1.3. Thermal analysis

Thermal analysis provides important data towards understanding the structure-property relationships and controlling the technology for molecular design with the aim of industrial production of different polymeric materials, especially fibre reinforced composites. Moreover, it is a useful technique to determine the thermal stability of the materials. Additionally, it permits to quantify the amount of possibly damaging, deteriorating volatiles, such as the moisture uptake during a hydrothermal treatment, which can cause deterioration in the composites [17]. Some investigations focusing on the thermal degradation of the natural fibres and their composites have been performed. Kita et al. reported that the degradation of lignin in cellulose fibre sets in at around 200°C, and other polysaccharides, mainly cellulose, are oxidised and degraded at higher temperature [78]. The thermal degradations of the individual components and the composite based on sisal and polypropylene in an inert atmosphere were compared by Joseph. The sisal fibre was found to degrade at lower temperature compared to the PP matrix. Most of the cellulose in the sisal fibre is decomposed at a temperature of 350°C, whereas PP decomposes at a temperature of 398°C. The major peak of the degradation in the case of sisal-PP composite was observed to shift to higher temperature, namely 476°C, compared to sisal fibre and PP, suggesting that the thermal stability of the composite is higher than those of the fibre and pure PP due to fibre/matrix interactions [17]. The thermal behaviour of flax and hemp was also characterised by Wielage. The fibres were degraded slightly between 200°-220°C in air, above this temperature irreversible degradation of the fibres occurs [79]. The thermal degradation of PP and viscose fibre in both nitrogen and synthetic air were studied and compared in a research by Paunikallio et al. [80]. The thermal stability of the natural fibres can be influenced by some fibre surface treatments. In a study of Mohanty et al., an improvement of the thermal stability of the henequen and kenaf fibres was observed after NaOH treatment at the concentration of 5% for 1 hour [81]. The acetylation of jute fibre was investigated by Rana et al. and showed an improvement in thermal resistance compared to untreated fibre [82]. However, treatment of the jute fibre with PF and CNSL-PF carried out by Mitra et al. showed a reduction of the thermal stability of the treated fibre [83].

Nevertheless, the thermal analysis of the natural fibre reinforced composites with and without modification has not been studied in depth so far, especially in air. Therefore, the aim of our research in this part is to study the thermal stability of the jute fibre, polypropylene resin and composites with and without modification under two atmospheres, namely nitrogen and air. Thermal gravimetry (TG) and derivative thermo-gravimetry (DTG) were carried out using a TGA Q500, TA instruments. The samples were heated from -50°C to 200°C with a heating rate



of 10K/min. The sample weight as a function of temperature is recorded, the data indicate a number stages of thermal breakdown, weight loss of the material in each stage, etc. Both TG and DTG provide information about the nature and extent of degradation of the materials [17]. The data are presented in section 5.1.5 and 5.3.4.

#### 4.1.4. Atomic Force Microscopy (AFM)

AFM measures the topography of surfaces on the molecular scale. As the AFM probes the atomic interaction between surfaces, it can also be used to map the adhesion, friction, stiffness or other kinds of interaction such as magnetic or electric forces. For topography, there are two imaging modes of AFM: contact mode and intermittent contact or “tapping mode”. Tapping mode tends to be more applicable to imaging polymeric samples in air, particularly for soft samples, as the resolution is similar to contact mode while the forces applied to the sample are lower and less damaging. Tapping mode operates by scanning a tip attached to the end of an oscillating cantilever across the sample surface. The cantilever is oscillated at or near its resonance frequency with an amplitude ranging typically from 20 nm to 100 nm. The tip lightly “taps” on the sample surface during scanning, contacting the surface at the bottom of its swing [84]. The vertical position of the scanner at each (x, y) data point in order to maintain a constant “setpoint” amplitude is stored by the computer to form the topographic image of the sample surface (Fig. 23).

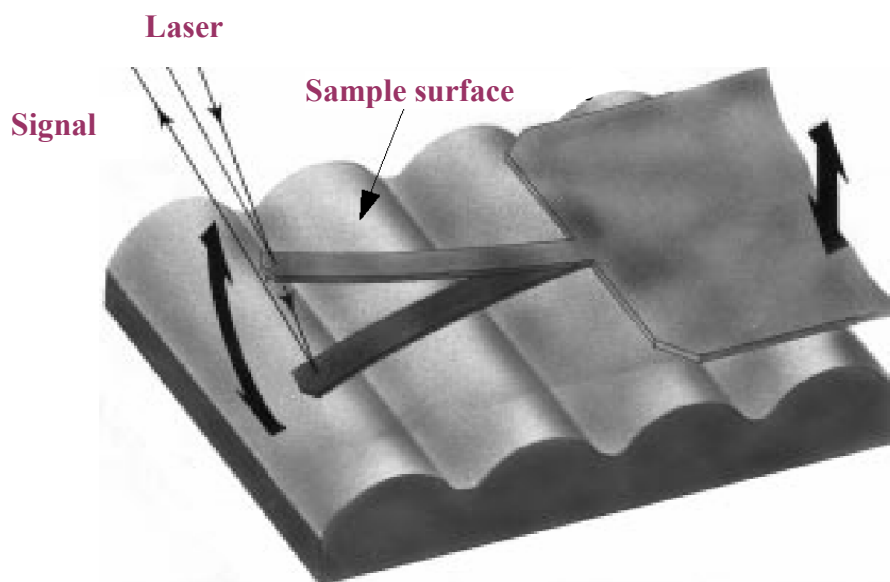


Fig. 23. Principle of detection of oscillating cantilever [84]

The mean roughness of the fibre surfaces can be calculated and compared. Roughness parameters derived from ASME B 46.1 (the American Society of Mechanical Engineers, Surface Roughness, Waviness and Lay) were calculated based on the following definitions [85, 86, 87]:

❖ Image mean roughness ( $R_a$ ): The arithmetic average of the absolute values of the surface height deviations measured from the mean plane within the cursor box ( $4\mu\text{m}^2$ ).

$$R_a = \frac{\sum_{i=1}^N [Z_i - Z_{cp}] }{N} \quad (\text{Eq.14})$$

where

$Z_{cp}$ : the surface height ( $Z$ ) of the center plane.

$Z_i$ : the current  $Z$  value.

$N$ : the number of points within a given area.

❖ Maximum height roughness ( $R_{\text{max}}$ ): The difference in height between the highest and lowest points on the surface relative to the Mean Plane.

So far, using AFM for investigating the natural fibre has been not performed often. An AFM investigation of flax fibre surface was carried out by George, who is one of very few researchers who did the AFM research for the natural fibre. The AFM image of untreated and silane treated fibre in force modulation mode showed the higher roughness of the treated fibre comparing to untreated fibre [88]. Especially, there has not been quantitative estimation of the roughness of the natural fibre surface up to now.

In this research, the investigation of the jute fibre surface before and after pull-out tests was carried out by using AFM (a Digital Instruments D3100, USA, nanoscope III a or nanoscope IV + controller). In tapping mode, a piezo stack excites a silicon cantilever's substrate vertically at its resonant frequency with a drive amplitude of 200 mV. As the cantilever is oscillated vertically, the reflected laser beam reveals information on the deflection of the cantilever and therefore indirectly or vertical height of the sample surface. A silicon cantilever (NANOSENSORS, Germany) with normal spring constant of 7 N/m and a tip radius of approximately 10 nm was used with resonant frequency of 245 kHz. Several images were recorded at different locations to verify the reproducibility of the observed features. The AFM images of the fibres of two polypropylene and epoxy composites systems before and after pullout tests, as well as the calculated roughness are displayed in section 5.2.2.

#### **4.1.5. Scanning Electron Microscopy (SEM)**

Morphological analysis of the fibre can be also carried out using SEM. This is the most widely used of the surface analytical techniques. High resolution SEM has proved an invaluable tool for studying surface topography and failure analysis. The technique enables qualitative three-dimensional (3-D) imaging of surface features, however, it does not easily lend itself to quantitative surface roughness characterisation. This can be overcome by complementing SEM investigations with atomic force microscopy. In SEM, a highly focused scanning electron beam bombards the surface causing large numbers of secondary electrons to be generated, the intensity of which is governed by surface topography. The method is suitable for all materials, but non-conducting materials must be given a thin conductive coating sputtered gold, which can alter or mask the true surface morphology. The resolution of topographical features is approximately 5 nanometres. SEM is often used to survey a surface before more specialised techniques are employed. In this study, the scanning electron microscope LEO 435 VP (Leo Elektronenmikroskopie) operating with an acceleration voltage of 5 to 10 kV was used to investigate the fibre surface and the fracture surface of the composites.

## 4.2. Model composites

### 4.2.1. Micro-mechanical analysis

It is well established that the level of interfacial adhesion is a fundamental importance in determining the transfer of stress from a relatively low modulus matrix to a high modulus fibre in a discontinuous fibre-reinforced composite system. A strong and durable interface is required between the fibre and matrix for the resulting composite to have good mechanical properties [89]. There are three main types of micromechanical test for evaluating the properties of the fibre/matrix interface (Fig. 24), namely the fragmentation [90], the microindentation [91] and the single fibre pull-out test, which may be subdivided into a pull-out test [92] and microbond test [93].

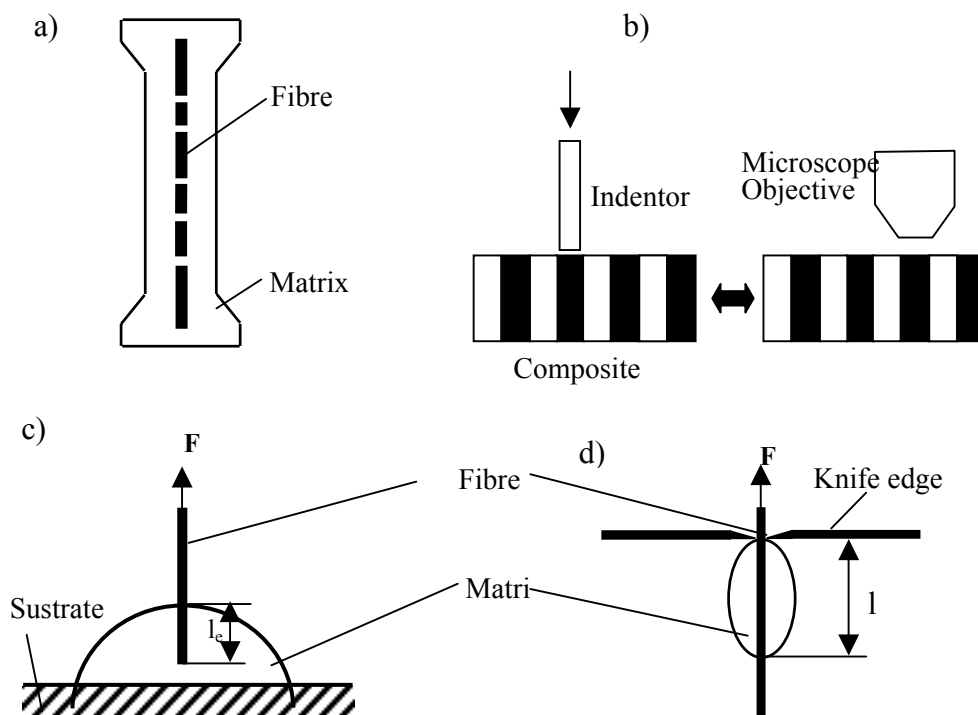


Fig. 24 Micromechanical tests: (a) fragmentation, (b) microindentation, (c) pull-out and (d) microbond test.

Amongst the micromechanical testing methods for evaluating fibre/matrix interfacial properties of fibre-reinforced composites, the pull-out test is widely used due to its simple sample preparation and measurement [94].

### 4.2.2. Pull-out test

In this test, one fibre end of a single fibre is embedded vertically in a block of resin to a controlled depth. This sample is placed in a tensile test machine and the other fibre end is

gripped with a special glue or clamp of the machine. The fibre is pulled from the resin block and the load as well as extension is recorded in a Force-displacement curve (Fig. 25). In the curve, there are three parts corresponding to three stages of a pullout test. The first part ( $0 \leq F \leq F_d$ ), the curve is nearly linear due to linearly elastic property of fibre-matrix system and the fibre-matrix interface remains intact. When the external load reaches the critical value,  $F_d$  (called de-bond force), the fibre begins to de-bond off the matrix through interfacial crack propagation [95, 96]. At this second stage ( $F_d \leq F \leq F_{\max}$ ), the force continues increasing with the fibre end displacement (or with crack length), because frictional load in de-bonded regions is added to the adhesive load from the intact part of the interface. After reaching a peak load,  $F_{\max}$ , the crack propagation becomes unstable, the whole embedded length fully de-bonds and the measured force drops from  $F_{\max}$  to  $F_b$ . From this moment until complete pullout, the “tail” force is due to frictional interaction between the fibre and the matrix [97].

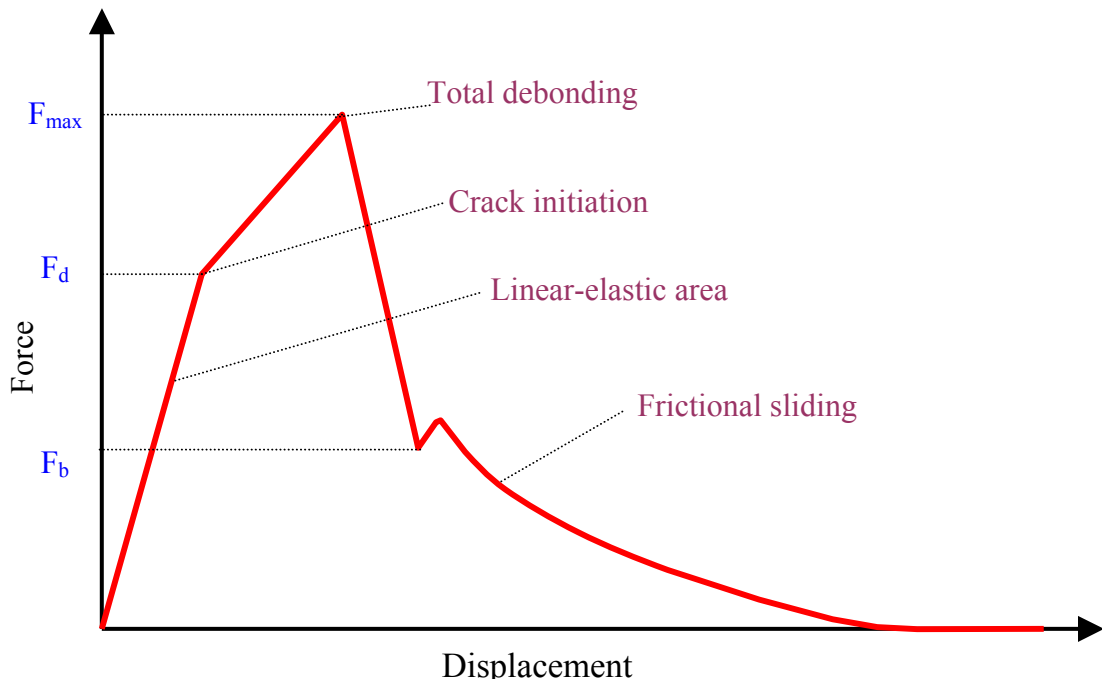


Fig. 25 A typical plot of pull-out force versus displacement

The quality of interfacial bonding is characterized by calculating the apparent interfacial shear strength (apparent IFSS,  $\tau_{app}$ ) and post-debonding friction ( $\tau_f$ ) [93, 98, 99, 100].

$$\tau_{app} = \frac{F_{\max}}{\pi d_f l_e} \quad (\text{Eq. 15})$$

and

$$\tau_f = \frac{F_b}{\pi d_f l_e} \quad (\text{Eq. 16})$$

Where

$F_d$ : Maximum force

$F_b$ : Minimum force

$d_f$ : the fibre diameter.

$l_e$ : the embedded length.

The main advantage of the pull-out test is that without considering composite processing variables, good performance the composites may be selected before their laborious and material-consuming preparation step [37].

There has been some research using the single fibre pull-out test method for estimating the interfacial shear strength of natural fibre composites. The apparent shear strength of composites based on two types of flax fibres and a number of matrices including high and low density polyethylene, polypropylene and maleic anhydride modified polypropylene was investigated and compared by Stamboulis et al. [101]. The addition of small proportion of maleic anhydride to the polypropylene and polypropylene-ethylene propylene diene terpolymer blends was observed significantly increased the shear strength of the flax fibre reinforced composites. Machado et al. assumed that the introduction of functional groups in the matrix reduced the interfacial stress concentration preventing fibre-fibre interactions which are responsible for premature composite failure. On the other hand, the presence of maleic anhydride functional groups can make the esterification of flax fibre takes place increasing the surface energy of the fibres to a level closer to that of the matrix. Therefore, a better wettability and interfacial adhesion were obtained [102]. The interfacial adhesion of sisal fibre with both matrices, including thermosetting resins (polyester, epoxy and phenol formaldehyde) and thermoplastic resin (LDPE) was investigated by Joseph et al. Interfacial bonding was found to be maximum in sisal fibre reinforced phenol formaldehyde composites due to chemical bonding between phenol formaldehyde pre-polymer and the guaiacyl group of lignocellulose. The interfacial bonding in sisal-LDPE composites is low due to the divergent behaviour in polarity of the fibre and the matrix [103]. Pull-out tests of sisal reinforced polyester biocomposites were performed by Syndenstricker, evidencing the improvement of interfacial adhesion by NaOH and N-isopropyl- acrylamide treatments of the fibres [37]. The influence of fibre surface modifications on the interfacial shear strength of the composites based on sugar cane Bagasse fibres and polystyrene was assessed by Edgar et al. The improved extent of IFSS followed the order: non-treated fibres < fibre treated with NaOH or

silanized with 3-(trimethoxysilyl)-propylmethacrylate<<fibres grafted or coated with polystyrene. All the treatments applied to the sugar cane bagasse fibres were found to improve the binding properties of their interface with polystyrene. A significantly increase in IFSS was achieved through a combination of treatments due to the synergistic of the surface treatments techniques [104].

In this work, the apparent interfacial shear strength of jute fibre composites based on both polypropylene and epoxy matrices with the modification of the matrix and the fibre were estimated using single fibre pull-out test. First, the single fibre model composites were prepared by putting resin into a special aluminium carrier and the whole unit was set into a self-made sample preparation equipment designed and constructed at the Institute of Polymer Research Dresden. Single fibre were embedded into the resins perpendicularly at a pre-selected embedding length (50-500  $\mu\text{m}$  for polypropylene and 40-150  $\mu\text{m}$  for epoxy resin) and controlled atmosphere and temperature. The epoxy composite samples were then cured at 80°C for 6h, as recommended by the manufacturer. Then the pull-out test was carried out on a self-made pull-out apparatus (Fig. 26) with force accuracy of 1 mN and displacement accuracy of 0.07  $\mu\text{m}$ . An adhesive contact was formed between the studied fibre and a matrix fixed on a substrate, the force,  $F_{\text{max}}$ , required for pulling the fibre out of the matrix was measured.

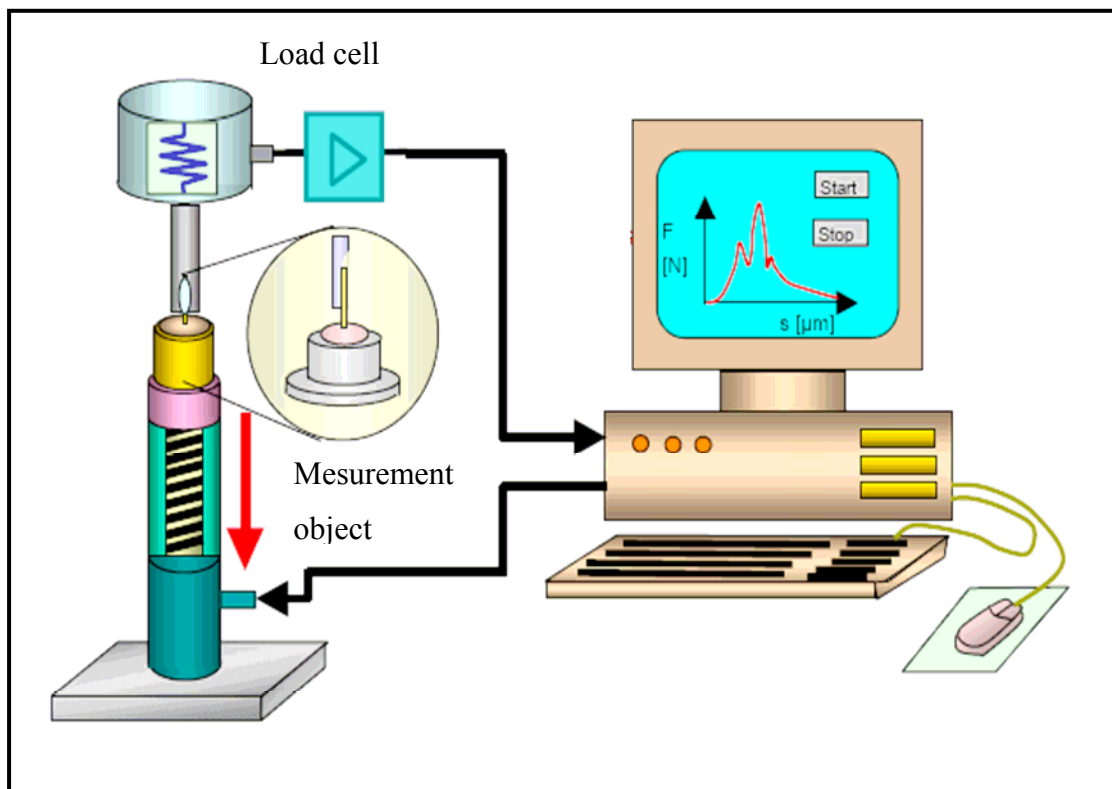


Fig. 26. Schematic of single fibre pull-out test equipment

The test was done with a loading rate of 0.01  $\mu\text{m/s}$  at ambient conditions. The free fibre lengths were kept as short as possible ( $<0.5\text{ mm}$ ) and the installation was stiff enough to discern the “kinks” in force-displacement curves [97, 105]. After testing, the fibre diameter  $d_f$  was measured microscopically at two perpendicular views and five different positions along the fibre for each viewing angle and the bond strength between the fibre and the matrix was characterized by the values of the apparent interfacial shear strength ( $\tau_{\text{app}}$ ) and post-debonding friction ( $\tau_f$ ), following the equation (15) and (16), respectively. Each fibre/matrix combination was evaluated by about 15 to 20 single tests. The influences of the modifications on the interfacial adhesion between the jute fibre and PP as well as epoxy matrix estimated by pull out test are displayed in section 5.2.1.

#### **4.2.3. Analysis of fracture surfaces (Fractography)**

AFM was used to investigate the topography of the jute fibre surfaces and to study the failure mode of single fibres after pull-out tests. The debonded fibre pieces after pull-out tests were used for the examination. The principle of this measurement is the same compared with section 4.1.4.

#### **4.2.4. Aging of micro-composites**

A major restriction in the successful use of natural fibres in durable composite applications is their high moisture absorption due to the hydrophilic behaviour of the fibre. Swelling of fibres can lead to micro-cracking of the composite and therefore to degradation of mechanical properties. Many studies focus on the effect of aging condition on physical and mechanical properties [22, 106, 107, 108]. However, mainly macro-composites are studied. Micro-mechanical measurements are sensitive to the interphase, they should provide valuable information on the effect of aging on the adhesion behaviour. Therefore, one objective of this work is to investigate the environmental effect on their micro-mechanical behaviour by single fibre pull-out test. For this test, the single fibre composite samples were firstly prepared as mentioned above. Next, they were kept in a desiccator containing water to get the relative humidity (RH) of 95% for 7 days. The pull-out test then was carried out to estimate apparent adhesion strength and to compare with the control samples.



## 4.3. Composites

### 4.3.1. Fibre length and content

#### 4.3.1.1. Fibre length distribution

It should be noted during compounding and injection moulding, fibres are damaged resulting in shorter fibre lengths. This process is more promoted for glass and other man-made fibres than for natural fibres. The main reason is high fibre attrition, depending on fibre content, viscosity of the polymer melt, melt-flow velocity, etc. The average fibre length remaining after processing is an important factor for the strengthening of a composite [23]. The fibre length distributions in injection moulded composites based on PP matrix were investigated [109, 110]. The fibre length distributions in the injection moulded part and granulates of the hemp reinforced biodegradable matrix composites estimated by Keller showed no further shorting of the fibre during injection moulding [111]. The influence of the injection moulded processing on the final fibre length of the polypropylene composites based on abaca, jute and flax fibres investigated by Biagotti et al. showed the minor effect with the higher fibre content and a more significant size reduction of the flax fibre due to its more rigid behaviour [112]. However, the flax fibre was observed by Hornsby et al. to be significantly less susceptible to breakage than wheat straw fibre during melt compounding processing of the polypropylene composites [113]. The influences of the sisal fibre length on the mechanical properties of the sisal/PP composite were studied by Jayaraman and presented a steady increase of the impact strength with increasing fibre length [114].

To confirm if variation of the jute fibre dimensions exists during composite process, one part of our study is measurements of the fibre length,  $L_f$ , and diameter,  $d$ , before (compound granules) and after (composite plates) injection moulding process.

PP was removed from jute/PP composites (granules and plate) by boiling in xylene (135°C) for 14 hours. Fibres were spread between a glass slide and a cover plate. The lengths and diameters of extracted fibres were measured by the analySIS Software program (SIS) (Soft Imaging System, GmbH, Münster, Germany) using a semi-automatic two points measuring mode and by Image Scan Multi program (SCAN) from Minolta Company. It should be noted that the cross-section of jute fibres is oval or polygonal, however it was adapted to a circular one in this work. Because of the great scatter usually observed for natural fibres, the values of fibre dimensions for each system are a rough approximation based on more than six hundred individual tests.

Average fibre lengths were statistically analysed to obtain the cumulative distribution function  $P(l)$  [115]:

$$P(l) = \frac{\sum_{i=0}^l N_i}{\sum_{i=0}^{\infty} N_i} \quad (\text{Eq. 17})$$

where

$P(l)$ : the cumulative probability to find fibres with length shorter or equal to  $l$

$N_i$ : the number of fibres with length  $i$

The results and discussions are displayed in section 5.3.1.

#### 4.3.1.2. Fibre content

The volume fraction of the fibre  $V_f$  was obtained from fibre mass content  $M_f$  by the following relationship [111]

$$V_f = \frac{M_f \times \rho_m}{M_f \times \rho_m + (1 - M_f) \times \rho_f} \quad (\text{Eq. 18})$$

where

$\rho_f$ : fibre density

$\rho_m$ : matrix density

$M_f$ : the mass fraction of the fibre

### 4.3.2. Static mechanical properties

In this work, tensile, impact and flexural tests were done for polypropylene and epoxy composite systems in order to study the effects of matrix or fibre treatments as well as fibre content on the mechanical properties of these composites.

#### 4.3.2.1. Tensile test

Among the many mechanical properties of plastic as well as composite materials, tensile properties are probably the most frequently considered, evaluated, and used throughout the industry. These properties are an important indicator of the material's behavior under loading in tension. Tensile testing provides these useful data: tensile yield strength, tensile strength at break (ultimate tensile strength), tensile modulus (Young's modulus), and elongation at yield and break. The tensile strength ( $\sigma$ ) is given by

$$\sigma = \frac{F}{b h} \quad (\text{Eq. 19})$$

where

F: load

b: width of the sample

h: thickness of the sample

Strain or elongation is defined as:

$$\varepsilon = \frac{\Delta l}{l_0} \quad (\text{Eq. 20})$$

where

$\Delta l$ : is the extension

$l_0$ : the initial gauge length

The Young's modulus in tension ( $E_t$ ) is the slope of the stress vs. strain curve evaluated at small strains, where the response is linear.

Dog-bone shaped specimens with the dimensions of  $160 \times 10 \times 4$  mm were used for testing the tensile behaviour of polypropylene composites, injection moulded. However, for study epoxy composites, transverse plates with the dimension of  $250 \times 25 \times 2$  mm were used. Using the Universal testing machine Zwick 1456, the tensile test was performed according to ISO 527-2.

The use of modelling is reported in some literature in order to predict the mechanical properties of the composites. In our work, models are used to compare the experimental data of the jute/polypropylene composites with the possible performance expected by these models. An effective use of fibre strength is dependent on both the interfacial adhesion properties and the critical fibre length. The micro-mechanical evaluation was done by using single fibre pull-out test. It is well known that fibre length plays an important role in the mechanical performance of fibre reinforced composites. Using the Kelly-Tyson theory, the critical fibre length, defined as the minimum fibre length where the maximum allowable fibre tensile stress can be achieved, is roughly calculated as:

$$l_c = \frac{\sigma_f d}{2\tau_{app}} \quad (\text{Eq. 21})$$

where

$\sigma_f$ : the fibre strength at gauge length equal to the critical fibre length

$\tau_{app}$ : the apparent interfacial shear strength

$d$ : the fibre diameter

Using a modified ‘rule of mixture’ takes into account the interfacial properties for the strength of natural fibre/polymer composites,  $\sigma_c$ , as a function of volume fraction [116].

$$\sigma_c = \left( \frac{\eta L_f \tau_{app}}{d} - \sigma_m \right) V_f + \sigma_m \quad (\text{Eq. 22})$$

where

$\sigma_m$ : tensile strength of matrix

$V_f$ : the fibre volume fraction

The Hirsch model combined parallel and series ‘rule of mixtures’ models [117] was used to determine the Young’s modulus of the composite as the following equation:

$$E_c = \beta(E_m V_m + E_f V_f) + (1 - \beta) \frac{E_f E_m}{E_m V_f + E_f V_m} \quad (\text{Eq. 23})$$

where

$\beta$ : a factor of efficient stress transfer between fibre and matrix.

$E$ : the Young’s modulus.

$c, m, f$ : refer to the composite, matrix and fibre, respectively.

#### 4.3.2.2. Bending test

The epoxy composite samples were used for this test by using the machine Zwick according to ISO 178. For this three-point bending, the dimensions of the specimens are  $h \times (20 \times h) \times 15$  mm and the measurement is in transverse direction.

The modulus of elasticity ( $E_b$ ) and bending strength ( $\sigma_b$ ) are calculated the following equations:

$$E_b = \frac{m L^3}{4 b h^3} \quad (\text{Eq. 24})$$

and

$$\sigma_b = \frac{3 F L}{2 b h^2} \quad (\text{Eq. 25})$$

where

$E_b$ : bending modulus

$\sigma_b$ : bending strength

F: load

m: initial slope of the load vs. deflection curve

L: specimen length between two support points

#### 4.3.2.3. Impact test

The PSW 4 testing machine was used for this test of polypropylene composite according to ISO 179/1eU. The dimensions for the Charpy impact test are  $100 \times 10 \times 4$  mm without notch. Un-notched impact strength ( $a_{cU}$ ) is calculated by the following equation:

$$a_{cU} = \frac{W}{hb} \times 10^3 \quad (\text{Eq. 26})$$

Where

W: energy

b: width of the sample

h: thickness of the sample

### 4.3.3. Aging behaviour

#### 4.3.3.1. Model for the moisture diffusion process

With the recognition that moisture plays a significant role in influencing the mechanical behavior, the long-term durability of polymer and polymer matrix composites, numerous diffusion models have been proposed over the years for modeling hygrothermal effects in polymers and composites.

The moisture uptake of the materials follows Fick's law of diffusion, the fluid flux (F) is proportional to the concentration gradient ( $\nabla m$ ) [118]:

$$F = -D \times \nabla m \quad (\text{Eq. 27})$$

D: the diffusion constant. Fluid flux is taken as positive outward, therefore we get negative flux for an increasing concentration gradient. If the samples are thin and flat then the moisture transport may be approximated as one-dimensional. The conservation of mass for one-dimensional moisture transport follows the equation:

$$\partial m / \partial t = -\partial F / \partial x \quad (\text{Eq. 28})$$

The negative sign is again due to the outward positive sense of the flux. From the equations (27) and (28), the governing partial differential equation for one-dimensional Fickian moisture transport was received:

$$\partial m / \partial t = D \times \partial^2 m / \partial x^2 \quad (\text{Eq. 29})$$

Eq. (29) can be solved with the appropriate initial conditions (IC) and boundary conditions (BC) given as:

$$\text{IC: } m(x, 0) = m_i$$

$$\text{BC: } m(0, t) = m(h, t) = m_a \quad t > 0$$

where

$m_i$ : the initial fluid concentration in the sample.

$m_a$  : the constant fluid concentration at the free surface of the sample, taken to be the saturation value.

Equation (29) can be also solved as a series solution for moisture concentration in the sample as the following equation [119].

$$\frac{m(x, t) - m_i}{m_{sat} - m_i} = 1 - \sum_{j=0}^{\infty} \frac{\pi}{4} \times \left[ \frac{1}{2j+1} \times \sin\left(\frac{(2j+1)\pi x}{h}\right) \times \exp\left(\frac{-(2j+1)^2 \pi^2 D t}{h^2}\right) \right] \quad (\text{Eq. 30})$$

where

$m_i, m_{sat}$ : the initial and saturation values of fluid concentration in the sample, respectively.

$h$ : the sample thickness

It is assumed that the sample free surface concentration,  $m_a$ , is the saturation value. The total mass of moisture in the sample is found by integrating equation (30) over the volume of the sample can be obtained by the following expression [120].

$$M = \int m(x, t) dV = A \int_0^h m(x, t) dx \quad (\text{Eq. 31})$$

where A is the area of the sample face normal to the direction of moisture diffusion.

#### 4.3.3.2. Determination of diffusion constant

For a thin plate (thickness  $\ll$  length, width), The diffusion is assumed to be one – dimensional. According to Fick's law, the percent weight gain, % M, initially varies linearly with the square root of time, t [121].

$$\%M = \frac{[4 \times (\%M_{sat}) \times \sqrt{D_A}]}{h \times \sqrt{\pi}} \times \sqrt{t} \quad (\text{Eq. 32})$$

where

%M<sub>sat</sub>: the percent weight gain at saturation.

D<sub>A</sub>: the apparent diffusion constant.

h: the thickness of the sample.

The apparent diffusion constant D<sub>A</sub> may be determined from the slope of this linear region [122]:

$$D_A = \pi \left[ \frac{h^2}{16 \times (\%M_{sat})^2} \right] \times \left[ \frac{(\%M_2 - \%M_1)}{\sqrt{t_2} - \sqrt{t_1}} \right]^2 \quad (\text{Eq. 33})$$

where

%M<sub>1</sub> and %M<sub>2</sub>: plate percent weight gain at time t<sub>1</sub> and t<sub>2</sub>, respectively.

Since the apparent diffusion constant D<sub>A</sub> by Equation (33) is one-dimensional, it does not account for the diffusion taking place through the plate edges. Therefore the corrected diffusion constant D is given by Rao et al. [106, 123]

$$D = \frac{D_A}{\left[ 1 + \frac{h}{l} + \frac{h}{w} \right]} \quad (\text{Eq. 34})$$

where

h: the sample thickness

l: the sample length

w: the sample width

Usually water may act as a plasticizer when absorbed by the matrix and fibre, softening the materials and demaging some properties of the fibre reinforced composites. Moisture may also migrate along the fibre-matrix interface, affecting the adhesion. Moisture in composites reduces matrix-dominated properties, such as transverse strength, fracture toughness and impact resistance. Lowering of the glass transition temperature may also occur in epoxy resin with an increase in absorbed water. De-bonding can occur due to formation of discontinuous bubbles and cracking in the matrix [124].

The swelling of the jute fibre in the polypropylene composite was found by Karmaker et al. to have positive effects on the mechanical properties [22]. In contrast, the water absorption of the natural fibre/PP composites examined by Espert et al. showed a dramatical effect by the water uptake on the mechanical properties of the composites. Water saturated samples showed lower values of Young's modulus and stress at maximum load [125]. The modifications of the fibre have an influence on the moisture uptake behaviour. A moisture absorption of composites with silanized fibres reduced by about 10-20% compared to untreated fibres was observed by Gassan

et al. The fibre surface modification by epoxy functional  $\gamma$ -glycidoxypopyl trimethoxy - silane caused a reduction of moisture effects on the mechanical properties [42]. The moisture uptake behaviour of flax fiber reinforced polypropylene composites was investigated by Stamboulis et al. The use of maleic anhydride modified PP as a compatibiliser was observed to significantly decrease the diffusivity due to improved interfacial bonding [11]. The study by Yuan et al. confirmed that strong intermolecular fiber-matrix bonding decreases the rate of moisture absorption in bio-composites [126]. The influence of fibre surface treatments on the water absorption behavior of sisal/epoxy composites was characterized by Min et al. The acetylation of the sisal fibre significantly improved the water resistance due to increased hydrophobicity or the masking of surface cells. For continuous sisal/epoxy laminates with exposed fibre ends, the fibres control mainly the water absorption. With the chemical treatment of the fibre surface, the water resistance of the composites can be improved by blocking splits in the fibres. For discontinuous composites without intentionally exposed fibre ends, the interfacial adhesion governs the water absorption behaviour. It may be concluded that improving fibre/matrix interfacial adhesion can enhance the water resistance of the composites. The influence of water absorption on the mechanical properties of the composites was also investigated. The presence of water in the fibre resulted in a decreased tensile strength of the composites, but lead to increased Young's modulus and impact strength [107].

For jute/ polypropylene composite systems of our study, the samples with dimension of 80 x 80 x 2 mm were dried before exposition to the controlled environments. The relative humidities (RH) are 50% and 95%. The weight of the samples was measured at different time intervals at an accuracy of 1 mg until it reached the equilibrium state. From these values, the moisture diffusion constant was calculated following the equations in section 4.3.3.2 and compared to estimate the influences of the modifiers. The results are displayed in section 5.3.6.

Furthermore, the moisture-saturated samples were used for dynamic mechanical test in order to determine the influence of moisture to the dynamic mechanical properties, which have been rarely studied so far for natural composites. The results are displayed in 5.3.8.

On the other hand, the aging behaviour of jute reinforced epoxy composites was investigated by immersing in distilled water at room temperature. The dimension of the unidirectional composites sample is 40 × 10 × 2 mm. After immersion in water, samples were removed at different time, wiped with filter paper to remove surface water and weighed. The weight change was determined until the equilibrium values reached. From the obtained data, the water diffusion constant was calculated following the equations in section 4.3.3.2 and compared to estimate the influences of the modifiers. The results are displayed in section 5.4.4.



#### 4.3.4. Dynamic Mechanical Thermal Analysis

Dynamic mechanical analysis has been widely used for investigating the structures and viscoelastic behaviour of polymeric materials. It determines the relevant stiffness and damping characteristics for various applications. The dynamic behaviour includes also direct relevance to a range of unique polymer applications, concerned with the isolation of vibrations or dissipation of vibrational energy in engineering components. In polymer composite systems, the introduction of the fibre in a polymeric matrix leads to a reduction in mobility of the macromolecular chains in the vicinity of the fibre. Generally, that leads to the increase in the temperature of the main relaxation associated with the glass transition [127]. The dynamic properties are expressed in terms of storage modulus, loss modulus and damping factor which are dependent on temperature, time and frequency.

The dynamic mechanical behaviour of short jute fibre reinforced polypropylene composites was studied by Rana et al. The storage modulus was observed to increase with increase of fibre content and further increase with addition of the compatibilizer Epolen G-3002. The  $\tan \delta$  peak was shifted to higher temperature as the amount of fibre loading increased [128]. Similarly, the influence of fibre surface treatment by MAHgPP on the dynamic mechanical properties of jute reinforced polypropylene was investigated by Gassan and Bledzki. It was shown that maleic anhydride polypropylene co-polymer increases the level of adhesion between polypropylene and jute fibre [129]. A marginal improvement in storage modulus was observed for chemically treated fibre composites, including polymethylene polyphenyl isocyanate (PMPPIC), toluene diisocyanate/ polypropylene glycol (TDI-PPG) and  $\text{KMnO}_4$ , which is due to the increase in interfacial stiffness achieved through more intense fibre-matrix interaction, i.e. there exists a better interfacial adhesion between fibre and the PP matrix. The maximum improvement was observed in the case of maleic anhydride modified sisal/PP composites. Both storage and loss modulus was seen to decrease with increasing temperature. Dynamic modulus was found to increase with increasing frequency [127]. Investigation of dynamic mechanical behaviour of vinylester resin matrix composites reinforced with untreated and alkali treated jute fibres was carried out by Ray et al. The storage modulus was observed to increase with increasing fibre loading in the composites and decrease with increasing in the temperature. The loss modulus values corresponding to the  $T_g$  were found to increase considerably in the composites compared to the resin. With the increase in the fibre loading, when treated, the second peak, which is at a temperature higher than the  $T_g$ , shifted to a higher temperature and the corresponding loss modulus value also increased. The second peak, however, shifted to a lower temperature for the

composites with the treated fibres. The damping parameter ( $\tan \delta$ ) was observed to reduce drastically on incorporation of the untreated fibre in the composites. However, an increasing trend of the  $\tan \delta$  value of both the transition peaks was seen in the case of the alkali treated fibre composites with 35 vol. % fibre loading [31]. The effects of alkali treated kenaf and hemp fibres on the dynamic mechanical properties of the cashew nut shell liquid matrix composites were carried out by Sharifah et al. The composites based on fibres treated by 6% NaOH solution were found to have higher storage moduli and lower  $\tan \delta$ , corresponding to the trends of higher flexural modulus and lower work of fracture, respectively [130].

The investigation of the dynamic mechanical behaviour of polypropylene as well as epoxy composites in this work is used to estimate the effect of fibre loading, matrix and fibre treatments as a function of temperature. The short fibre reinforced polypropylene and unidirectional jute-epoxy composite specimens used for this test have the dimensions of 10 x 40 x 2mm. The test was done by using a two-point bending system DMA 2980, TA Instruments at a frequency of 1 Hz. The samples were cooled to  $-50^{\circ}\text{C}$ , then heated to  $180^{\circ}\text{C}$  at a heating rate of 2 K/min in a nitrogen atmosphere. The dynamic storage modulus ( $E'$ ), loss modulus ( $E''$ ) and loss factor ( $\tan \delta$ ) of the specimens were determined as a function of temperature. The discussions of the obtained results are presented in section 5.3.5 and section 5.4.3.

## 5. Results and discussion

### 5.1. Jute fibres

#### 5.1.1. Fibre mechanical properties

The tensile strength was determined for the jute fibre of different lengths, as mentioned in detail in section 4.1.1. As expected, the tensile strength of natural fibres in the fibre direction depends on the gauge length and exhibits considerable scatter (Table 10), due to the statistical distribution of flaws such as pits and nodes [131] and not uniform cross-section of fibre. Nevertheless, the specific tensile strength (strength/density) of jute fibre is similar to that of glass fibres ( $\sim 580 \text{ MPa/g cm}^{-3}$ ) and highlights the application for lightweight composites.

Table 10. Tensile strength of jute fibres (J1)

Gauge length (mm)	Tensile strength $\pm$ s.d.* (MPa)	Specific tensile strength (MPa/g cm <sup>-3</sup> )	Weibull distribution parameters	
			Weibull-modulus, m	Characteristic strength, $\sigma_0$ (MPa)
5	770 $\pm$ 243	550	2.9	743
10	629 $\pm$ 228	449	2.6	611
15	610 $\pm$ 198	436	3.3	601
20	582 $\pm$ 223	416	2.8	577

\*s.d.: standard deviation

As shown in the Weibull plots of Fig. 27 and Table 10, the fibre tensile strength tends to decrease with increasing gauge length from 5mm to 20mm. This result is as expected, since the probability of critical defects causing fracture increases with increasing length. The single fibre used for the test is the technical fibre, which is composed of shorter elementary fibres as seen in Fig. 28. They are bonded together by the relatively weak pectin. With the larger gauge length, therefore, the possibility of the failure taking place at the interface is higher and at lower stress.

The Weibull modulus calculated using the strength distribution (Fig. 27) for four gauge lengths is in the range of 2.6 to 3.3. On the other hand, the Weibull modulus can also be determined from the fibre length dependence of fibre mean strength (Fig. 29), however, it is about 5. This is substantially higher than the Weibull modulus measured from the distribution of tensile strength. The effect of fibre cross-section area variability on the measured Weibull modulus is not commonly studied. Generally speaking, a fibre with larger cross-section area should have greater chance to have a bigger flaw, therefore, it is expected to be weaker than that with a smaller

cross-section area. For natural fibres, there is a distribution of individual fibre cross-section area, shape within a roving as well as within a single fibre, so that the tested volume will vary even at a fixed gauge length. Thus, the measured strength distribution will be created by the overlap of the distribution of strength due to the volumetric distribution of flaws and due to the variable fibre volume. Because of this effect, the natural distribution of fibre strength will be artificially broadened, reducing the measured Weibull modulus from the distribution of tensile strength.

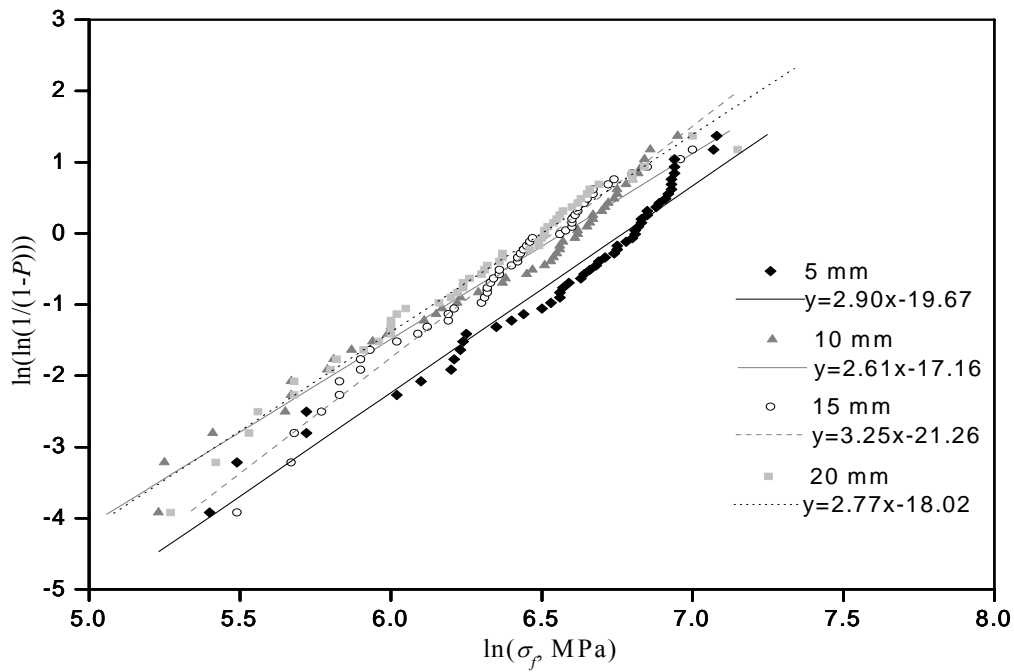


Fig. 27. Weibull plot of fracture probability as a function of jute fibre tensile strength for different gauge lengths

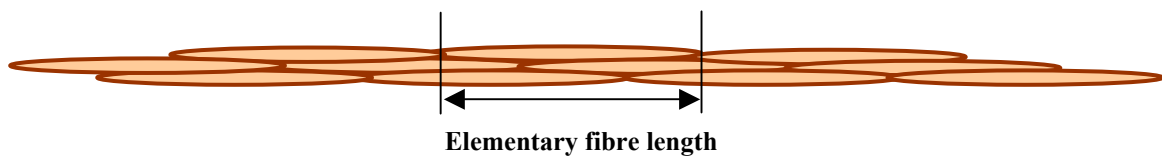


Fig. 28. Schematic of a technical fibre

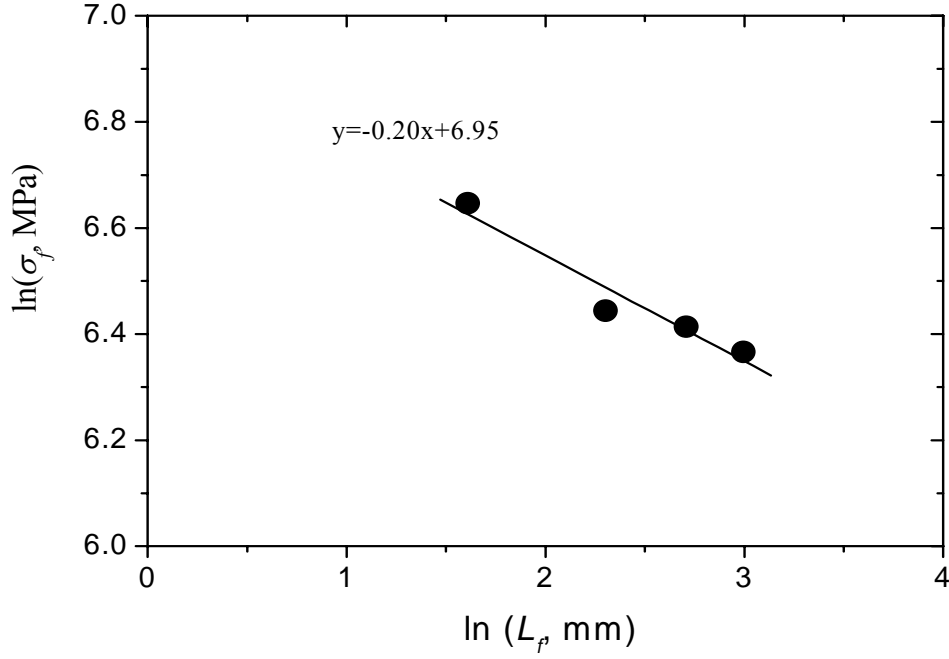


Fig. 29. Variations of jute fibre tensile strength as a function of gauge length

Notably, the measured tensile strength actually increased with jute fibre cross-sectional area at a constant fibre length despite the scatter (Fig. 30). This is inconsistent with the general statistic failure behaviour for brittle materials, where the strength tends to decrease with increasing volume because of an increase of the probability of critical defects. This finding suggests that the intrinsic tensile properties of jute fibre is proportional to fibre cross-sectional area associated with its more perfect circle shape and regular form of the cross sections [132]. It is reported that jute fibre has a cellulose content of more than 60 % and a microfibril angle in the range of 7-12 ° to the fibre axis [131]. These structure characters are strongly maturity dependent and in turn, affect significantly the overall mechanical properties of natural fibres. However, the Weibull theory assumes a random distribution of flaws within the volume of the samples with same properties. Thus, it is clear that the tensile strength of the natural fibre has been grossly oversimplified in the previous commonly used Weibull model.

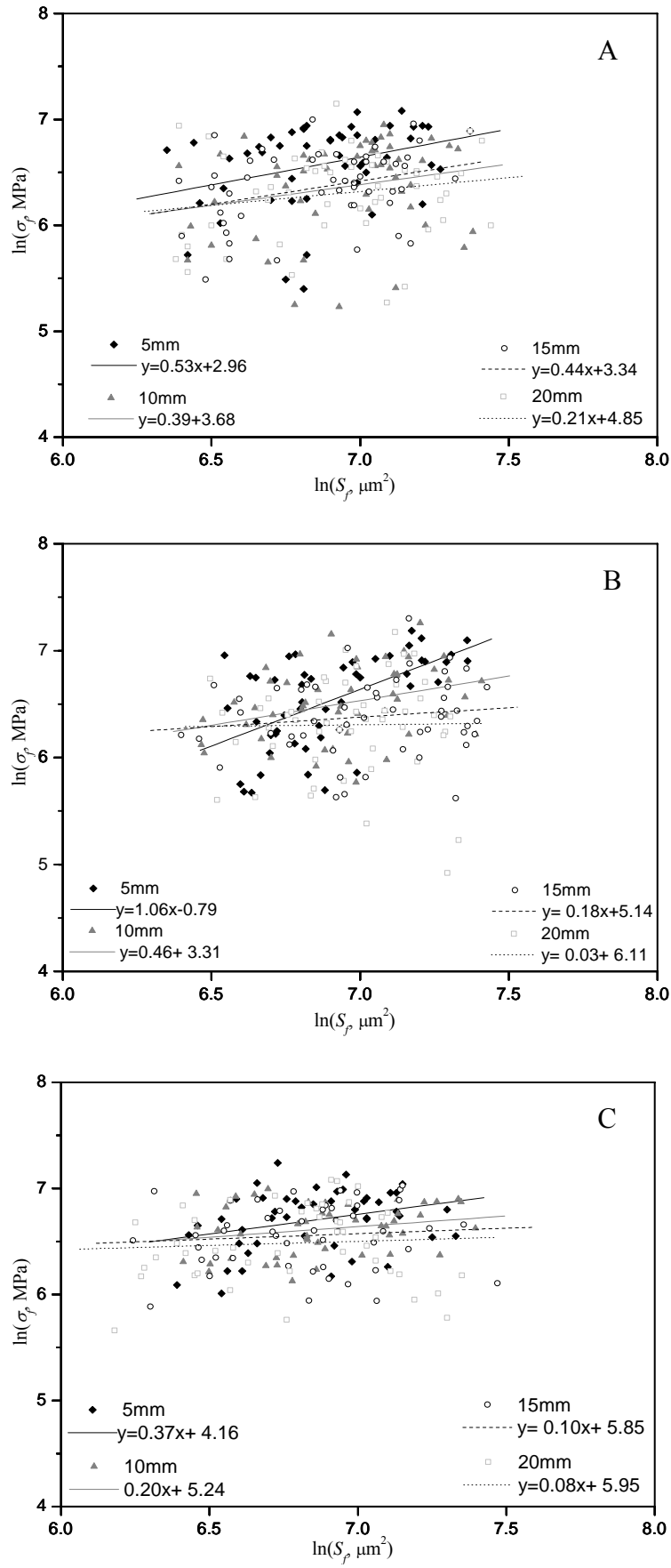


Fig. 30. Variations of jute fibre tensile strength as a function of fibre cross-section area of (A) J1, (B) J2 and (C) J3

## 5.1.2. Mechanical properties of treated fibre

### 5.1.2.1. Alkaline treatment

The de-waxed jute fibres were treated by NaOH 1wt% and 5wt% for various periods of time and at room temperature. Weight loss of jute fibre at different conditions of alkaline treatment was displayed in Fig. 31. The weight loss of the fibre increased by the increase of time of treatment at the same NaOH concentration. The weight loss of the fibre in NaOH 5% is higher than that in NaOH 1% at the same period. It can be expected that the reaction between the NaOH and hemicellulose, which is thought to consist principally of xylan, polyuronide and hexosan and to be very sensitive to the action of NaOH [14], increased with increasing alkali concentration. At the alkali concentration of 1 %, the weight loss was observed to increase gradually. However, in NaOH concentration of 5%, the fibre weight decreased very fast during the first 30 minutes, then slightly decreased with increasing time. To get the optimal condition of alkali treatment of the fibre, the properties of the fibre and the composite based on the jute fibre treated by NaOH 1% for 4h and NaOH 5 % for 10 minutes and 12 hours with a weight loss of 5.93, 7.32 and 9.75 %, respectively, were investigated.

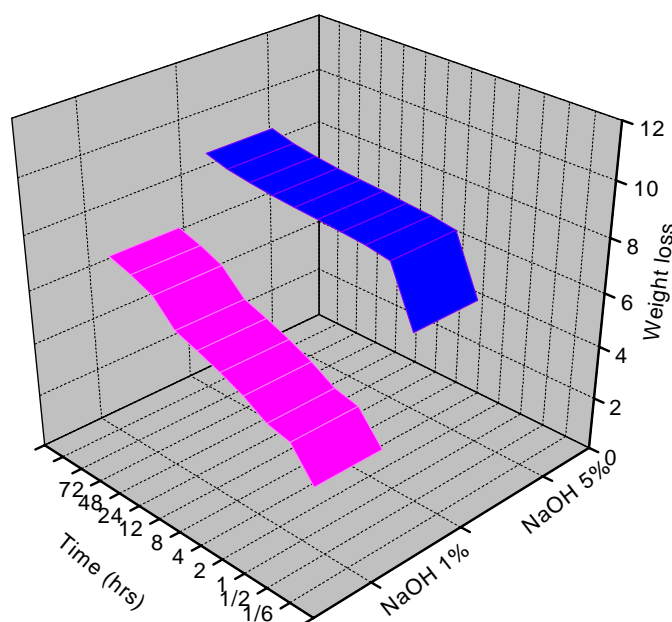


Fig. 31. Weight loss (%) of jute fibre at different conditions of alkali treatment

Although the main composition of jute fibre is cellulose, the non-cellulosic components called cementing such as lignin and hemicellulose also play an important part in determining the characteristic properties of the fibres. The removals of hemicellulose and lignin by alkali-treatment aimed improving some properties of the fibre as well as composites. Fig. 32 shows

fibre tensile strength calculated by Weibull statistics as mentioned in section 4.1 for differently alkali treated J3 fibres.

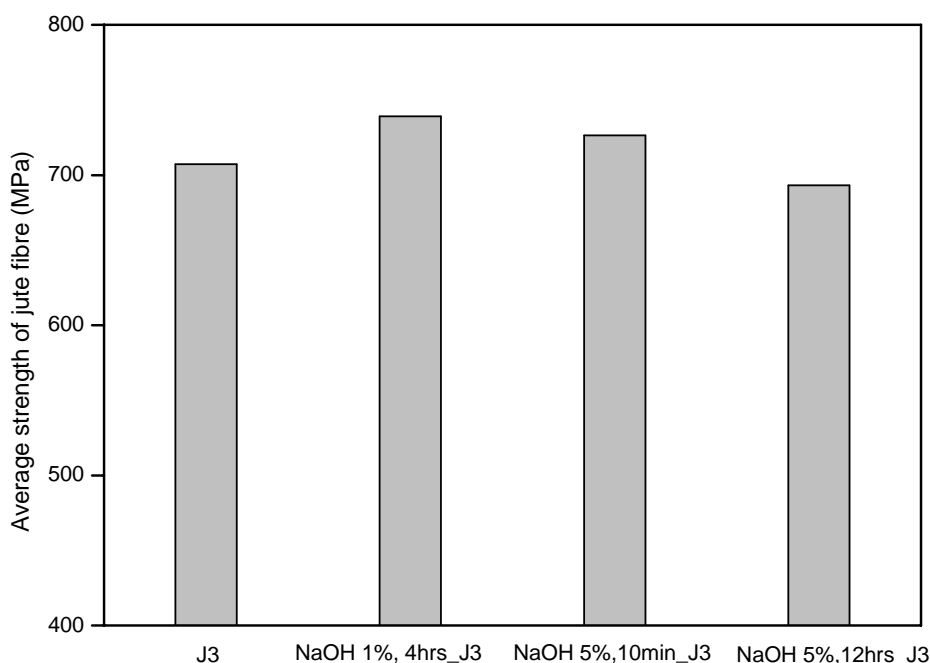


Fig. 32. Fibre tensile strength calculated by Weibull statistics for differently alkali treated J3 fibres.

It was found that a mild NaOH treatment (NaOH 1%, 4hours) improves the strength of the fibre. It can be expected that due to alkaline treatment, hemicellulose and lignin are removed, the inter-fibrillar region is likely to be less dense and less rigid, that makes the fibrils more able to rearrange themselves along the direction of tensile loading. When jute fibres are stretched, such arrangements among the fibrils would result in better load sharing and hence in higher stress development in the fibre [14]. However, at more extreme conditions (NaOH 5%, 12 hours), the NaOH treatment hardly caused further increasing in tensile strength of the fibre but some damages of the fibre happen caused by the attack of NaOH on the cellulose. Consequently, NaOH 1%, 4 hours were assumed the optimal condition of alkali treatment for the fibre tensile strength.

#### 5.1.2.2. Silane treatment

The jute fibres were pre-treated by NaOH 1% for 4 hours and then treated by silane coupling agent (Y9669) or a mixture of silane and epoxy dispersion (APS+XB). As shown in Fig. 33, the treated fibres have a very small difference in fibre tensile strength calculated by Weibull statistic



compared to untreated fibre. It can be confirmed that the sizings have an insignificant effect on the strength of the fibre.

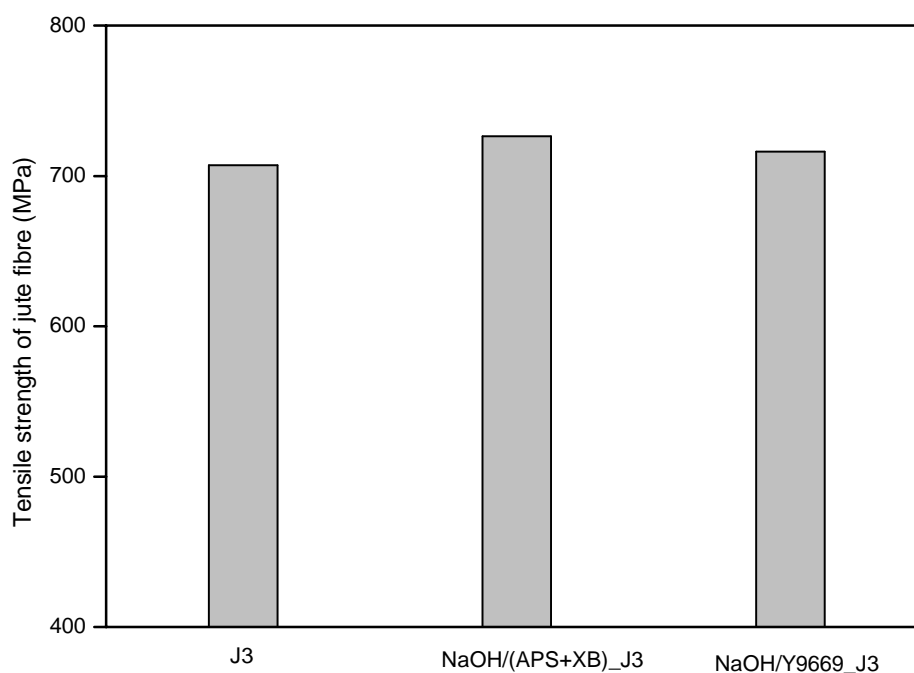


Fig. 33. Influences of difference fibre treatments on fibre tensile strength calculated by Weibull statistics

### 5.1.3. Wetting of the fibres

A typical curve from dynamic contact angle measurement of jute fibre by the Wilhelmy technique is given in Fig. 34. The irregular shaped graph of the tensiogram due to hysteresis indicates that the wetting force of the liquids in both advancing and receding phases varies randomly from one position to another on the fibre surface. That can be assumed due to high roughness and chemical contamination as well as heterogeneity of the jute fibre surface. The contact angles shown in Table 11 present the effects of the fibre surface treatments. The alkaline treatment significantly decreases the contact angle of jute fibre with the polar liquid like water. However, the fibre surface treatments by combinations of alkaline treatment and silane coupling agent (Y9669) or mixture of silane and epoxy dispersion (APS + XB) increase the contact angle of the fibre with water and decrease that in the case of toluene. It is caused by higher hydrophobicity of the fibre surface after these treatments.

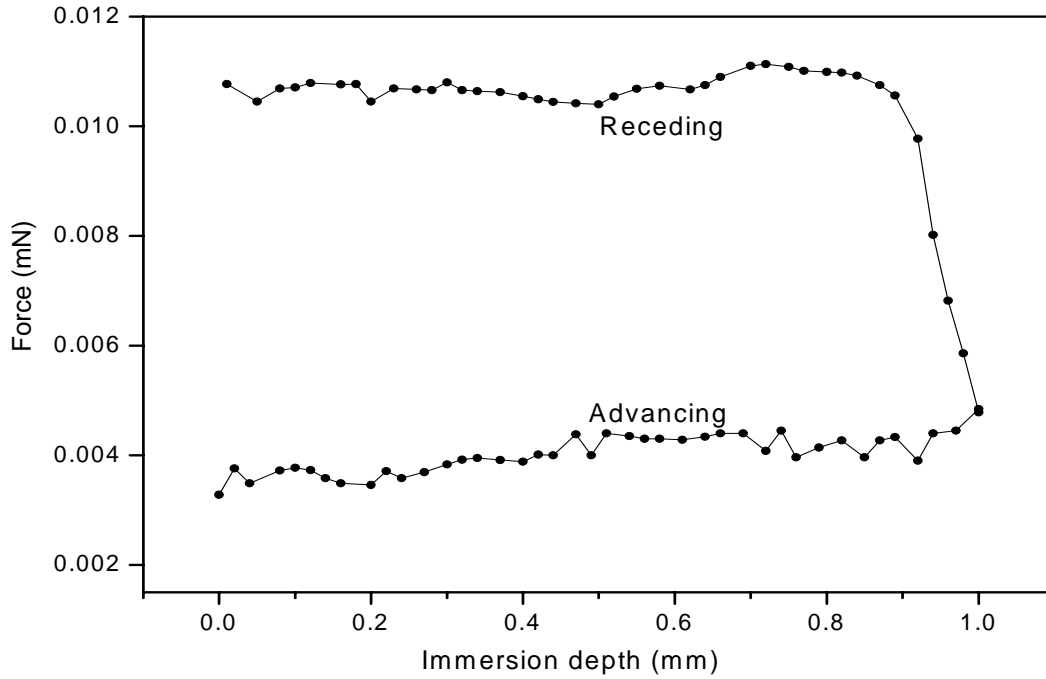


Fig. 34. Force vs. immersion depth for jute fibre (J3) in water

Table 11. Advancing contact angle of untreated and treated jute fibre (J3)

Liquids	Untreated-J3	NaOH_J3	NaOH/(APS+XB)_J3	NaOH/Y9669_J3
Toluene	$28.4 \pm 4.2$	$27.9 \pm 6.3$	$14.1 \pm 4.1$	$11.5 \pm 3.4$
$\alpha$ -bromonaphthalene	$49.5 \pm 3.1$	$48.6 \pm 5.9$	$29.6 \pm 3.9$	$32.9 \pm 4.2$
1,5-pentadiol	$43.1 \pm 3.7$	$42.3 \pm 7.1$	$39.7 \pm 3.7$	$40.6 \pm 2.6$
Water	$66.5 \pm 4.9$	$49.5 \pm 5.8$	$73.8 \pm 4.5$	$72.6 \pm 3.9$

From the cosine of the advancing contact angle and plotting  $(W_a / 2 * (\gamma_{lv}^d)^{1/2})$  versus  $(\sqrt{\gamma_{lv}^p} / \sqrt{\gamma_{lv}^d})$  using the equations in section 4.1.2, in Fig. 35, the dispersive and polar parts of the fibre surface energy were determined.

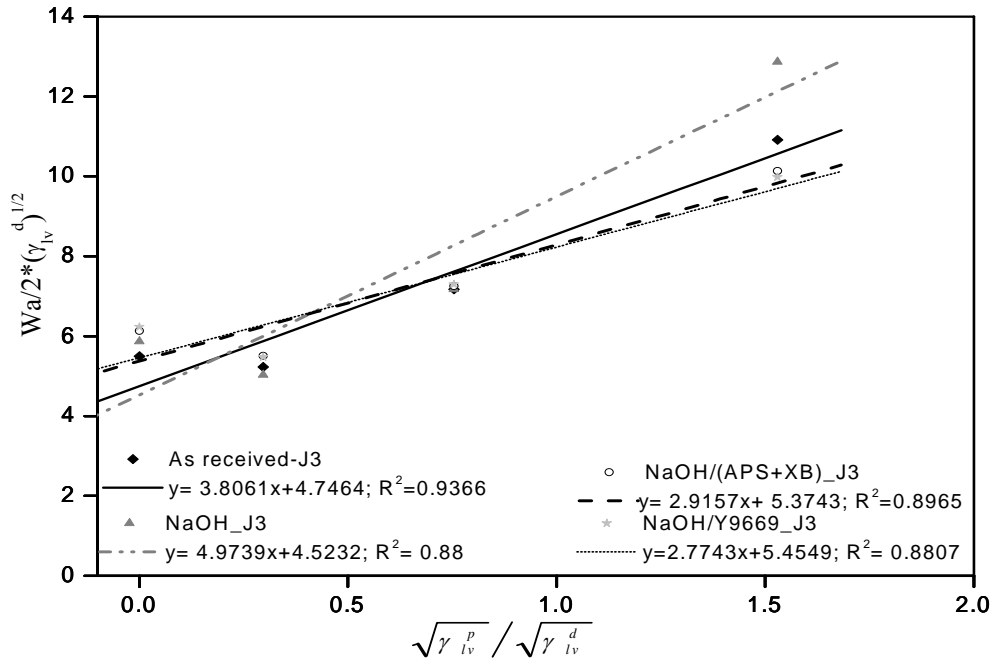


Fig. 35. Diagram to estimate the fibre surface energy

These components were obtained from the best linear fit of the plots and are displayed in Fig. 36. It is clear that the alkali treated jute fibre has the highest surface free energy value, 45.2 mJ/m<sup>2</sup>. This is higher than the surface free energy of the untreated jute fibre, 37.0 mJ/m<sup>2</sup>. It can be seen in both increases of polar and non-polar components by alkaline treatment. It is possible that the treatment by dewaxing and then NaOH can also partially remove the impurities covering fibre surface such as waxes, fats, lignin, pectin and hemicellulose, reveal the fibrils and give a clean and rough surface topography to the fibre and also increase the voids or the gaps between crystalline cellulose [133, 134, 35]. That can be a reason for the increase of both components of the surface free energy. It is believed that a good wetting of the fibre by liquid matrix polymer is very important to establish a good interfacial adhesion. If the surface tension of reinforcing fibres greatly exceeds that of liquid matrix, they are likely to spread easily. Therefore, the increase of fibre surface free energy after alkaline treatment is also a reason for good sorption of the epoxy resin on the jute fibre surface in composite processing. That improves the fibre surface wet-out and mechanical interlocking with resin [133, 135].

The treatments of the fibre by NaOH/(APS+XB) and NaOH/Y9669 shown in Fig. 36 do not change fibre surface energy compared to untreated fibre. However, the dispersive component of NaOH/(APS+XB) treated fibre (28.9 mJ/m<sup>2</sup>) and NaOH/Y9669 treated fibre (29.8 mJ/m<sup>2</sup>) increases compared to that of untreated fibre (22.5 mJ/m<sup>2</sup>). These increases can cause the wetting improvement of the low polar epoxy resin on the fibre surface. On the other hand, the chemical

similarity between the polymer matrix and the sizing also can be a reason for a good wetting of resin on the fibre surface in the composites.

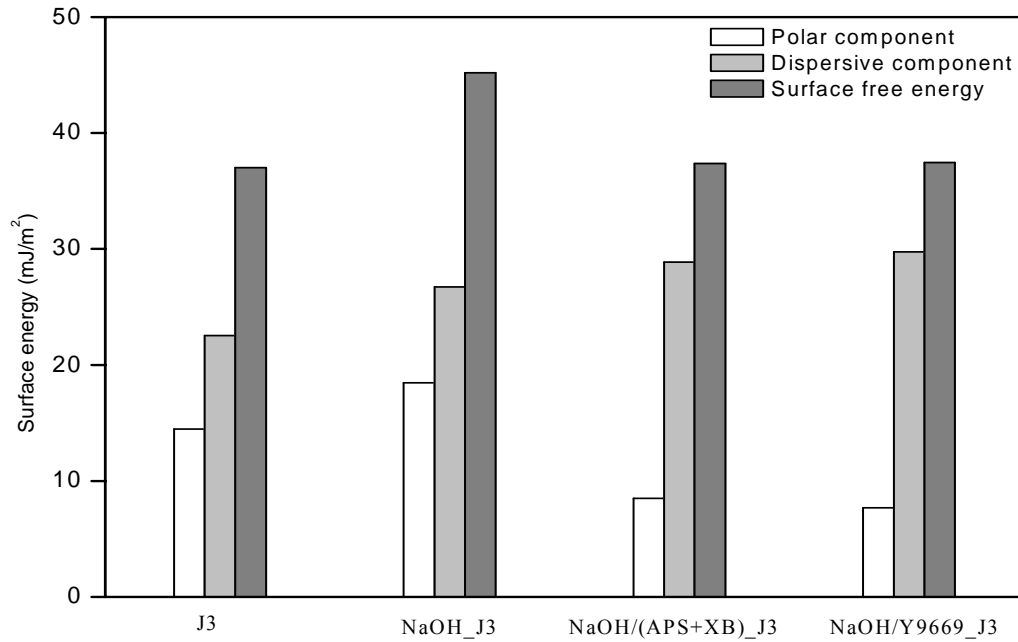


Fig. 36. Surface free energy, polar and dispersive components of untreated and treated fibre

#### 5.1.4. Moisture absorption

Since moisture absorption of fibres plays a very important role in the reinforcement, the hydrophilic character of jute fibre was investigated. With the moisture absorption, the jute fibres swell laterally, and presumably the water molecules intervene between the chains constituting the fibre so that the secondary valence forces are weakened, thus facilitating the slippage of the chain. That leads to changes in the physical properties of the fibre as well as the composites [136]. It has been shown that moisture absorption of a fibre bundle takes place in three stages: during the first stage there is diffusion through the air from the water vapour to the fibre surface, the second stage involves diffusion through the air in the spaces between fibres from the surface of the bundle to the surface of a single fibre and the third stage involves diffusion from the surface of a fibre to its interior [12]. Thus, the time needed for the water absorption and diffusion coefficient for the fibre specimen is difficult to determine exactly by Fick's law. Fig. 37 shows the moisture absorption content,  $M$ , of jute yarn as a function of time at two different relative humidities (RH). Here, we fit the experimental data with the following equation:

$$M = M_{sat} \frac{(Kt)^\alpha}{1 + (Kt)^\alpha} \quad (\text{Eq. 35})$$

where  $M_{sat}$  is the saturated moisture absorption content. Parameters  $K$ ,  $\alpha$ , and  $t$  are the rate constant, index factor, and exposure time, respectively. It can be observed that both the saturation moisture content and adsorption speed of jute fibres increases with increasing relative humidity. Specifically, the saturated moisture absorption value of jute (J1) at 95% RH is 21.5 wt%, whereas at 50% RH it levels up at 10.1 wt %.

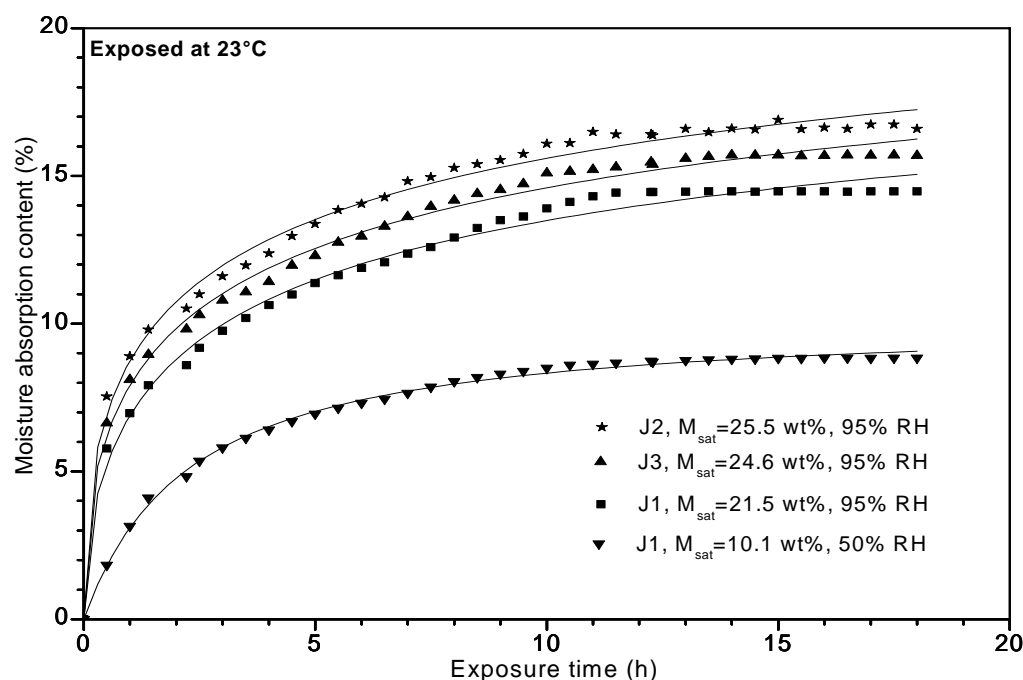


Fig. 37. Moisture absorption of jute fibres as a function of exposure time at 95% and 50% of relative humidity

Jute fibre from different sources have different moisture absorption behaviour depending on chemical compositions and the treatments following harvesting. It was clearly observed that J2 has the highest saturated moisture content ( $M_{sat}$  = 25.5 wt%), then J3 with  $M_{sat}$  = 24.6 wt% and J1 has lowest value ( $M_{sat}$  = 21.5 wt%) at the same relative humidity (95%). According to the data, the moisture absorption of jute fibres is very fast during the first two hours, which should be associated with the first and second stages of water diffusion. The presence of many hydroxyl groups on the molecular structure makes jute fibres hydrophilic. It is expected that the NaOH treatment of the jute fibre (J3) increase moisture absorption, while the silane modifications of NaOH pre-treated fibre decrease hydrophilic properties (Fig. 38). A high moisture absorption may cause application issues and requires further research work. For application, a low absorption is ideal, this may be reached either by fibre surface modification or improved interfaces.

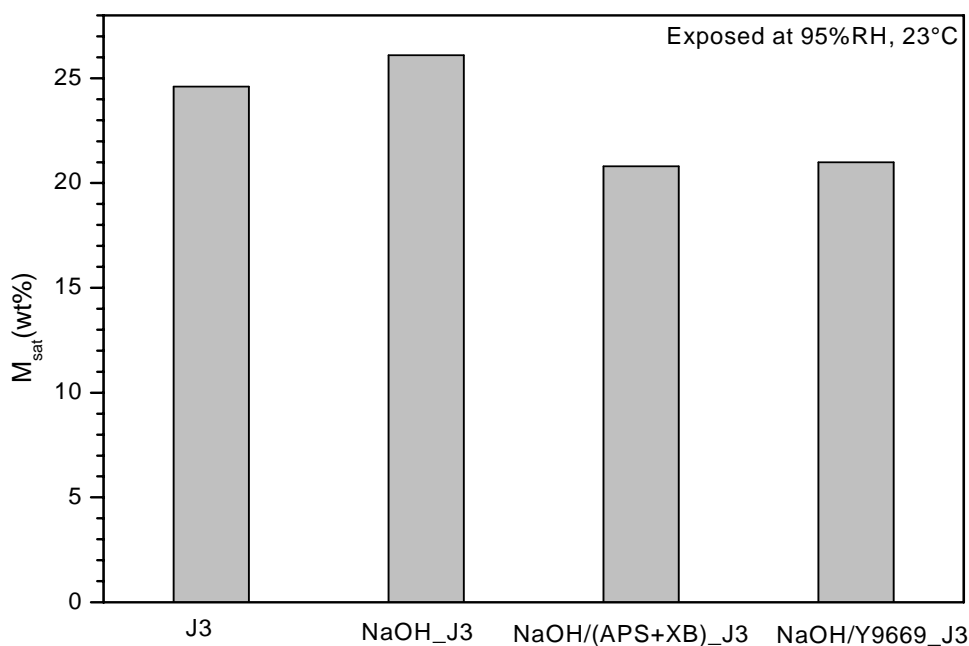


Fig. 38. Saturated moisture content values of untreated and treated fibres

### 5.1.5. Thermal behaviour

For the manufacturing of composites, the thermal stability of the fibre is very important. Some fibre treatments can influence its thermal stability as evidenced from TGA analysis (Fig. 39).

The thermal analysis of jute fibre (J3) with and without treatments was performed in nitrogen atmosphere. DTG curves show the main three-stages process of untreated jute fibre corresponding to three peaks. The first very small peak  $<100^{\circ}\text{C}$  corresponds to the heat of vaporisation of water absorbed in the fibre. The second peak at about  $286.8^{\circ}\text{C}$  is due to the thermal degradation of hemicellulose and the glycosidic linkages of cellulose and the very strong third peak at about  $352.7^{\circ}\text{C}$  indicates the degradation of cellulose, leading the formation of char. It is clearly seen that the second peak disappears in the DTG curves of treated fibre, due to considerable removal of hemicellulose during alkaline treatment. On the other hand, the TG curves of the treated fibres shifted to slightly higher temperature show the slightly higher thermal stability of treated fibre. The residual char left at  $600^{\circ}\text{C}$  increased considerably from 5% to 12-25% in the cases of treated fibres. It was proposed that besides removing hemicellulose, NaOH treatment can give rise to a lignin-cellulose complex, therefore the NaOH treated fibre becomes more stable and this was reflected in the increased amount of residual char [32]. An increase in thermal resistance and residual char formation in the cases of NaOH/(APS+XB) and

NaOH/Y9669 treatments may be caused by the reactions between the active groups in sizings and hydroxyl groups of the fibres.

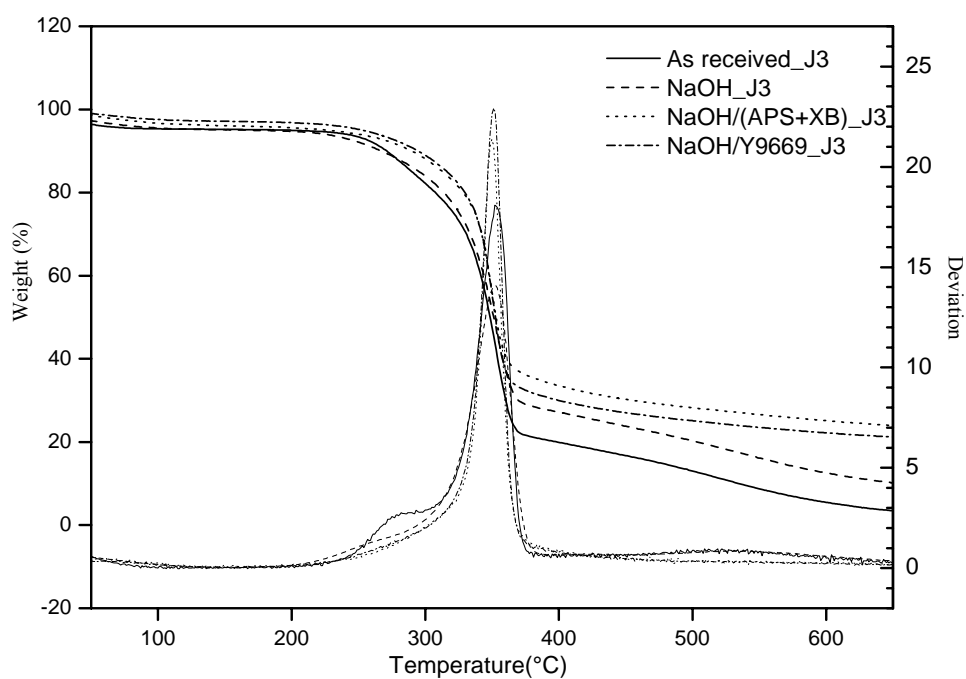


Fig. 39. TG and DTG curves of treated and untreated jute fibre (J3)

## 5.2. Micro-composites

### 5.2.1. Micro-mechanical behaviour

#### 5.2.1.1. Untreated jute fibre composites

Two composite systems with polypropylene and epoxy matrix were tested using the single fibre pull-out test. Fig. 40 presents typical force-displacement curves. Results in Table 12 show lower apparent interfacial shear strength ( $\tau_{app}$ ) and post-debonding friction ( $\tau_f$ ) of polypropylene matrix systems compared to epoxy matrix system. That can be explained due to the lack of reactive group in the non-polar polymer chain of polypropylene, the adhesion between the fibre and the polymer is poor. In the case of epoxy matrix, the chemical reactions at the interface play a very important role in interfacial adhesion [58]. Specifically, epoxy ring opening at the interface and form covalent bonds with the fibre. The acid-base interactions as hydrogen bonds between the cured epoxy network and the fibre surface was noted in the adhesion phenomenon [137]. Therefore, the apparent interfacial shear strength of the jute fibre reinforced epoxy systems was found to be higher than that of polypropylene systems. It can be attributed to the lack of reactive group in the non-polar polymer chain of polypropylene. Interestingly, the treatments of matrix in PP system and of fibre in epoxy matrix show the increasing of both apparent interfacial shear strength and post-debonding friction (Table 12).

#### 5.2.1.2. Treated matrix composites

For polypropylene matrix treatment, the MAHgPP coupling agent (Ex) used is able to act as a compatibiliser for polar natural fibre and non-polar polymer matrices. The strong interfacial adhesion between the fibre and exxelor treated PP matrices can be seen in (Fig. 41). Moreover, the improvement of the interfacial adhesion of PP matrix system by using coupling agent (2 wt% Ex) is strongly influenced by the properties of PP. Using 2 wt% Ex as a coupling agent, improves the adhesion strength to a greater extent in higher molecular weight PP1 with lower melt flow rates than lower molecular weight PP2. The apparent interfacial shear strength increases by 91% for PP1 and by 68% for PP2. This is supposed to be due to creation of stronger interfaces in higher molecular weight polypropylene by interdiffusion of chains.



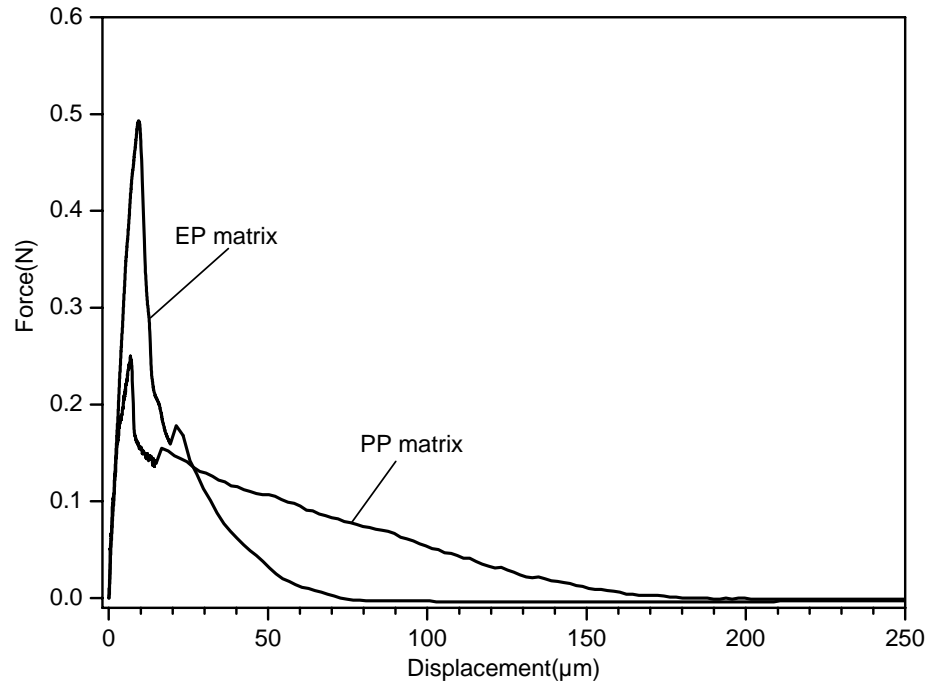


Fig. 40. Typical force-displacement curves for pull-out test of PP and EP matrix composites

Table 12. Effect of matrix and fibre treatments on apparent interfacial shear strength and frictional strength.

Fibre	Matrix	$\tau_{app}$ (MPa)	$\tau_f$ MPa)
J1	PP1	$10.33 \pm 3.03$	$5.36 \pm 1.52$
J1	PP1 + 2% Ex	$19.77 \pm 5.61$	$9.83 \pm 3.2$
J1	PP2	$9.71 \pm 1.55$	$6.95 \pm 0.99$
J1	PP2 + 2% Ex	$16.31 \pm 5.01$	$9.7 \pm 3.19$
J3	EP2	$42.74 \pm 8.47$	$13.8 \pm 4.67$
NaOH_J3	EP2	$59.58 \pm 12.29$	$16.27 \pm 2.51$
NaOH/(APS+XB)_J3	EP2	$63.95 \pm 13.77$	$14.64 \pm 6.32$
NaOH/Y9669_J3	EP2	$62.85 \pm 10.07$	$17.71 \pm 5.63$

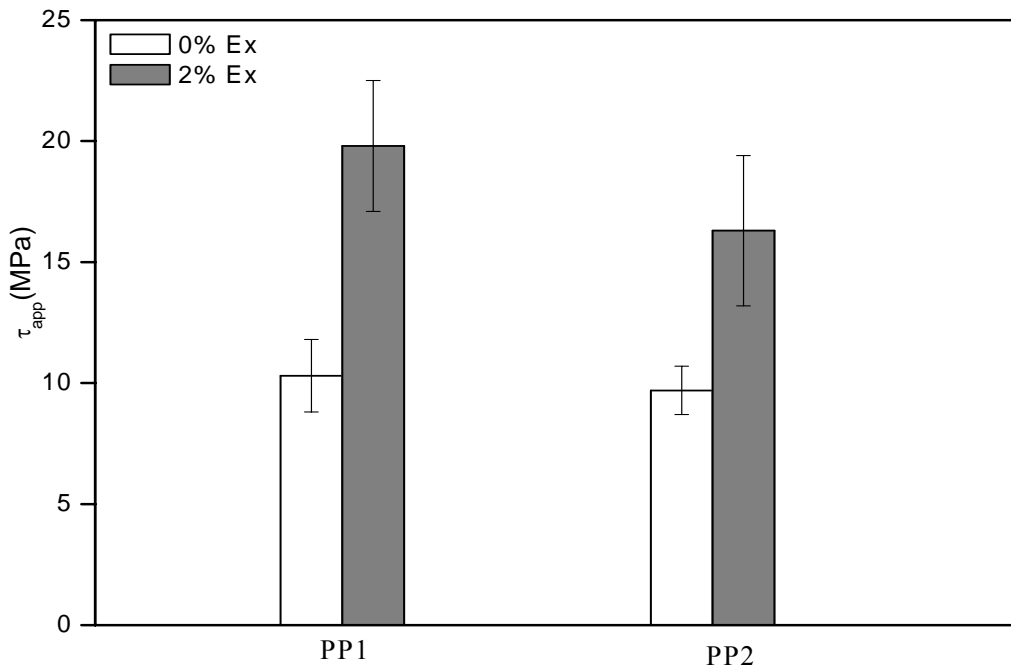


Fig. 41. Apparent interfacial shear strength in jute/PP systems

#### 5.2.1.3. Treated fibre composites

The fibre surface treatments improve significantly the interfacial strength in epoxy composite system (Table 12, Fig. 42). Alkaline treatment of the fibre increases the local interfacial bond strength of the epoxy composite from  $42.74 \pm 8.47$  MPa to  $59.58 \pm 12.29$  MPa. The stronger interaction between NaOH treated fibre and EP matrices can be caused by removing the cementing during dewaxing and alkali treatment, making a cleaner and rougher fibre surface (section 5.2.2.2), which enhances the mechanical interlocking with the matrix. Moreover, wettability of the resin on the NaOH treated fibre surface increased (as mentioned in section 3.4.2.2) is also a reason for stronger interfacial adhesion.

The obtained values in Table 12 also show the more enhancement of the adhesion strength while combining some different fibre surface treatments, including alkaline treatment (NaOH 1%, 4 hours) and coupling agent 3-Phenylaminopropyl-trimethoxy-silan (1%, 1hour) or sizing including 3-Aminopropyl-triethoxysilane (1%) and Epoxy dispersion XB 3791 (1.5%) for 1 hour. The apparent interfacial shear strength of the epoxy composite based on NaOH/(APS+XB)\_treated and NaOH/Y9669\_treated fibres were increased to 62.85 and 63.95 MPa from 42.74 MPa, respectively. It is assumed that NaOH treated jute fibre exhibited micro-pores on the fibre surface, the coupling agent as well as sizing penetrated into the pores and formed a mechanically interlocked coating on the fibre surfaces. Moreover, the fibre surface

treatments caused better wettability, and in turn, a strong fibre-matrix interface bond as mentioned in section 3.4.2.2.

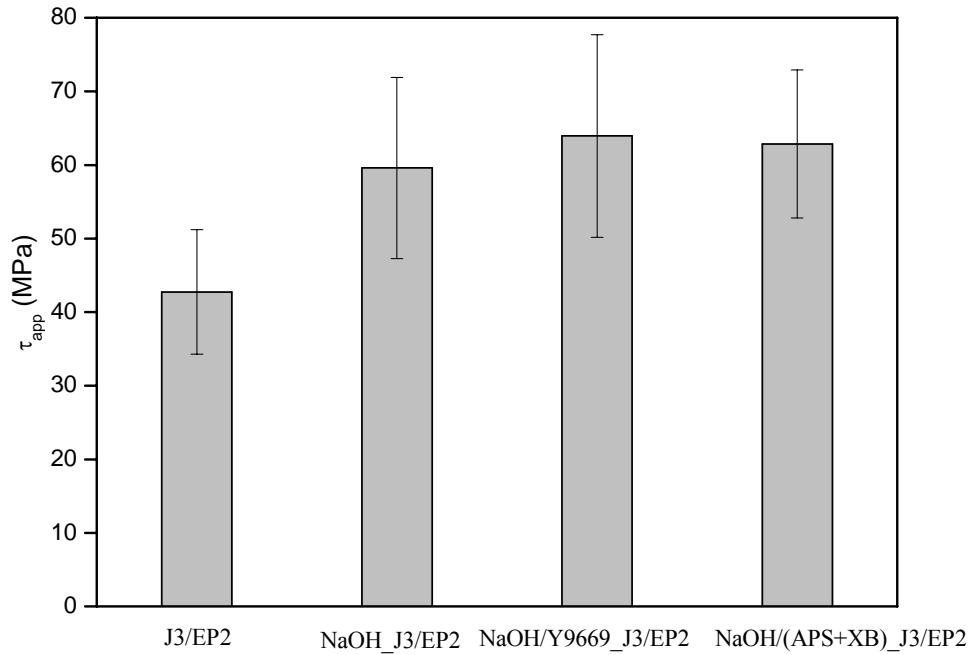


Fig. 42. Apparent interfacial shear strength in jute/epoxy systems

It is said that interfacial bond strength is strongly affected by specimen geometry and embedded length [138]. The relation between the apparent interfacial shear strength and fibre diameter as well as embedded length of jute fibre reinforced polypropylene and epoxy matrix systems with and without treatment are shown in figures from Fig. 43 to Fig. 47. It is observed that with increases of fibre diameter and embedded length,  $\tau_{app}$  of both matrix systems decreases. The high scatters of  $\tau_d$  values vs. fibre diameter and embedded length of both matrix systems implied the inhomogeneities of the jute fibre such as: geometry, varied fibre diameter, fibre surface structure, the bonding of sizing on the fibre surface and the straightness of the fibre ends [139].

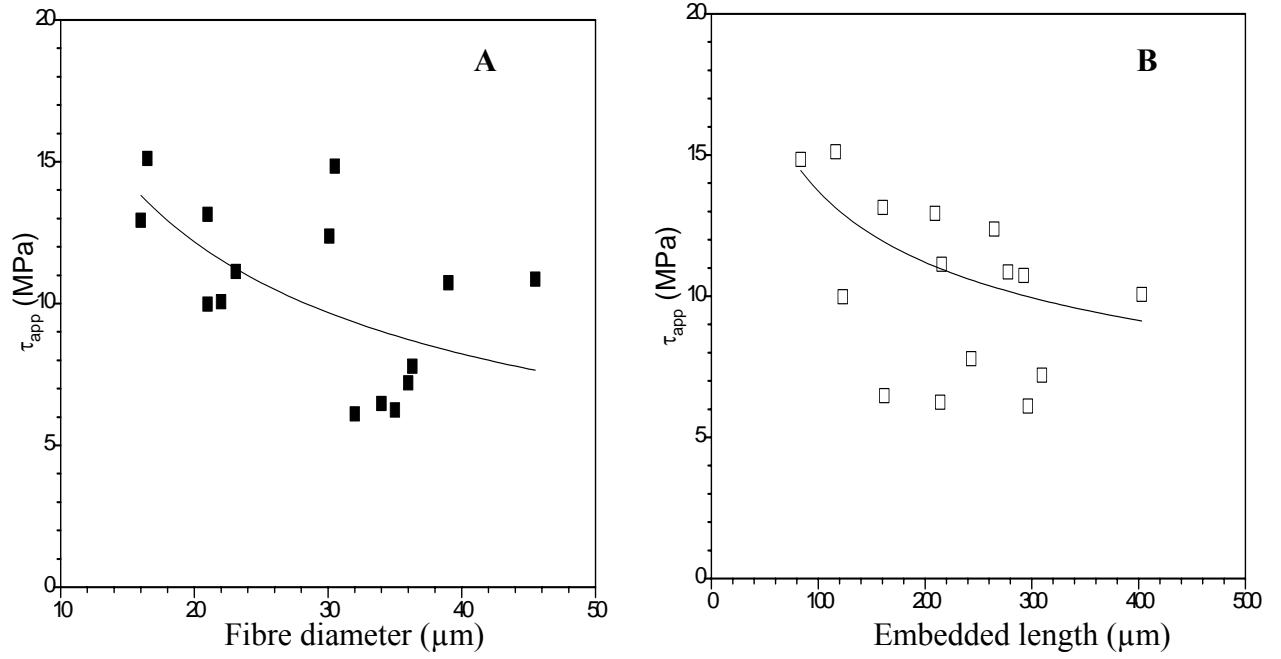


Fig. 43. Apparent IFSS as a function of (A) fibre diameter and (B) embedded length of J1/PP1 system

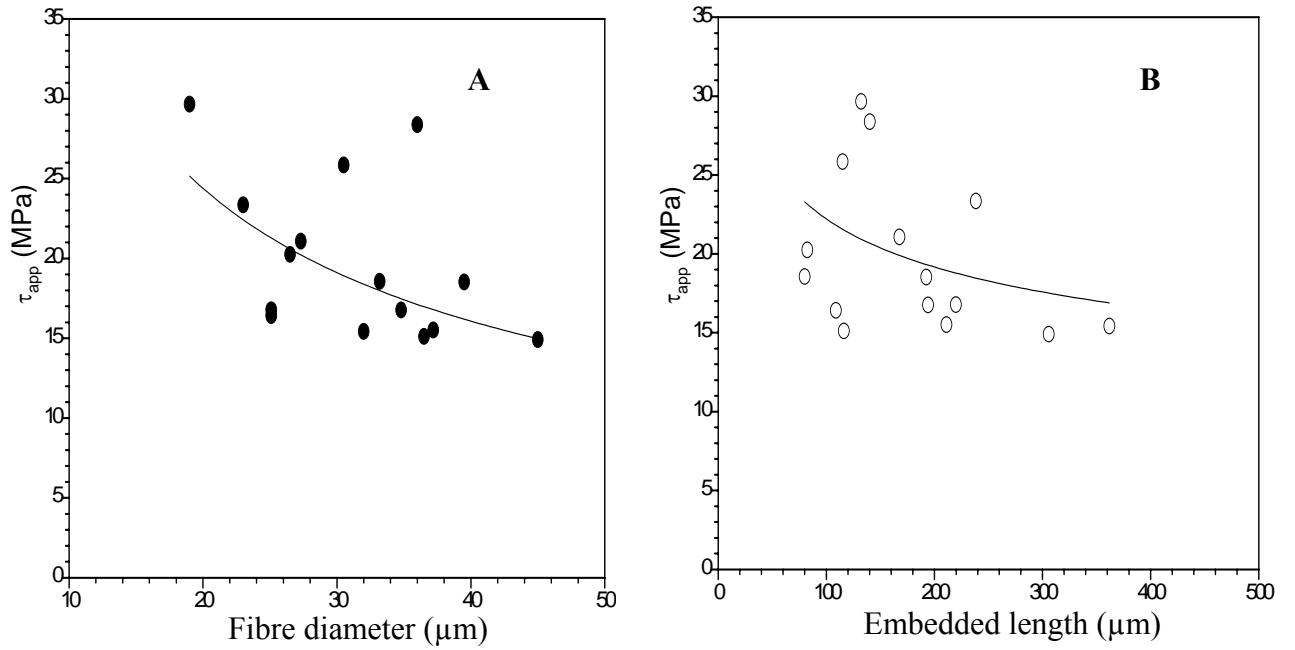


Fig. 44. Apparent IFSS as a function of (A) fibre diameter and (B) embedded length of J1/(PP1+Ex) system

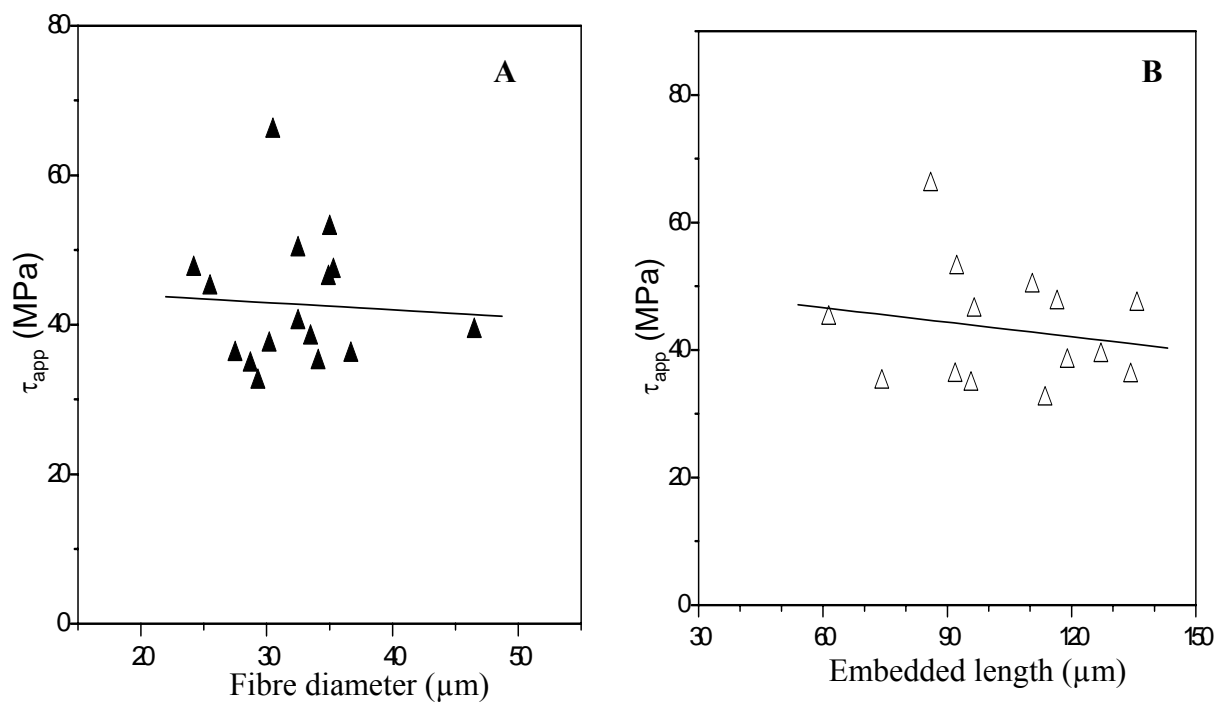


Fig. 45. Apparent IFSS as a function of (A) fibre diameter and (B) embedded length of J3/EP2 system

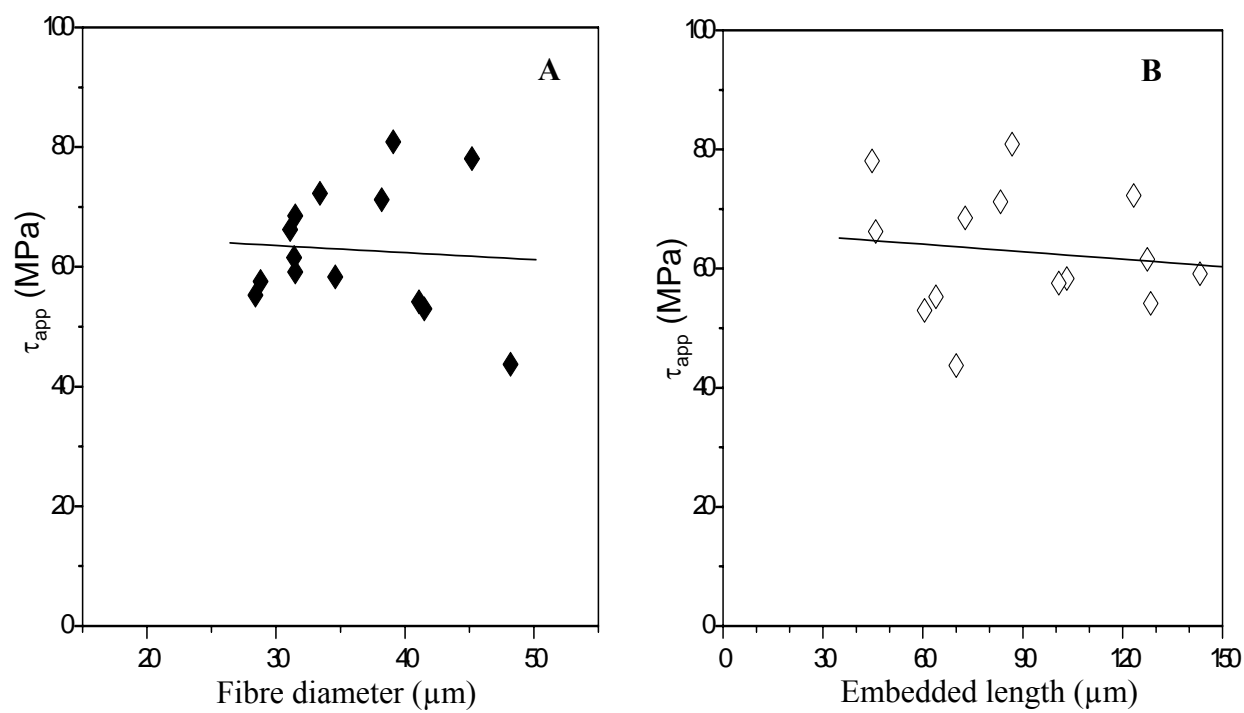


Fig. 46. Apparent IFSS as a function of (A) fibre diameter and (B) embedded length of NaOH/(APS+XB)\_J3/EP2 system

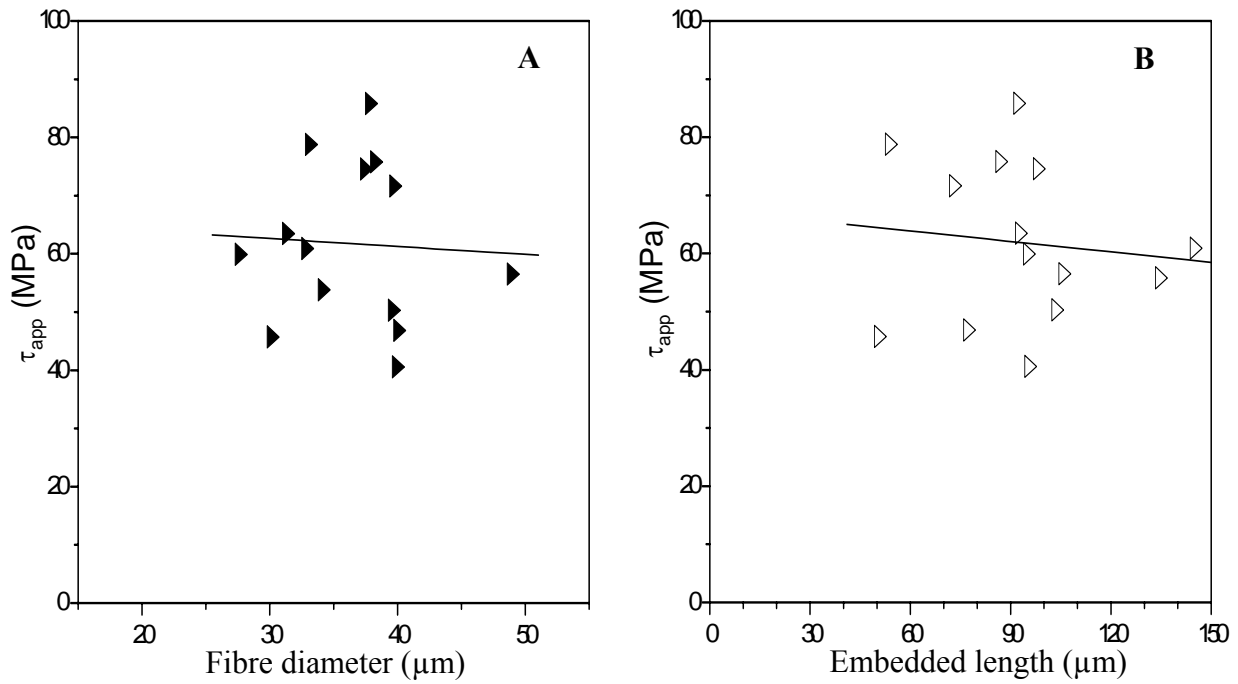


Fig. 47. Apparent IFSS as a function of (A) fibre diameter and (B) embedded length of NaOH/Y9669\_J3/EP2 system

## 5.2.2. Morphology of the fibre fracture surfaces

### 5.2.2.1. Influences of matrix modifications

The changes in fibre surface topography after pull-out test of polypropylene composites following matrix modifications were characterised using AFM (Fig. 48). It is interesting that the roughness of pulled-out fibre surfaces in the case of modified PP1 ( $R_a=12$  nm,  $R_{max}=88$  nm) and PP2 ( $R_a=14$  nm,  $R_{max}=126$  nm) is much lower than that of unmodified PP1 ( $R_a=26$  nm,  $R_{max}=209$  nm) and PP2 ( $R_a=27$  nm,  $R_{max}=235$  nm), respectively (Fig. 49). It is assumed that due to poor wettability of non-polar PP matrices on polar jute surface, the matrices can only contact with the flat areas but not with the deeply porous areas. Therefore, the deeply porous areas were revealed and just little matrices remained and form islets on the flat areas after pull-out. That causes higher roughness of pulled-out fibre surface in unmodified matrix composite systems. However, the PP matrices modified by 2 wt% Ex seem to be more polar and can have better wetting on polar jute surface. They may fill even the deeply rough areas and have good contact with the fibre surface. As mentioned above, the formations of hydrogen and covalent bonds between the modified matrices and the fibre surface significantly enhance interfacial adhesion. That can restrain removing the resin out of the deep holes on the fibre surface. Therefore, the roughness of the pulled-out fibre surfaces in the case of matrix modification is lower compared to that of the non-modified sample, as seen in a suggested model displayed in Fig. 50.

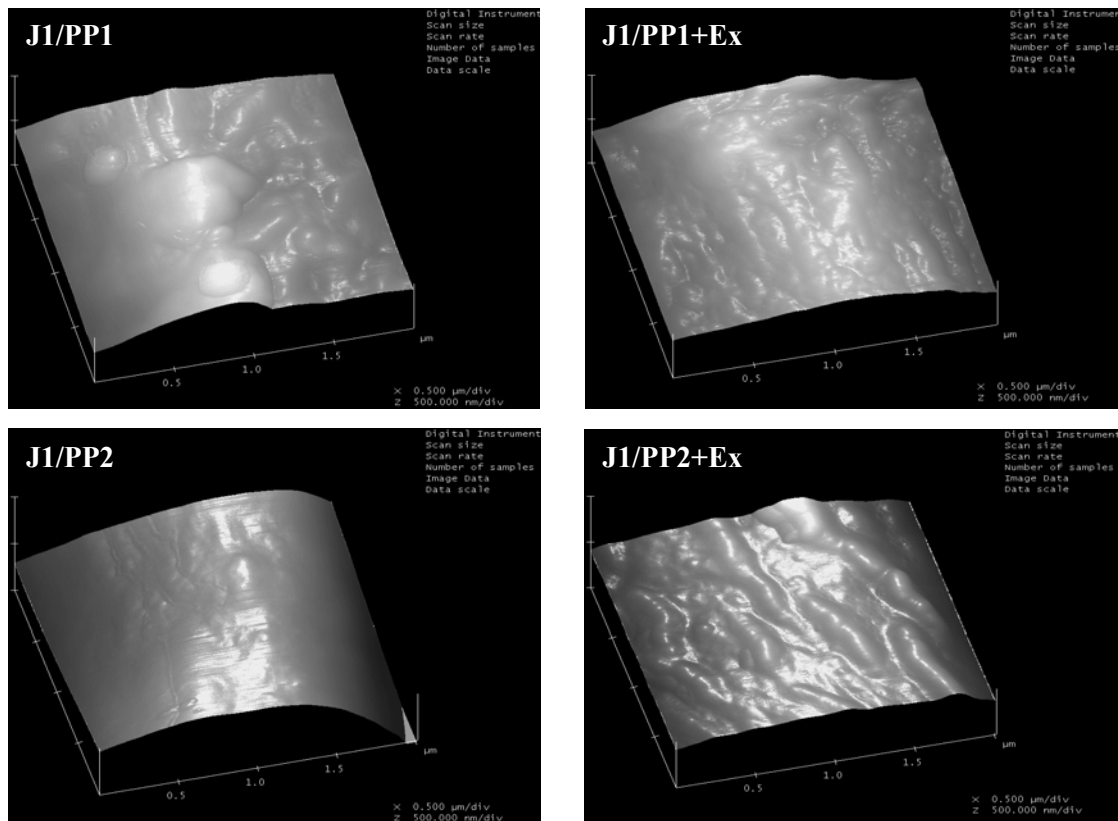


Fig. 48. Three-dimensional AFM topographical images of fracture surfaces of pulled-out jute fibres from unmodified and modified polypropylene composites (size:  $2 \times 2 \mu\text{m}$ )

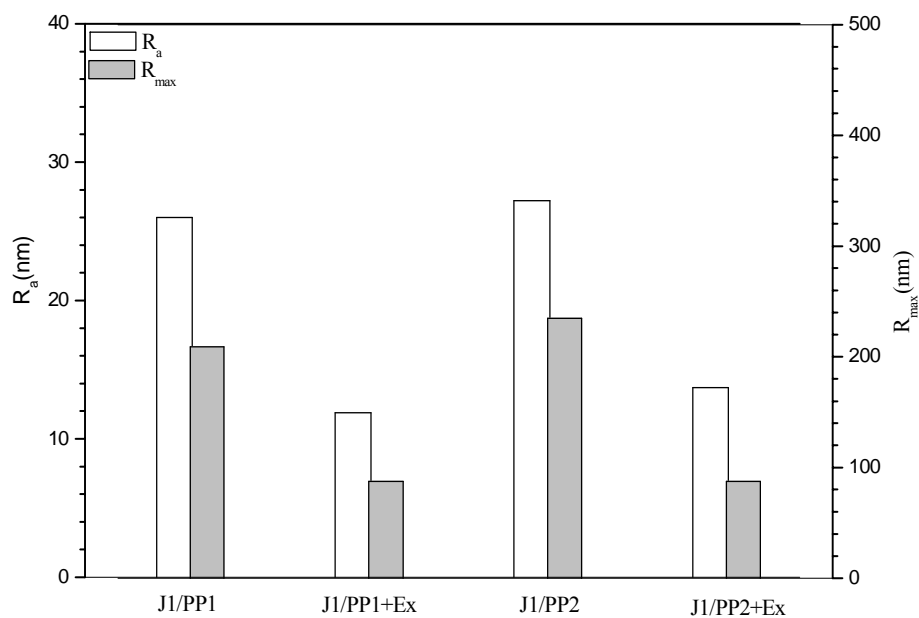


Fig. 49. Comparison of image mean roughness ( $R_a$ ) and maximum height roughness ( $R_{max}$ ) of the fibre after pull-out test from PP1 and PP2 matrices with and without modifier

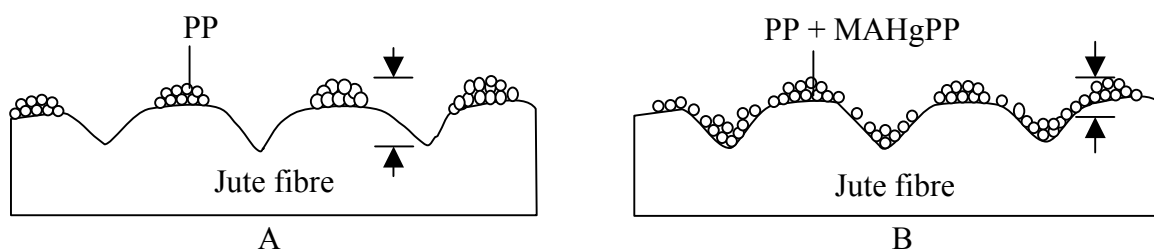


Fig. 50. Schematic model of (A) unmodified and (B) modified PP matrix composites after pullout test

#### 5.2.2.2. Influences of fibre modifications

AFM topographical images of the fibres before and after modification were shown in Fig. 51. These images have been used to visualize the surface roughness of the jute fibre with different modifications. Compared with untreated fibre surface, the NaOH-treated fibre shows rougher surface due to the removing of the surface cementings, which is also clearly seen in SEM micrographs (Fig. 52). Its mean roughness and maximum height roughness (Fig. 53) are 31 and 607 nm, respectively, which are higher than those of unmodified fibre ( $R_a = 24$  nm and  $R_{max} = 291$  nm). The jute fibres after pre-treatment by NaOH modified by coupling agent Y9669 and sizing APS+XB show the different influences on the morphologies. The image of NaOH/Y9669 treated fibre is rougher ( $R_a = 33$  nm and  $R_{max} = 307$  nm) comparing to only NaOH treated fibre. It can be observed apparently in Fig. 52D that besides sized coating layers, the fibre surface also contains some coalescence of sizing, which is likely soft. In contrast, the NaOH-pretreated fibre surface modified by a mixture of APS and XB shows much more smooth ( $R_a = 21$  nm and  $R_{max} = 151$  nm) than above two cases. It was proposed that the surfactants in epoxy dispersion (XB) may cause a good dispersion of partly polymerized APS and XB in aqueous solution of treatment agents, which prevents coalescence. Consequently, the fibre surface with the coating layers of APS+XB is less rough.

Comparing to the fibres before pull-out tests (light grey columns in Fig. 53), both mean and maximum roughness of the fibre surfaces after pull-out test (dark grey ones) increase. The roughness of pulled-out modified fibres was found to be higher than that of untreated fibre system. It is proposed that better bonding results in a strong tear at the interface, therefore, extensive stretched resin with high peaks remained on the modified fibre surfaces, which are also clearly seen in SEM photographs of tensile fracture surface displayed in Fig. 83 B. A schematic model of the fibre surface after pull-out from the composites based on NaOH, NaOH/(APS+XB) or NaOH/Y9669 treated jute fibre and epoxy matrix was suggested in Fig. 54.



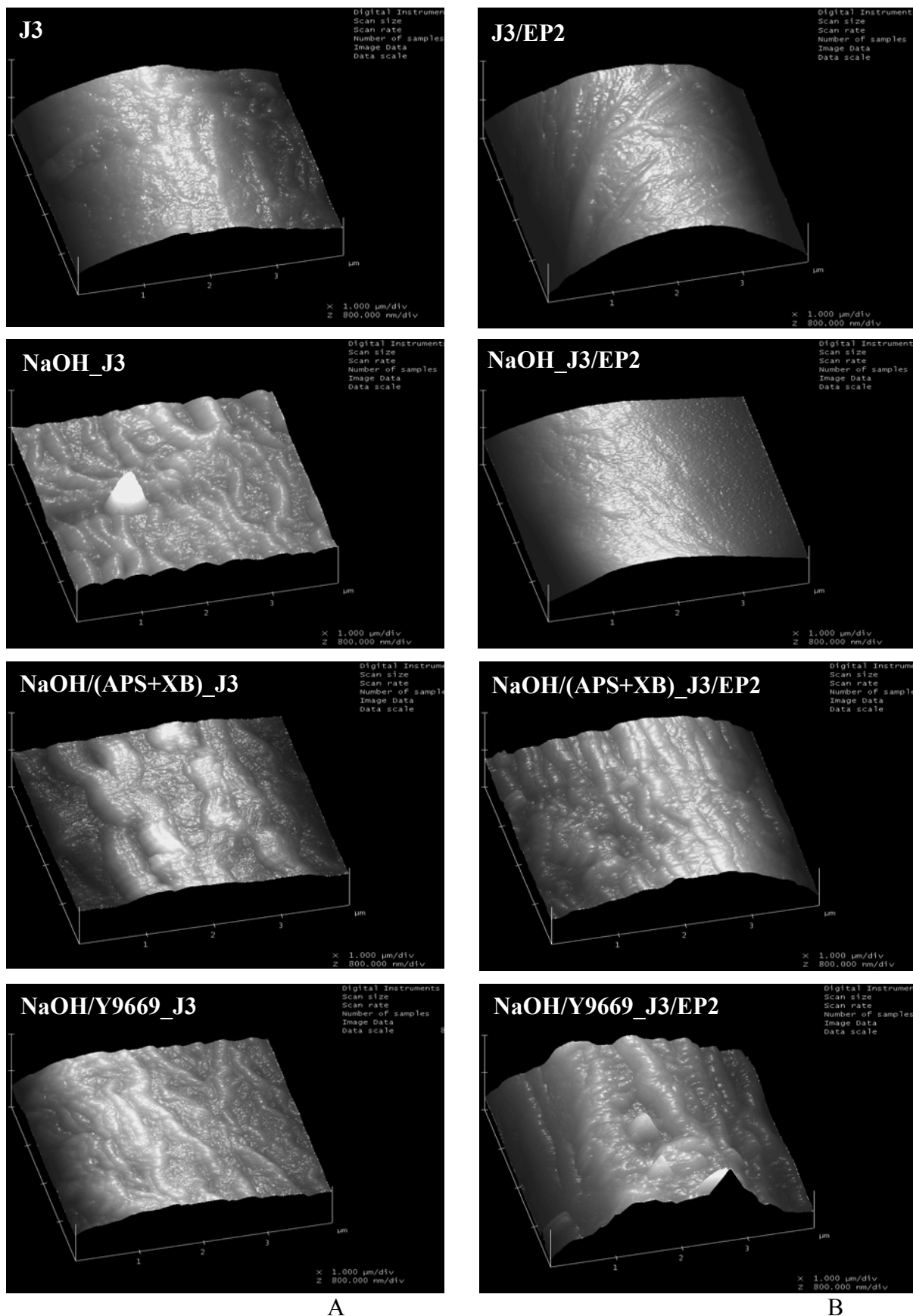


Fig. 51. Three-dimensional AFM topographical images of unmodified and modified fibre surfaces (A) before and (B) after pull-out test; (size:  $4 \times 4 \mu\text{m}$ )

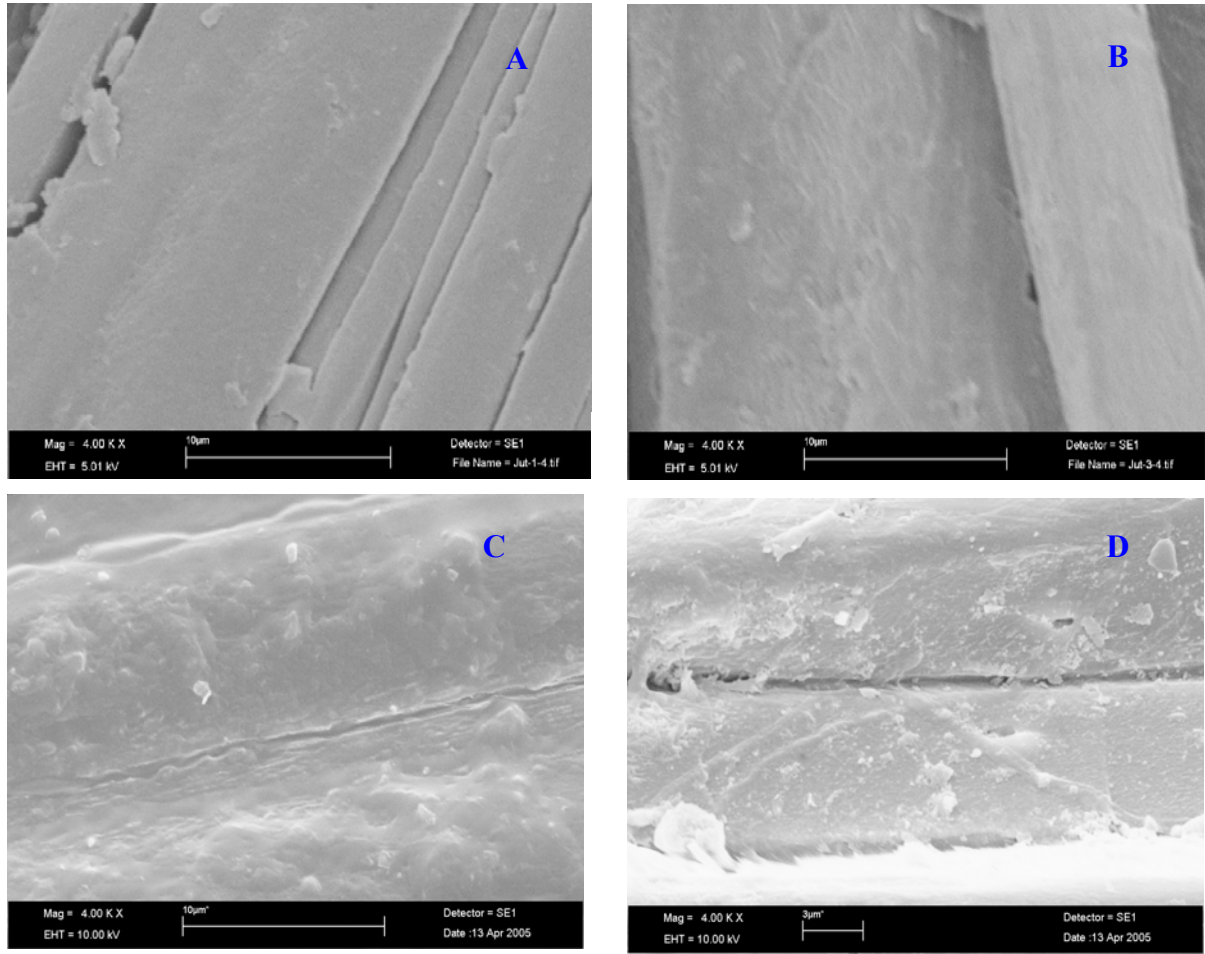


Fig. 52. SEM photographs of the jute fibre with different modifications (A) untreated\_J3, (B) NaOH\_J3, (C) NaOH/(APS+XB)\_J3 and (D) NaOH/Y9669\_J3

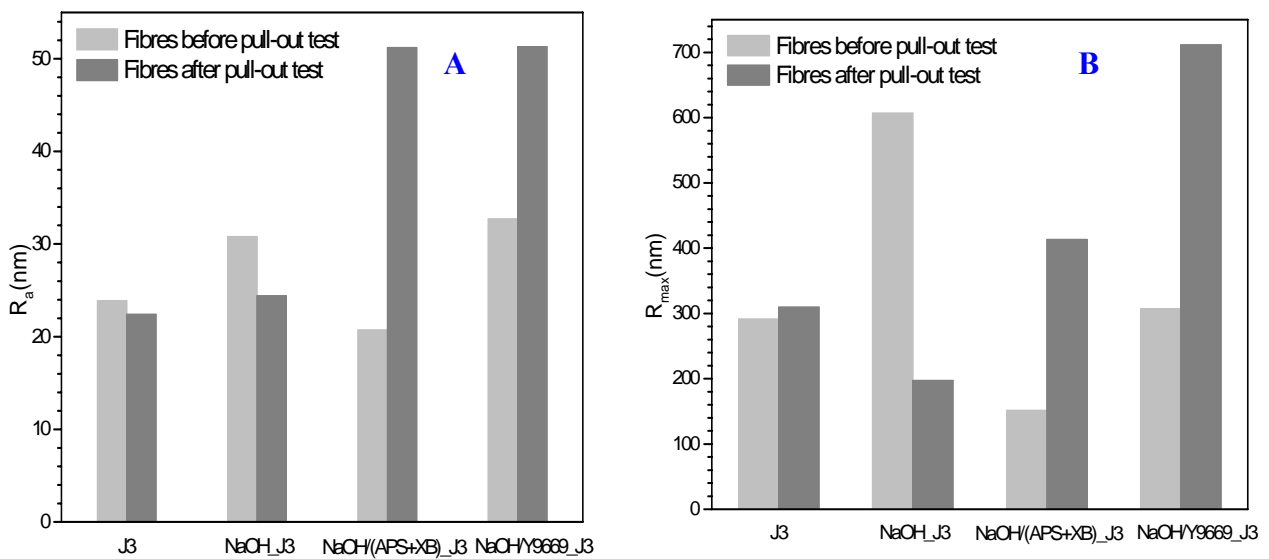


Fig. 53. Comparison of (A) image mean roughness and (B) maximum height roughness of the treated and untreated fibres before and after pull-out test from epoxy matrix

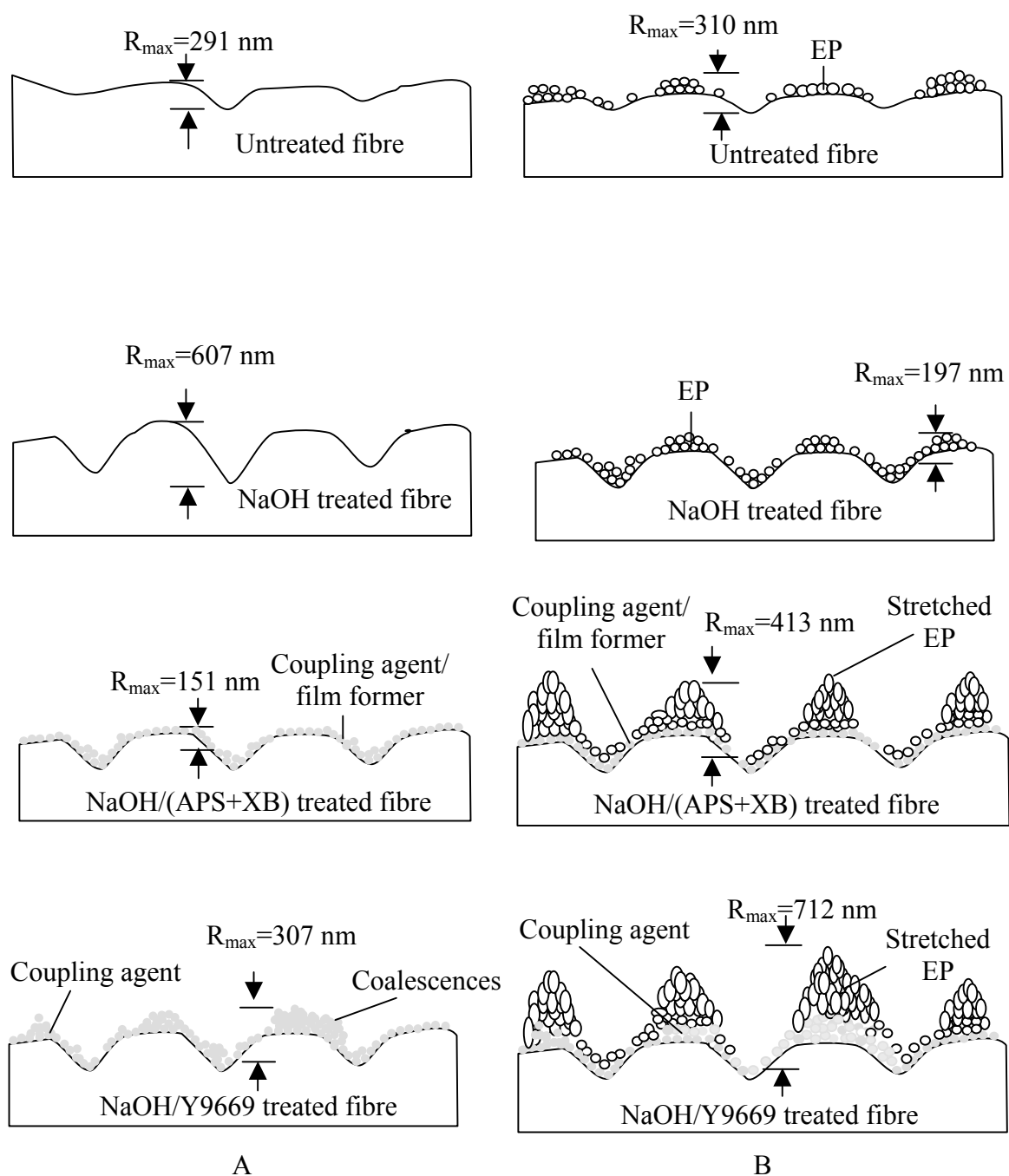


Fig. 54. Schematic model of untreated and treated fibre surfaces of (A) before and (B) after pullout tests

### 5.3. Jute/PP composites

The matrix treatment of PP by coupling agent maleic anhydride grafted polypropylene has been found to be the most efficient in improving interfacial adhesion of nature fibre composites [18, 20, 15, 76]. The MAHgPP's ability to enhance the composite properties depends on many factors, such as type of MAHgPP (graft level, random or block copolymer, molecular weight), miscibility of MAHgPP with the PP matrix, PP grade, composite processing conditions, etc. In order to chose the most economic and technological suitable one, three kinds of MAHgPP namely Exxelor PO 1020 (Ex), Polybond 3200 (PO) and TPPP 8012 (TP) were used for pre-investigations. It was found that all the MAHgPP grades result in improved tensile strength and impact toughness of jute reinforced PP except that in the case of using 2 wt% of TPPP the impact toughness decreased (Fig. 55 and Fig. 56). It is also observed that the improved degrees of these coupling agents are different and depend on their content. Exxelor revealed better mechanical properties than the other ones. That can be explained due to lower molecular weight of Ex the mobility of the MAHgPP molecule is higher and the MA group is more likely to reach the polar group on the fibre surface - this can say for the same kind of MAHgPP mean homopolymer, random or block copolymer. MAHgPP homopolymer tends to mix better with a PP homopolymer than with a PP copolymer [160]. The Exxelor amount of 2 wt% was expected to be the optimal content for PP matrix treatment. The content higher 2 wt% hardly contributes to a further increase. Therefore 2 wt% Ex was chosen to be optimum condition of treatment for investigating in detail the effect to the properties of jute reinforced polypropylene composites.

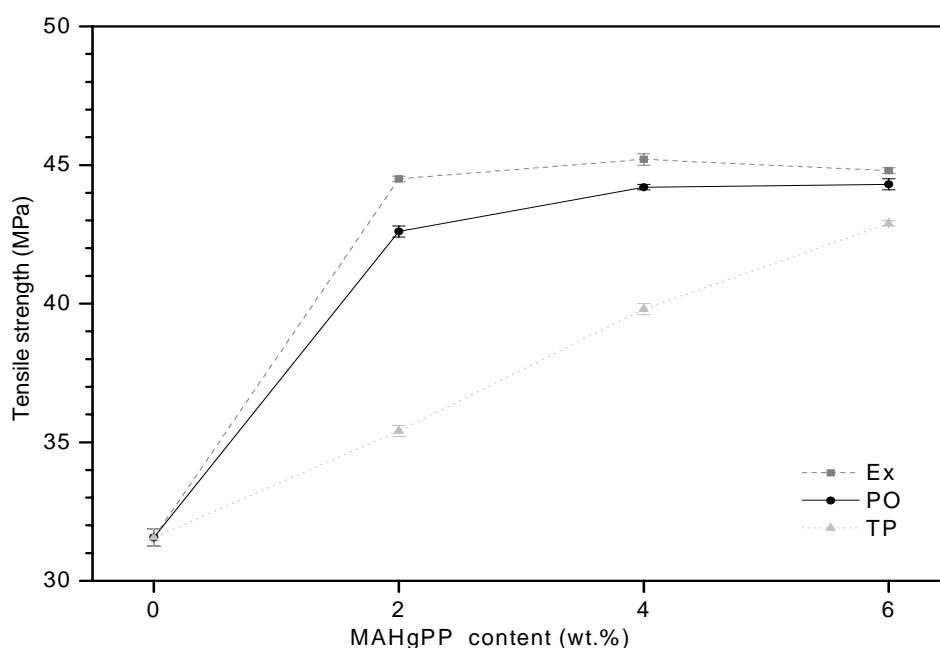


Fig. 55. Influences of three kinds of MAHgPP on tensile strength of jute/PP1 composites with fibre content of 19.78 vol%

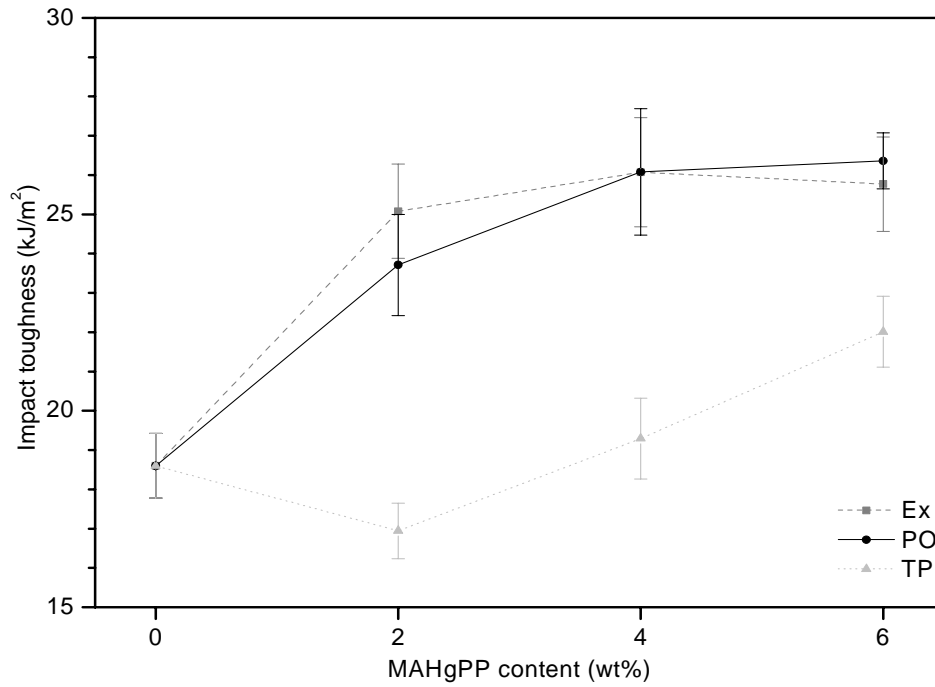


Fig. 56. Influences of three kinds of MAHgPP on impact toughness of jute/PP1 composites with fibre content of 19.78 vol%

### 5.3.1. Fibre length

It is well known that fibre length plays an important role in the mechanical performance of fibre reinforced composites. Table 13 summarizes the average fibre lengths and diameters derived from compound granules and plates. The data of compound granules indicates a strong decay of the fibre length due to the configuration of the screws during compounding and high viscosity/low temperature response. On the other hand, it should be noted that no significant changes in the fibre geometrical dimensions were observed after injection moulding, suggesting that no further cutting into shorter fibres or separated into elementary cells occurs during this processing step. Therefore, jute fibres are rather wear resistant during injection moulding.

Table 13. Average fibre length, diameter, and length/diameter ratio derived from compound granules and plates with 19.78 vol% fibre.

Samples	$L_f \pm \text{s.d.} (\mu\text{m})$	$d \pm \text{s.d.} (\mu\text{m})$	$L_f/d$
Granules	$243 \pm 162$	$23 \pm 15$	10.6
Plates	$244 \pm 154$	$22 \pm 12$	11.1

Fig. 57 and Fig. 58 show the distribution curves of length and length/diameter ratio. It can be observed that the distribution curves of fibre length very slightly move towards smaller values

with increasing fibre content. This phenomenon might be understood because higher fibre concentration promotes more damaging due to fibre-fibre interactions.

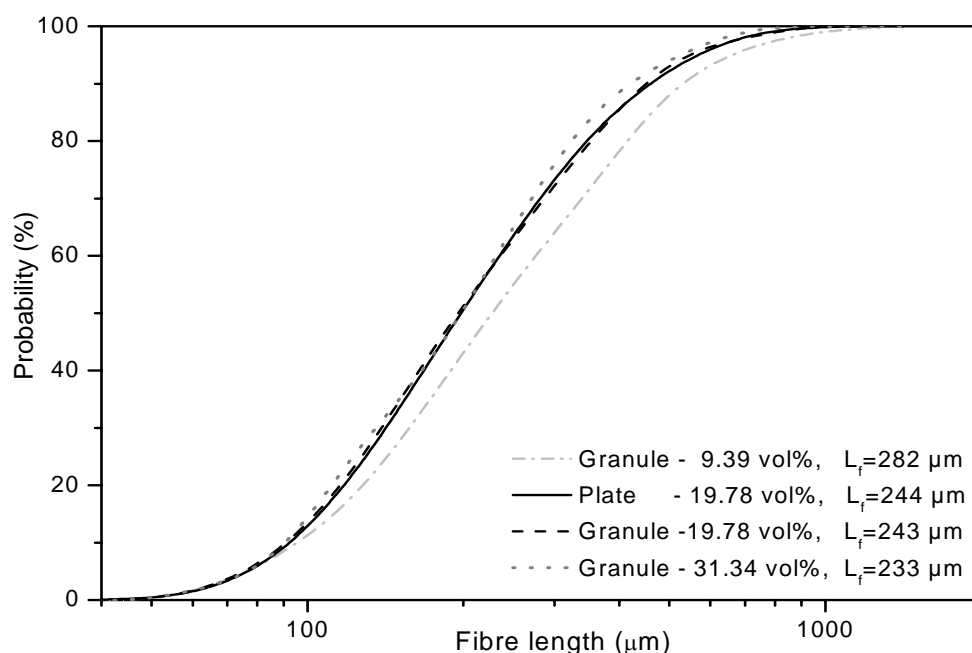


Fig. 57. Cumulated probability of fibre length in J1/PP1 + 2wt% Ex composites with different fibre content

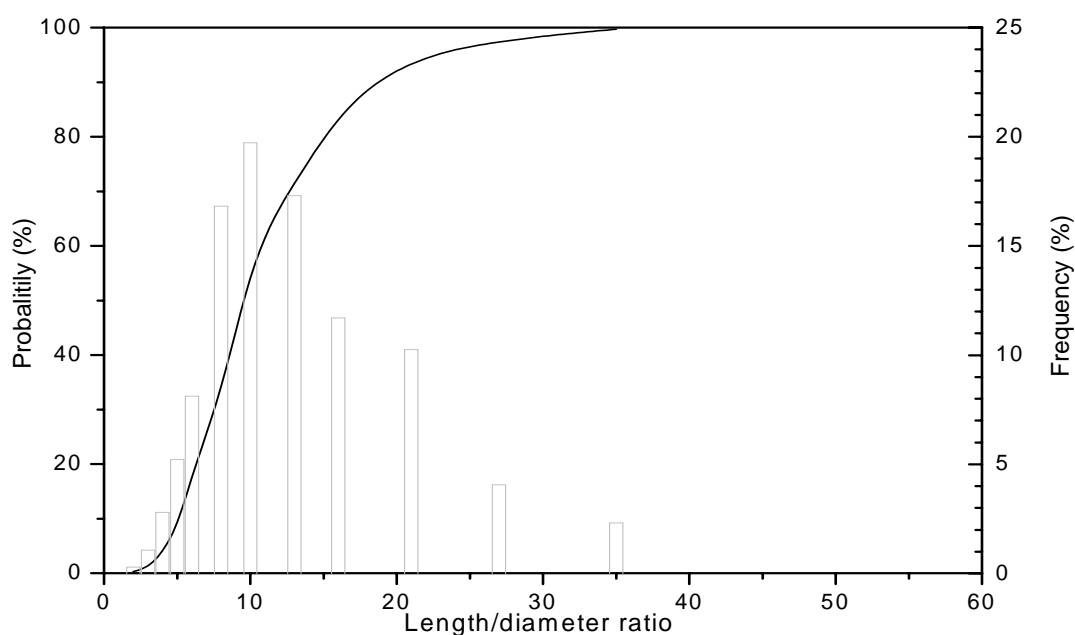


Fig. 58. Cumulated probability of fibre length/diameter ratios in J1/PP1 + 2 wt% Ex composite plate with fibre content of 19.78 vol%. A histogram of the frequency of length/diameter ratio is shown in the bar graphs.

On the other hand, fibre lengths of PP2 composites were observed to be slightly higher than those of PP1 composites (Fig. 59). It is possible that the higher molecular weight and higher viscosity of PP1 causes more fibre damaging. Furthermore, comparing the results obtained from SIS measured methods, the fibre lengths obtaining from SCAN seem to be slightly shorter. It is assumed that there is no fibre swelling effect by the solvent during measurement in the case of using SCAN method. However, this difference of the fibre length in two cases was very marginal, because the swelling has a minor effect for the fibre length.

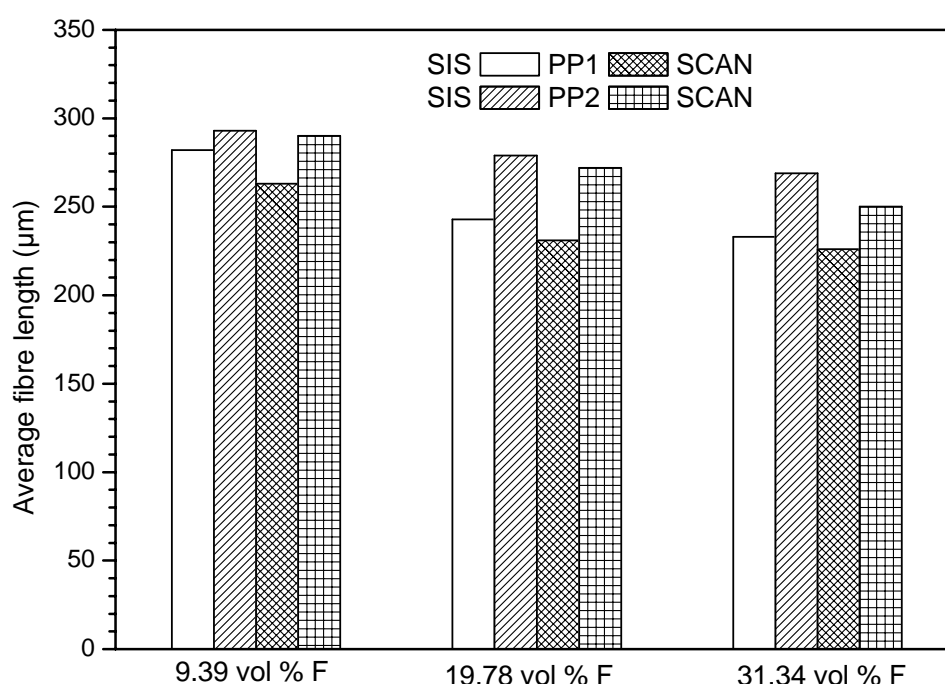


Fig. 59. Comparing average fibre lengths of PP1 and PP2 composites with MAHgPP, using both SIS and SCAN methods

### 5.3.2. Mechanical properties

Fig. 60 and Fig. 61 show the effect of the coupling agent Exxelor on the tensile strength and modulus of jute/PP composites. It is interesting to see that increasing tensile strength with increasing fibre content is only valid for the systems with the coupling agent. Using 2 wt % Ex as matrix modification increased the tensile strength of jute/PP composites with about 41% for PP1 and 28% for PP2 at the same fibre volume content. For the systems without coupling agent, the fibre acts as an included filler in the resin matrix, which actually weakens the composite because of poor interfacial adhesion.

Using the experimental data of  $\tau_d$  (Table 12) and  $\sigma_f$  value from the fit line in Fig. 29,  $l_c$  values (Table 14) were calculated and are in the region of 670-1117  $\mu\text{m}$  for different systems. As

aforementioned, the measured average fibre length in the short-fibre composite plate is far below the critical fibre length for all the systems in this study. This allows us to fit the equation (22) to the tensile values of various systems in Fig. 60 and use the fibre parameters and interfacial adhesion data in Table 12 and Table 13 gives values of the fibre orientation factor in the region of 0.10 to 0.36 and an average value of 0.23 (Table 14). This value is very close to the theoretical value for a random arrangement,  $\eta = 0.20$  [140] or 0.23 [141]. The significant variation of tensile strength for different systems indicates fibre alignment is not the only factor which affects mechanical performance; interfacial adhesion and how the fibre influences matrix properties also have a significant effect. Clearly, these theoretical lines based on the equation (22) correlated well to the experimental results, demonstrating the accuracy of the ‘rule of mixture’ theory, taking into account the interfacial adhesion properties, applied to natural fibres in PP matrix.

Table 14. The calculated critical fibre length and fibre orientation factor of polypropylene composites

Samples	$l_c (\mu\text{m})$	$\eta$
J1/ PP1	1074.6	0.18
J1/PP1+2% Ex	670.2	0.36
J1/PP2	1117.2	0.1
J1/PP2+2% Ex	778.1	0.28

Fig. 61 gives a comparison of the variation in the experimental and theoretical tensile modulus values of the jute/PP composites with fibre volume fraction. From the figure, it is clear that the Hirsch model given in 4.3.2.1 can adequately fit to the data. For all systems,  $E_c$  values increase almost linearly with increasing fibre content. In contrast to the tensile strength described above, the tensile moduli are not affected by the coupling agents. Generally, Young’s modulus reflects the capability of both fibre and matrix material to transfer the elastic deformation in the case of small strains without interface fracture. Therefore, it is not surprising that the tensile modulus is less sensitive to the variation of interfacial adhesion than the tensile strength which is strongly associated with interfacial failure behaviour.

Unlike the significant improvement of the tensile properties with increasing fibre content, the impact toughness decreases slightly (Fig. 62). It is attributed to a change from ductile to brittle fracture behaviour with increasing fibre content. Besides, the probability for fibre agglomeration



[117] also increases at higher fibre content, creating regions of stress concentration that require less energy to initiate or propagate a crack [37]. The important toughening mechanism in fibre reinforced polymer composites is crack-bridging by fibres associated with frictional sliding during fibre pull-out, which in general will be affected by the interfacial adhesion. Due to the improved stress transfer effect by the coupling agent, the impact toughness for jute/PP1 matrix composite increased by about 40%. However, the impact toughness of PP2 matrix composites was not significantly affected by the coupling agent. It is believed that the deformation behaviour of PP is strongly dependent on its molecular weight. As demonstrated by above tensile test (see Fig. 60 and Fig. 61), the PP2 having lower molecular weight shows both lower strength and modulus values than the PP1 having higher molecular weight. It seems that the lower molecular weight of PP2 might promote polymer fracture rather than the deviation of the major crack path away from the polymer to the interphase region, resulting in less extensive interfacial debonding. Consequently, it reduces the sensitivity of interfacial adhesion contributions to toughness.

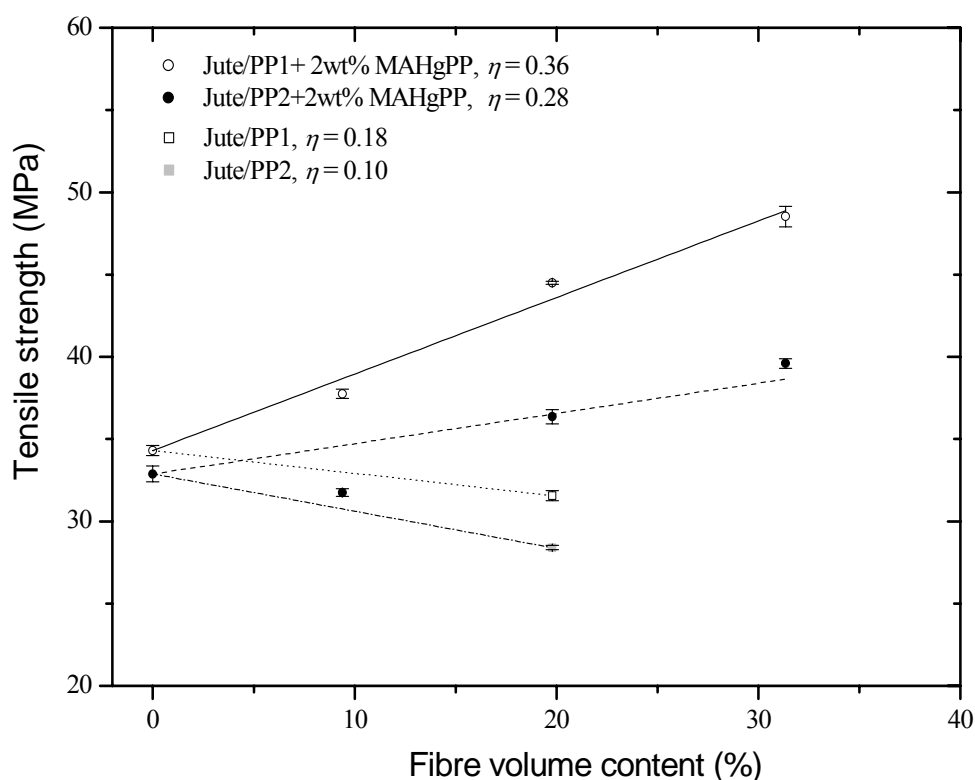


Fig. 60. Influences of interfacial adhesion on the mechanical properties of jute/PP composites.  
Experimental data of tensile strength as a function of the fibre volume content

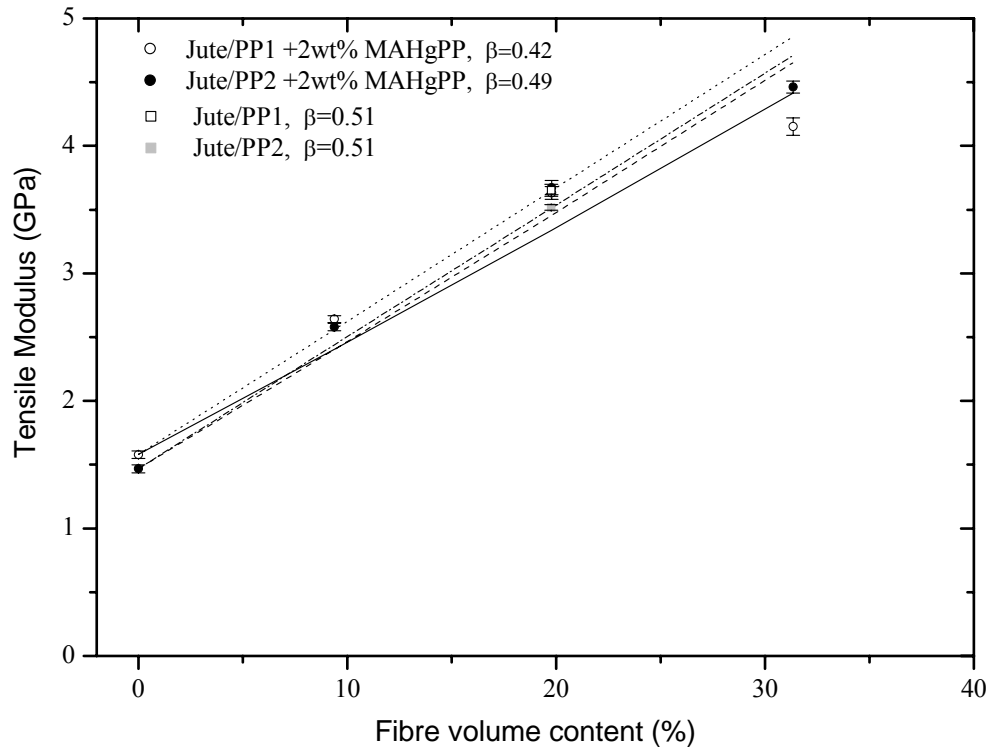


Fig. 61. Influences of interfacial adhesion on the mechanical properties of jute/PP composites.  
Experimental data of tensile modulus as a function of the fibre volume content

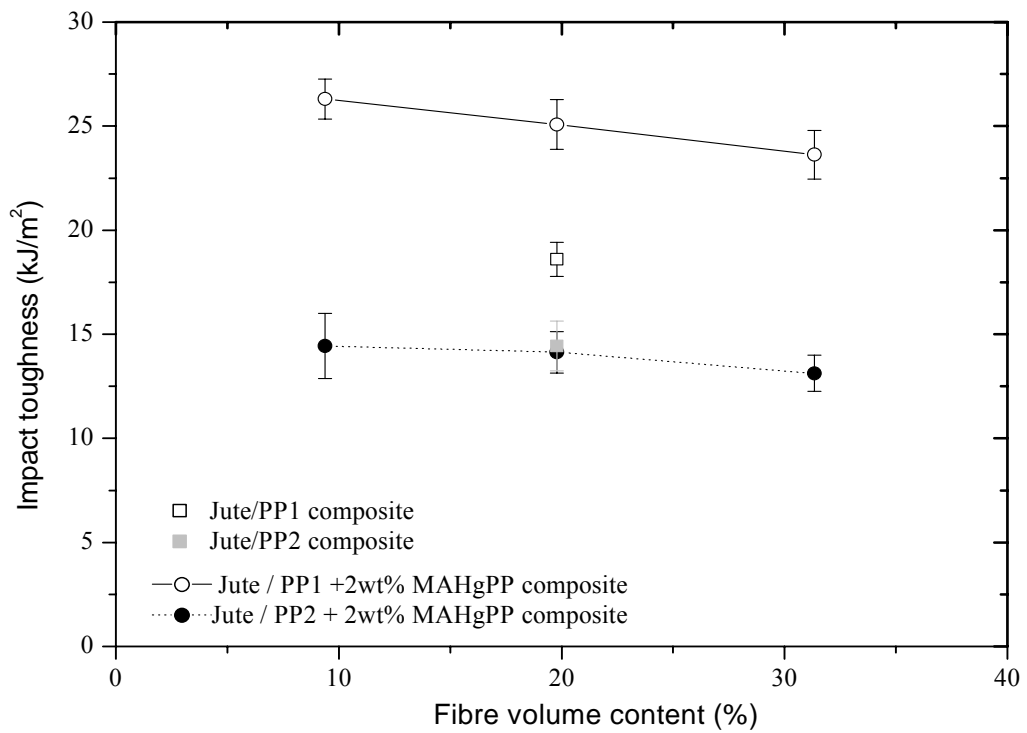


Fig. 62. Charpy impact toughness as a function of the fibre volume content  
for jute/PP composites

### 5.3.3. SEM

Scanning electron microscopy analysis of tensile fracture surfaces illustrates the improvement of the interaction between the fibre and matrix in polypropylene composites by the addition of Exxelor. The microscopic images of the fracture surfaces of untreated fibre composites based on PP1 and PP2 (Fig. 63 and Fig. 65) clearly show more and bigger pores than that exhibited by treated samples (Fig. 64 and Fig. 66). Moreover, there are more fibres pulled-out in the cases of untreated composites. These indicate that the interaction between the fibre and PP matrix in untreated composites is very weak, due to poor fibre-matrix compatibility. And with the using of 2 wt% Ex as a matrix modification, the interfacial bonding between the jute fibre and PP matrices is significantly improved. This finding corresponds with the results for mechanical properties discussed in the sections 5.2.1.2 and 5.3.2.

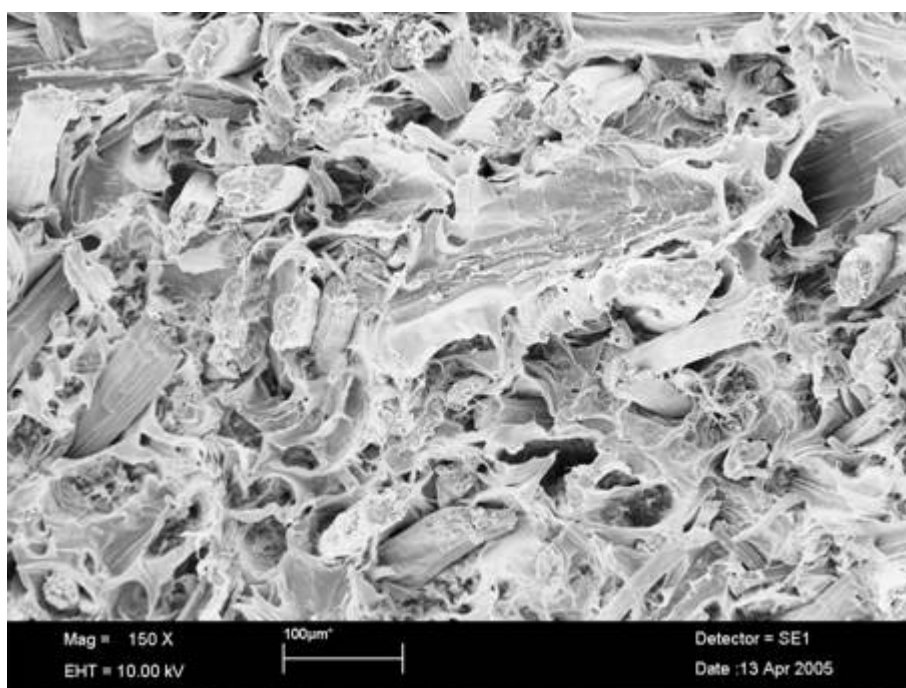


Fig. 63. Fracture surface of J1/PP1 composite broken in tensile test

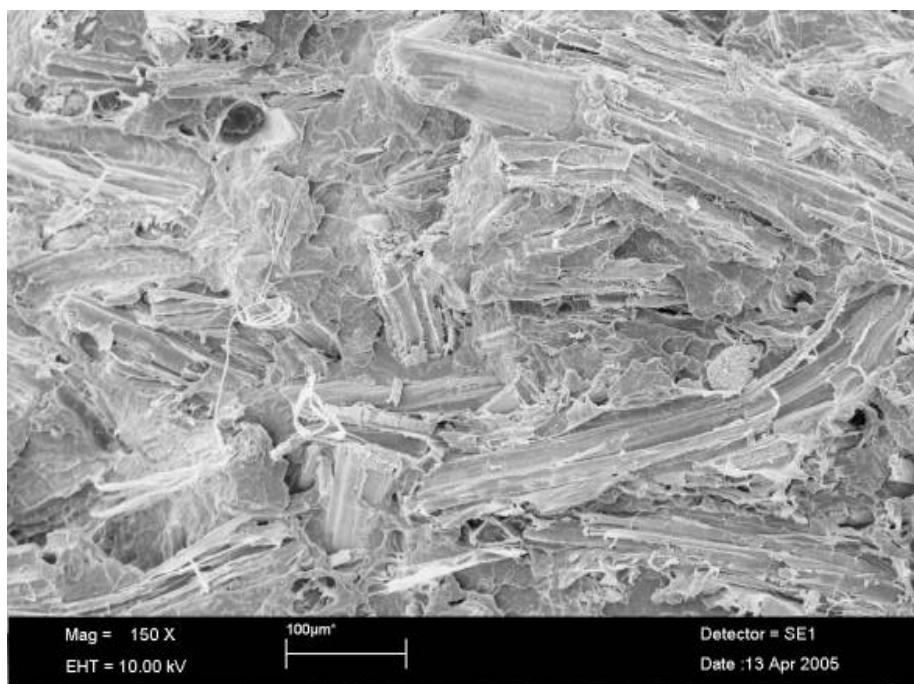


Fig. 64. Fracture surface of J1/PP1 + 2 wt% Ex composite broken in tensile test

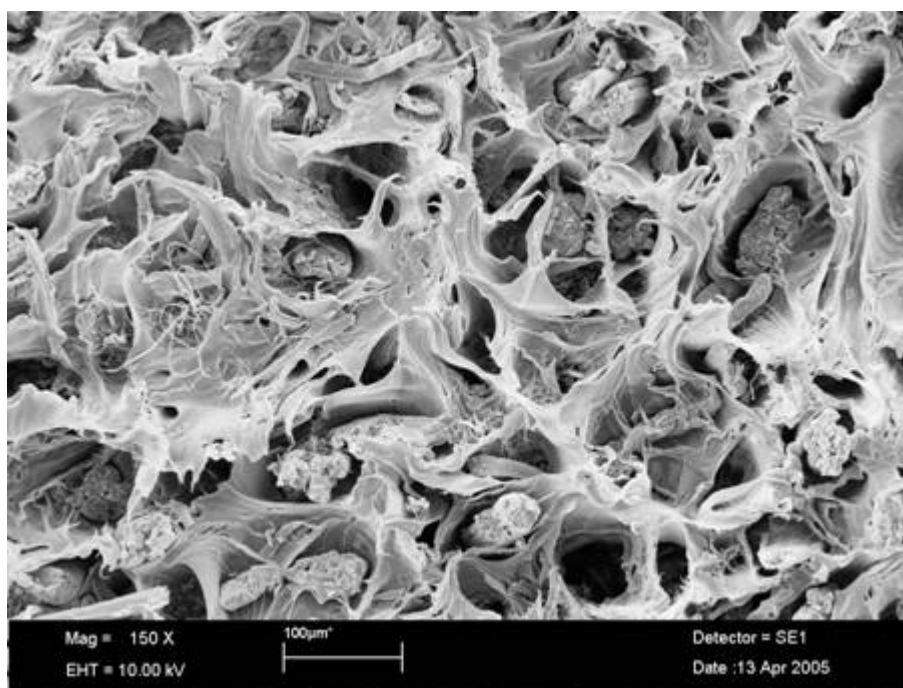


Fig. 65. Fracture surface of J1/PP2 composite broken in tensile test

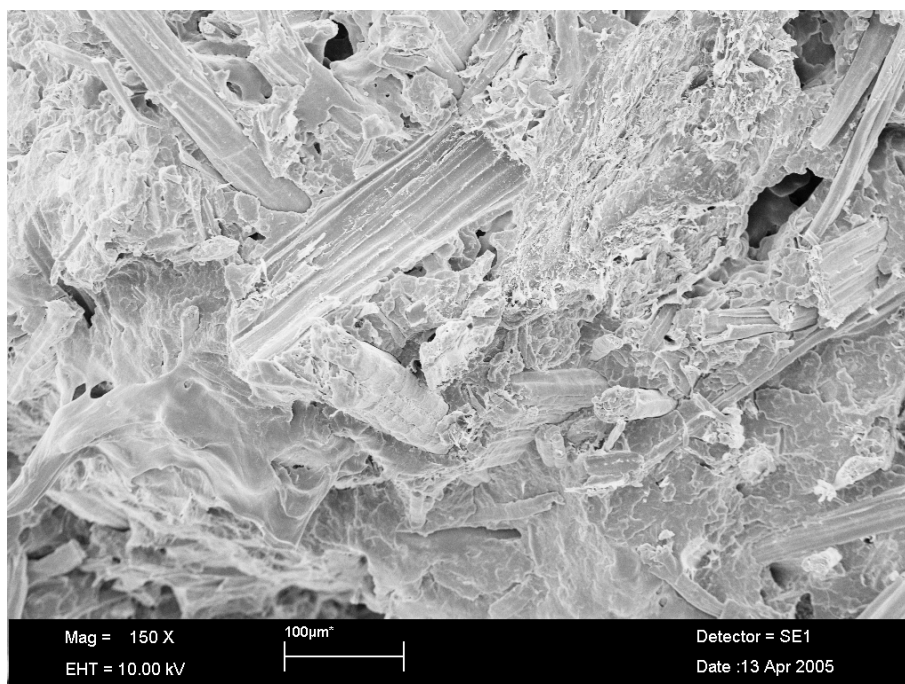


Fig. 66. Fracture surface of J1/PP2 + 2 wt% Ex composite broken in tensile test

### 5.3.4. Thermal analysis

#### 5.3.4.1. Effect of the atmosphere of measurement

During processing of polypropylene composites, jute fibres are exposed both to high temperature and trapped air, which might cause thermal degradation. If serious degradation of jute fibres happens during high melt processing temperature, the mechanical reinforcement effect of the fibre can be much decreased and lead to discolouration as well as unpleasant odour of the composites. Therefore, thermal gravimetric analysis was used to determine the high temperature degradation behaviour of the composites as well as their components under air and nitrogen atmospheres.

The DTG curves (Fig. 67) display the thermal behaviour of jute fibre, PP and jute/polypropylene composite with 19.78 vol% fibre in both air and nitrogen atmospheres. The DTG curves indicate the decomposition of jute fibre in nitrogen atmosphere (A-I) with three steps as described in section 5.1.5.

However, the thermal decomposition behaviour of the fibre is significantly different in air atmosphere during measurement (A-II). The degradation also comprises three steps (<100°C, 273.9°C, and 321.6°C, respectively), of which the main process is shifted to lower temperature. In addition, there is one more step with a peak at 441.7°C. In this step, the rest of the char is oxidised and the rest of the mass consumed [80].

Compared to jute fibre, the thermal degradation of polypropylene is much more influenced by the measured atmosphere. In nitrogen, PP degrades with a large single peak starting around 300°C. This peak corresponds to the thermal degradation of PP initiated primarily by thermal scissions of C-C chain bonds accompanied by a transfer of hydrogen at the site of scission [142]. However, thermal degradation of PP in air is significantly different from that in nitrogen. The thermal stability of PP in air is prominently reduced by oxidative dehydrogenation accompanied by hydrogen abstraction [143]. A broad weight loss rate peak around 299°C in air is observed at a much lower temperature than that in nitrogen (431°C) and the starting point of degradation is about 65°C lower than that in nitrogen (Fig. 67). It can be deduced that the thermal degradation of PP in air atmosphere is easier and faster comparing in nitrogen. The thermal stability of composites was found higher than that of both neat PP and the fibre in both nitrogen and air (Fig. 67). Two major peaks of jute/PP composite in nitrogen were clearly observed. The first minor peak at 346.1°C corresponds to the degradation of cellulose and the second major peak at 441.7°C mainly is the degradation of dehydro cellulose. However, these two peaks were nearly merged together and shift to lower temperature region in the purge air.

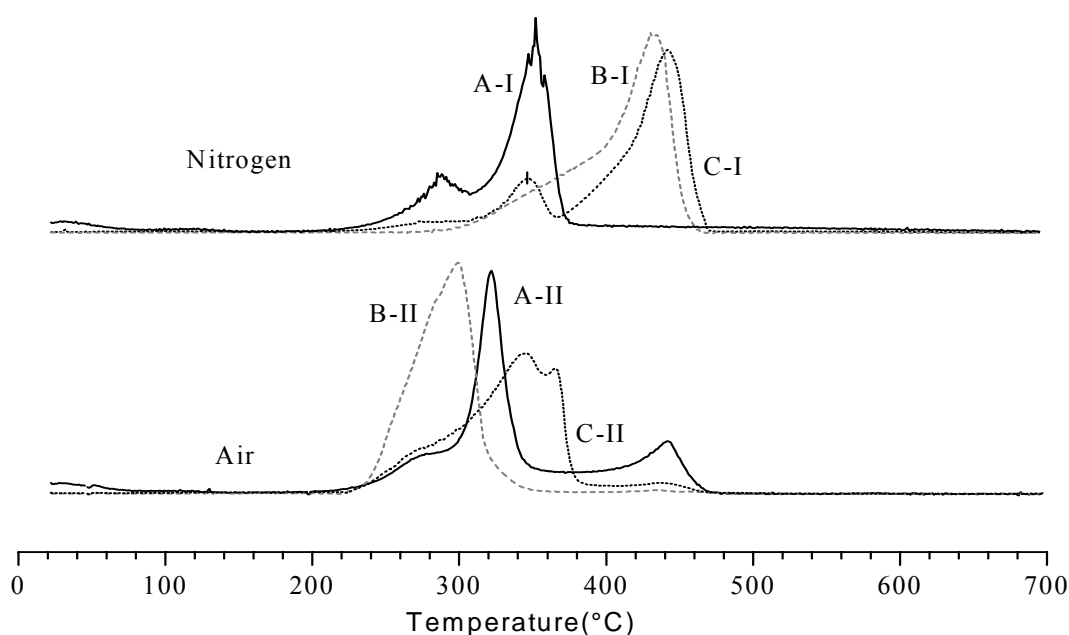


Fig. 67. DTG curves of (A) jute, (B) PP1 and (C) jute/PP1 composite 19.78 vol% fibre under nitrogen (I) and air (II) atmospheres

The higher thermal stability of the composite compared to the fibre and the matrix is also seen in Fig. 68. In which, the TGA curves of the composites moved to the right side mean higher temperature region compared to the fibre and the matrix in both air and nitrogen atmospheres.

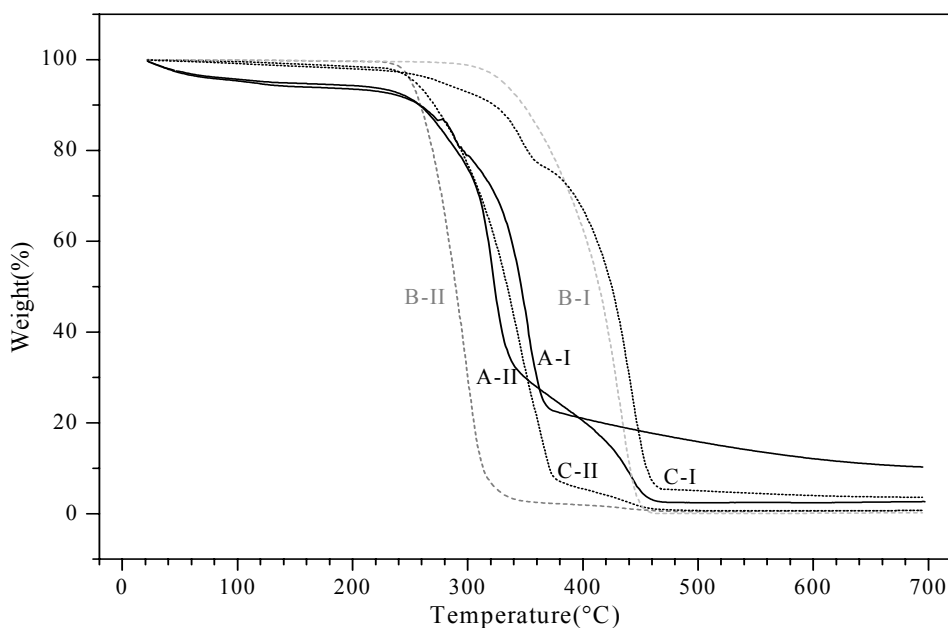


Fig. 68. TGA curves of (A) jute, (B) PP1 and (C) jute/PP1 composite 19.78 vol % fibre under nitrogen (I) and air (II) atmospheres

#### 5.3.4.2. Effect of modifier

The modification of jute/PP composite by using 2 wt% MAHgPP as a matrix modifier was observed to improve the thermal resistance. The TG curve of the modified composite moved slightly to a higher temperature region than that of non-modified composites (Fig. 69). This effect might be due to the stronger interaction between the fibre and matrix caused by the formation of the covalent bond at the interface. Thus, the thermal decomposition is shifted to high temperature.

#### 5.3.4.3. Effect of fibre content

Fig. 70 shows the influence of the jute fibre content on the thermal properties of modified composites. The TG-curves of jute/modified PP1 composites with different fibre content reveal different thermal resistance under nitrogen and air atmospheres. The thermal resistance of PP1 composites decreased with increasing fibre content in nitrogen atmosphere. This is in agreement with higher thermal resistance of propylene than jute fibre in nitrogen. However, the TG curves of these composites in air shifted towards a lower temperature region and thermal resistance of composites was found increase with fibre content due to lower thermal stability of polypropylene than jute fibre in air atmosphere, as mentioned in section 5.3.4.1.

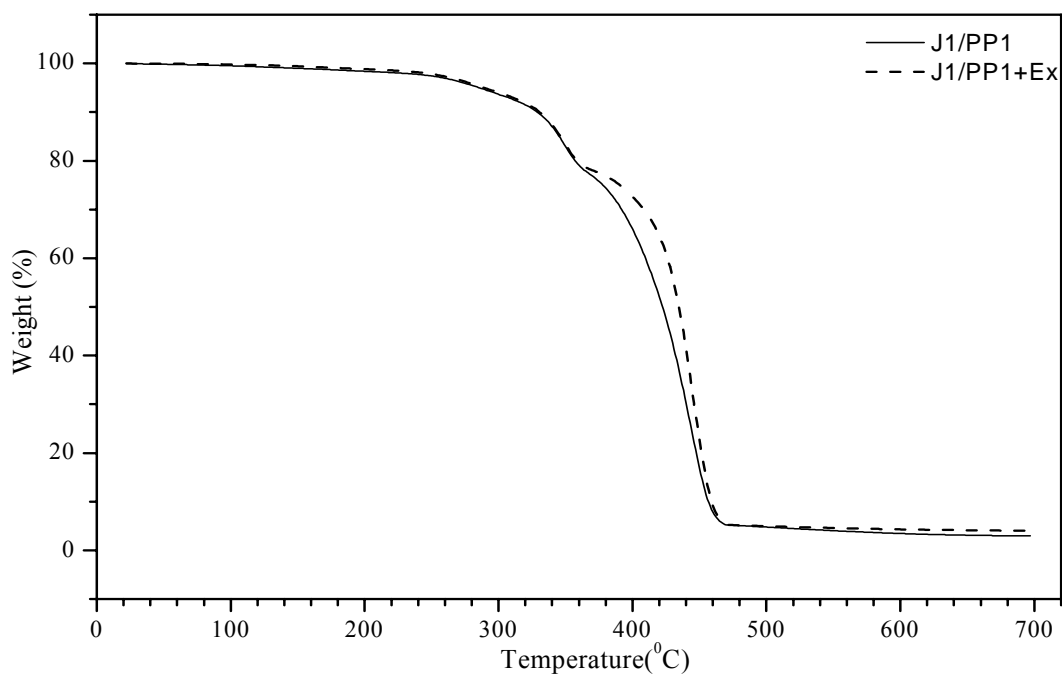


Fig. 69. Thermogravimetric curves of J1/PP1 composites with and without Ex modifier under nitrogen atmosphere at a fibre content of 19.78 vol%

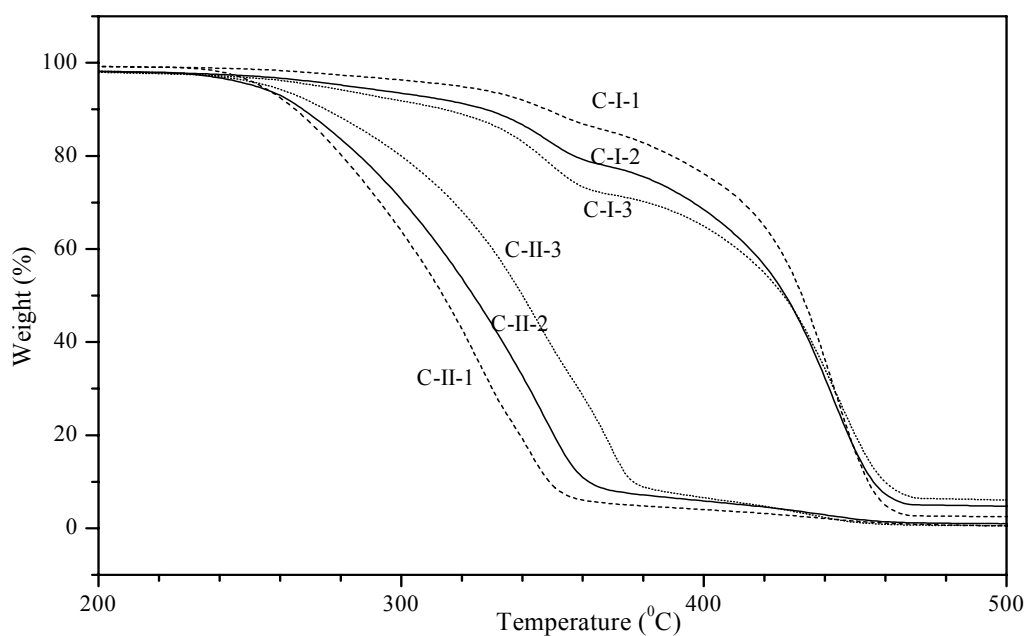


Fig. 70. Thermogravimetric curves of jute/PP1 + 2 wt% MAHgPP composites (C) under the nitrogen (I) and the air (II) with different fibre contents: 9.39 vol. % (1), 19.78 vol. % (2) and 31.34 vol.% (3)



### 5.3.5. Dynamic mechanical analysis

The dynamic mechanical properties of PP1 and jute/PP1 composites with and without modification in the 0° direction (flow direction during injection moulding) were evaluated. The storage modulus ( $E'$ ) as a function of temperature is depicted in Fig. 71. With increasing temperature,  $E'$  values of matrix PP1 and composite systems decreased. However, the decrease of matrix modulus in composites was compensated by the stiffness of the fibre. With increasing fibre content the storage modulus-temperature traces reveal a higher level of storage modulus.

The use of 2 wt% Ex as a coupling agent in J1/PP1 composite was found to slightly increase the storage modulus. At 19.78% fibre content, the storage modulus of jute/modified PP1 composite was slightly higher than that of jute/unmodified PP1 composite in the mostly temperature range of measurement. The increase in storage modulus indicated enhanced adhesion between fibre and matrix with the using coupling agent, leading to the better transfer of stress from matrix to the fibre.

Fig. 72 illustrates the evolution of loss modulus ( $E''$ ) and mechanical loss factor ( $\tan \delta$ ) with temperature. It was observed that in the modified composite system the loss modulus increased with fibre content. It is suggested that with increasing of fibre content, the energy losses increase owing to the interfacial friction between the matrix and the fillers under the action of the outside oscillation load [144]. On the other hand, the  $\tan \delta$  values increased as a function of temperature and reached the first maximum at the glass transition temperature of the amorphous part in PP (the  $\beta$  transition), then dropped and again reached the second maximum due to the presence of 'rigid' amorphous molecules present in the crystal ( $\alpha$  transition) [145, 146, 127]. With increasing fibre content,  $\tan \delta$  values dropped in jute/modified PP composites. The reason is that the fibres restrict the mobility of PP molecules in the relaxation process. The reduction in  $\tan \delta$  meant that, at the same temperature, the increase of storage modulus is greater than loss modulus with increasing fibre content. Furthermore, the decrease of mechanical loss factor was also denoted fatigue improvement [147] and an enhanced elasticity of the composites due to the high elasticity of cellulose fibre.

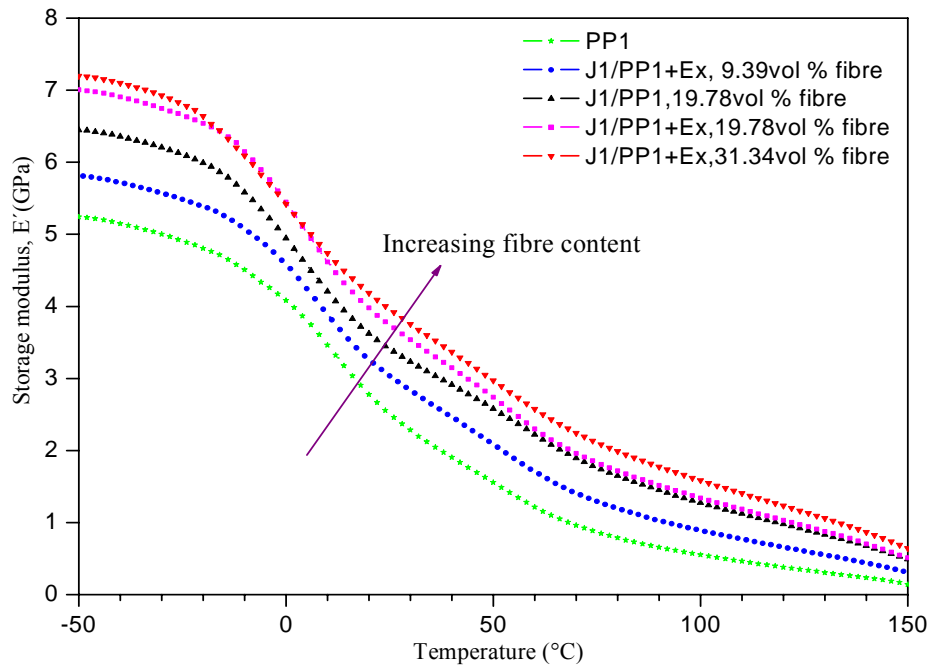


Fig. 71. Temperature dependence of storage modulus of PP1 and modified jute/PP1 composites at different fibre contents

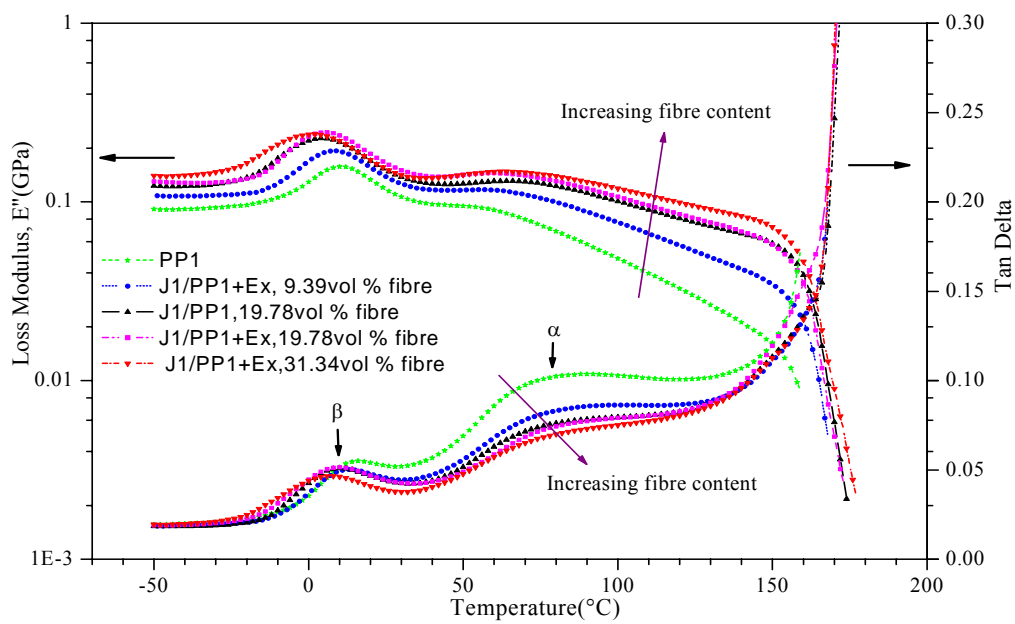


Fig. 72. Temperature dependence of loss modulus and tan delta of PP1 and modified jute/PP1 composites at different fibre contents

### 5.3.6. Moisture absorption behaviour

Samples are exposed to humidity as described in section 4.3.3.2. Fig. 73 also shows the moisture absorption behaviour of jute/polypropylene composites at different fibre contents, with and without modifier. The water content  $M_t$  rapidly increased at the first stage of absorption and gradually reaches the saturated values  $M_\infty$ . The ratio of  $M_t/M_\infty$  increases with the square root of exposed time  $t^{1/2}$  and the gradient of  $M_t/M_\infty$  versus  $t^{1/2}$  curve increase with fibre content. The hydrophilic character of natural fibres is responsible for the moisture absorption in the composites and therefore a higher content of fibres lead to a higher moisture absorption. It can be observed that when the fibre content is increased the saturation time is shortened. At the same fibres content, the saturation time of the modified composites is longer than that of the unmodified composites.

The equilibrium moisture content and the diffusion coefficient are summarized in Table 15. It is observed that the weight gain at saturation and the diffusion rates increased with fibre content. At the same fibre content, the unmodified composites present higher values of diffusion coefficient and equilibrium water content than the respective modified composites. This can be due to better adhesion between matrix and fibres, leading to fewer and smaller gaps in the interfacial region and also to more hydrophilic groups, as hydroxyl are blocked by the coupling [148]. Moreover, the PP1 matrix composites present lower values of the equilibrium water content and the diffusion coefficient than the respective composites with PP2 as matrix (Table 15)

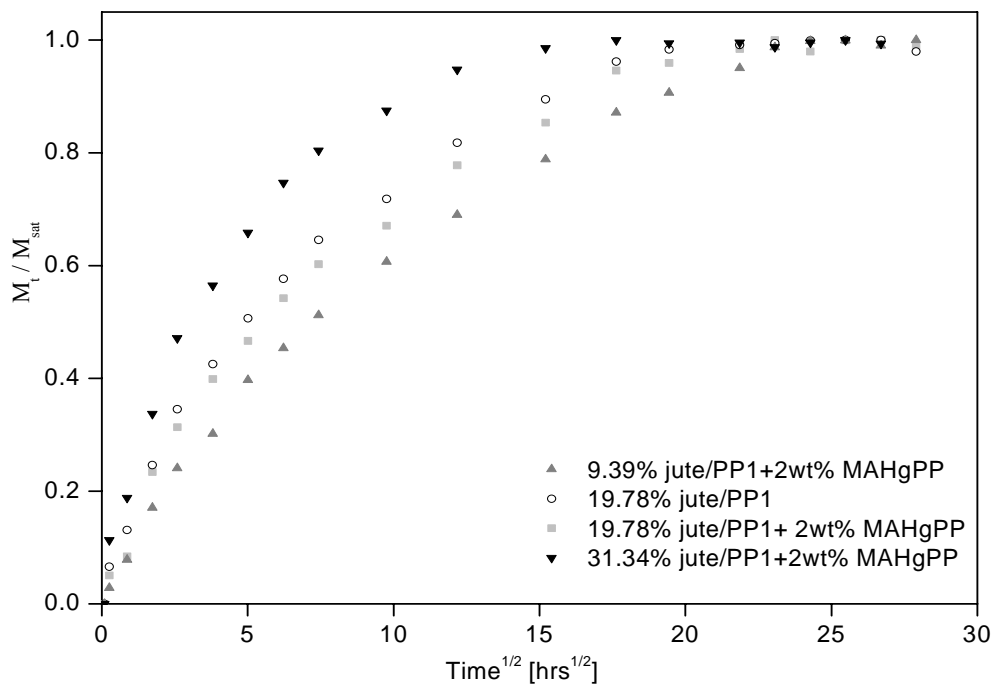


Fig. 73. Moisture absorption behaviour of jute/PP1 composites at 95 %RH

Table 15. Equilibrium water content ( $M_{\infty}$ ) and the moisture diffusion coefficient (D) of jute/polypropylene composites

Samples	PP1 composites		PP2 composites	
	$M_{\infty}$ (wt%)	$D \times 10^{-8}$ (mm <sup>2</sup> /sec)	$M_{\infty}$ (wt%)	$D \times 10^{-8}$ (mm <sup>2</sup> /sec)
J1/PP1+Ex, 9.39% Fibre	2.09	2.36	2.74	2.6
J1/PP1+Ex, 19.78% Fibre	4.5	4.04	5.32	4.33
J1/PP1, 19.78% Fibre	5.2	4.91	5.78	5.99
J1/PP1+Ex, 31.34% Fibre	7.11	9.16	8.03	9.85

### 5.3.7. Influence of moisture absorption on the tensile strength and interfacial adhesion strength of the composites

The tensile properties of PP and macro-composites were tested after exposing in moisture 95 %RH at 23°C and 70°C for 7 days. The influence of humidity aging on mechanical properties of the samples is shown in Fig. 74 A, B. Clearly, an increase of the tensile strength occurs for both PP polymer and composites in humidity aging conditions. It is also important to note that the effect of humidity on the mechanical properties of the composites depends strongly on the temperature, fibre content and time of exposure. The increase of tensile strength of modified samples was found to be higher than that of unmodified samples at the same fibre content for both aging conditions at 23°C and 70°C, 95 %RH for 7 days. At the same exposed time, the improving tensile strength of the composites by humidity aging was observed to be higher at 23°C than at 70°C. For PP2, the humidity aging at 70°C caused a decrease of tensile strength at the same fibre content compared to untreated samples.

The tensile strength increase after aging is presumably due to the swelling effect as a result of the presence of water and possibly improved both interfacial adhesion and fibre strength. As aforementioned, the fibre fracture is limited in our specimens because of the fibre length is much less than the critical length, thereby the contribution due to fibre strength increase can be neglected. To estimate the contribution of interfacial adhesion strength to composite properties under aging, therefore, we can simply deduce the following formula based on (Eq 22) and assume no variation of fibre orientation factor and fibre length during conditioning:

$$\tau_w = \frac{d[(\Delta\sigma_c) + \Delta\sigma_m(V_f - 1)]}{\eta L_f V_f} + \tau_{app} \quad (\text{Eq. 36})$$

$$\Delta\sigma_c = \sigma_{cw} - \sigma_c ; \quad \Delta\sigma_m = \sigma_{mw} - \sigma_m \quad (\text{Eq. 37})$$

where

$\tau_{app}$ : the apparent interfacial shear strength

$\tau_w$ : the interfacial adhesion strength after aging

$\sigma_{cw}$  and  $\sigma_{mw}$ : tensile strength of composite and pure PP polymer after aging, respectively.

It should be pointed out here that the values at high fibre volume content of 31.34% have extremely high standard deviation, which is possibly associated with structural damage when fibre swelling is dominated in the composites. Except of these values, the equation can be fitted well to other data in Fig. 74. The interfacial adhesion values ( $\tau$ ) were calculated based on (Eq.36) and shown in Fig. 75 (Columns). The calculated interfacial adhesion values were found to significantly increase for both PP1 and PP2 after humidity aging at 23°C. The increasing interfacial adhesion was observed with lower degree for PP1 and level off for PP2 after aging at 70°C.

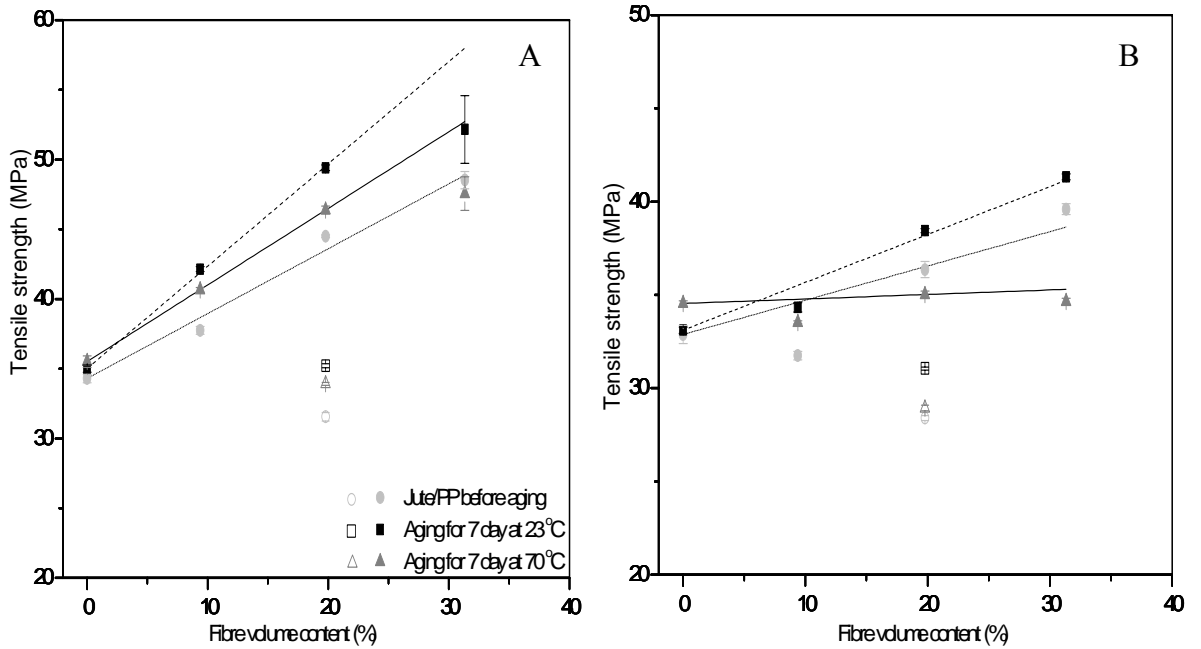


Fig. 74. Influence of humidity aging on tensile strength of neat PP polymer and composites based on (A) PP1 and (B) PP2, (filled symbols) with and (empty symbols) without Ex

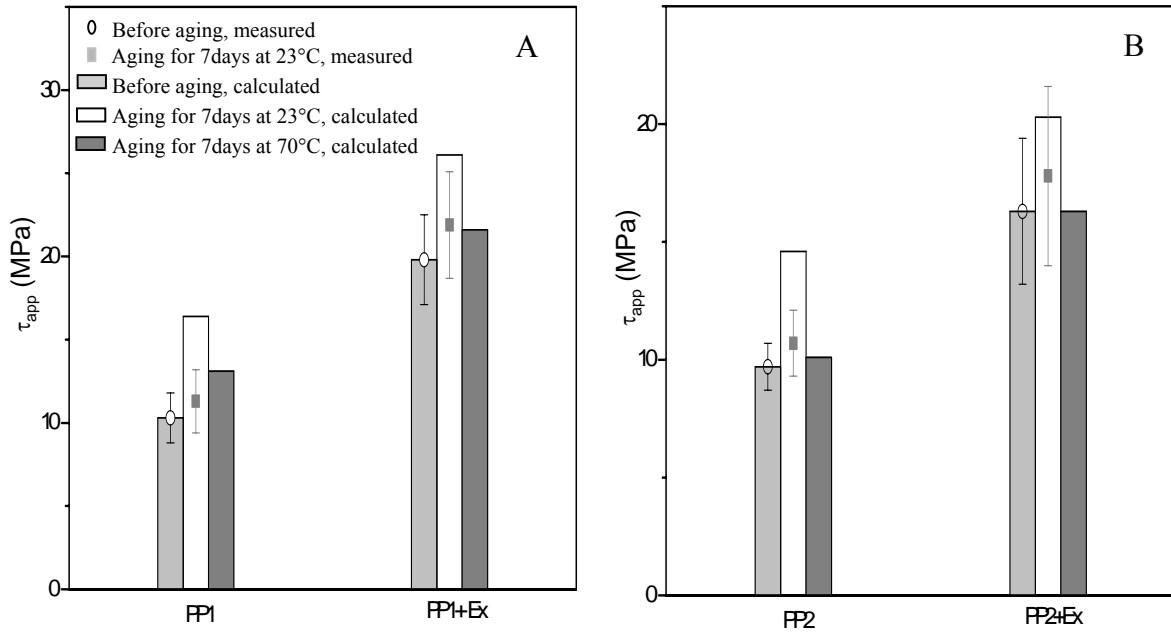


Fig. 75. Influence of humidity aging on interfacial adhesion strength of neat PP polymer and composites based on (A) PP1 and (B) PP2

This suggests that the major reason of composite tensile strength increase can be attributed to the improved polymer and interfacial adhesion strength after humidity aging. However at higher temperature of humidity aging, some damages happened at the same time of improving interfacial adhesion strength due to swelling.

To confirm the increase of interfacial adhesion strength due to swelling in humidity aging condition, the single fibre composites after aging in 95%RH at 23°C for 7 days were measured pull out test to get the interfacial adhesion strength. The experimental  $\tau$  values (symbols in Fig. 75) also shows an improvement of interfacial adhesion strength of the micro-composites by humidity aging. However, the experimental  $\tau_{app}$  values of the humidity aging are lower than the calculated  $\tau_{app}$  values. It could be explained that, the strength increases after aging mainly due to increase of interfacial shear strength ( $\tau_{app}$ ) in the micro-composite. However, the macro-composite strength increase is not only due to the interfacial shear strength increase but also depends on other factors such as: the increase of matrix strength, the increase of the composite strength after aging due to reduction of residual stress, which was formed during cooling of the injection moulding specimen. Therefore the calculated  $\tau_{app}$  values based on equation (36) are higher than the experimental  $\tau_{app}$  values.

### 5.3.8. Influence of moisture absorption on the dynamic mechanical behaviour

The influence of absorbed moisture on the temperature dependence of the storage modulus of jute/PP1 composites is shown in Fig. 76. Same as the control composites, the storage modulus of the aged composites was observed to decrease with increasing temperature and to increase with the increase of fibre content. At the same fibre content, the aged sample with modifier was found to have a higher storage modulus compared to the one without modifier.

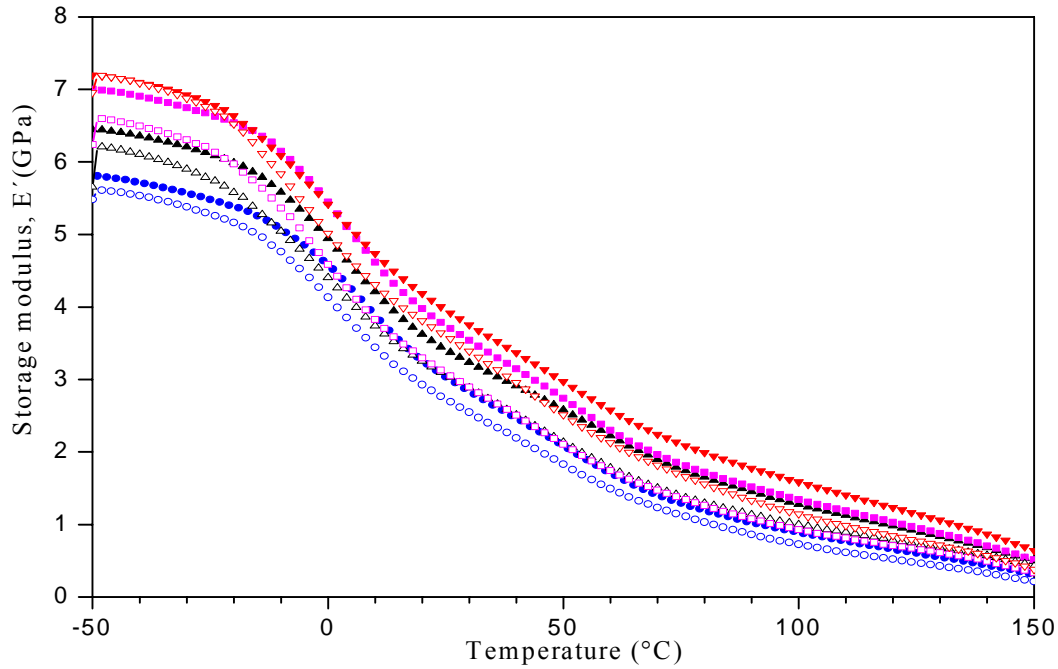


Fig. 76. Comparison of storage modulus of modified PP1 composites. Fibre content in control (filled symbols) and aged samples (empty symbols): ( $\circ, \bullet$ ) 9.39%, ( $\blacksquare, \square$ ) 19.78%; ( $\blacktriangledown, \triangledown$ ) 31.34% and ( $\blacktriangle, \triangle$ ) 19.78% without modifier

Comparing to the control samples, the storage modulus of moisture saturated samples was found to be lower at the same fibre content. Moreover, the glass-transition temperature, which decreased with fibre content, is lower in the cases of the aged composites compared to the control ones (Fig. 77). This may be explained as water molecules penetrate into the spaces between the cellulose molecular chains and facilitate the segmental motion in the amorphous region, therefore it has a plasticizing effect in the aged composites.

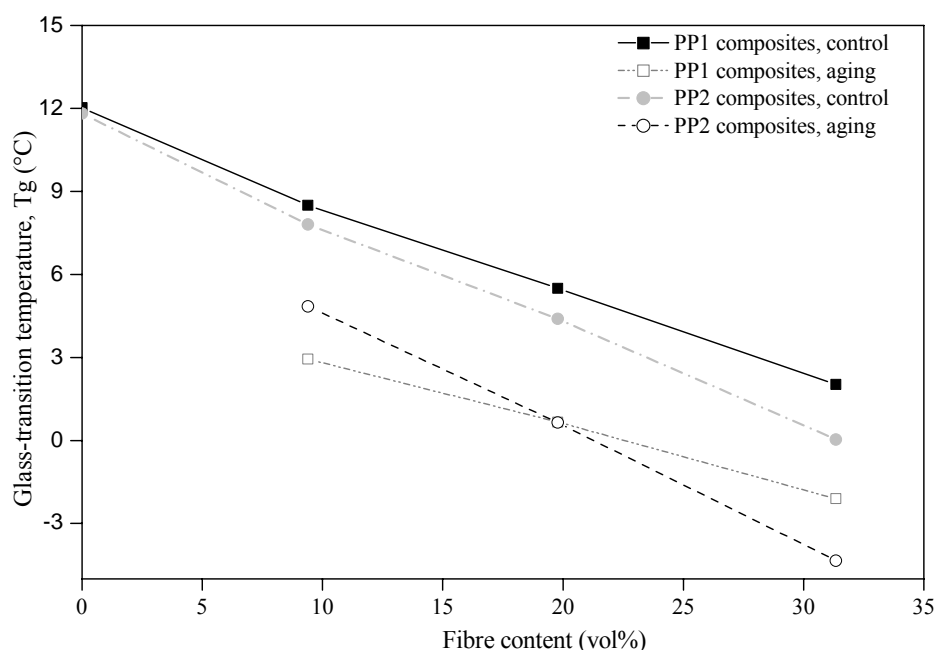


Fig. 77. Glass-transition temperature of modified PP composites before and after aging at different fibre contents

## 5.4. Jute/epoxy composites

### 5.4.1. Mechanical properties

#### 5.4.1.1. Alkaline fibre treatment

The influence of the alkaline treatment of jute fibres on the transverse tensile modulus and the transverse tensile strength of the unidirectional composites are shown in Fig. 78. It is clearly observed that the NaOH treatment improves the tensile strength but not tensile modulus. An improvement in the transverse tensile strength of the single layer fibre composites was observed with increasing from 19.71 MPa to 25.83 MPa in the case of fibre treatment by NaOH 1%, 4hours. This can be understood that the removal of the hemicellulose and a part of the lignin by alkali treatment can increase the interfacial adhesion between the matrix and NaOH treated fibre as explained in section 3.4.2.2. However, at higher alkali concentration (NaOH 5%), the tensile strength of the composites was observed to level off. It is possible that the interfacial adhesion is no further improved at higher concentration of NaOH. Therefore, the treatment condition of NaOH 1 wt%, 4 hours was assumed the optimal for the treatment.



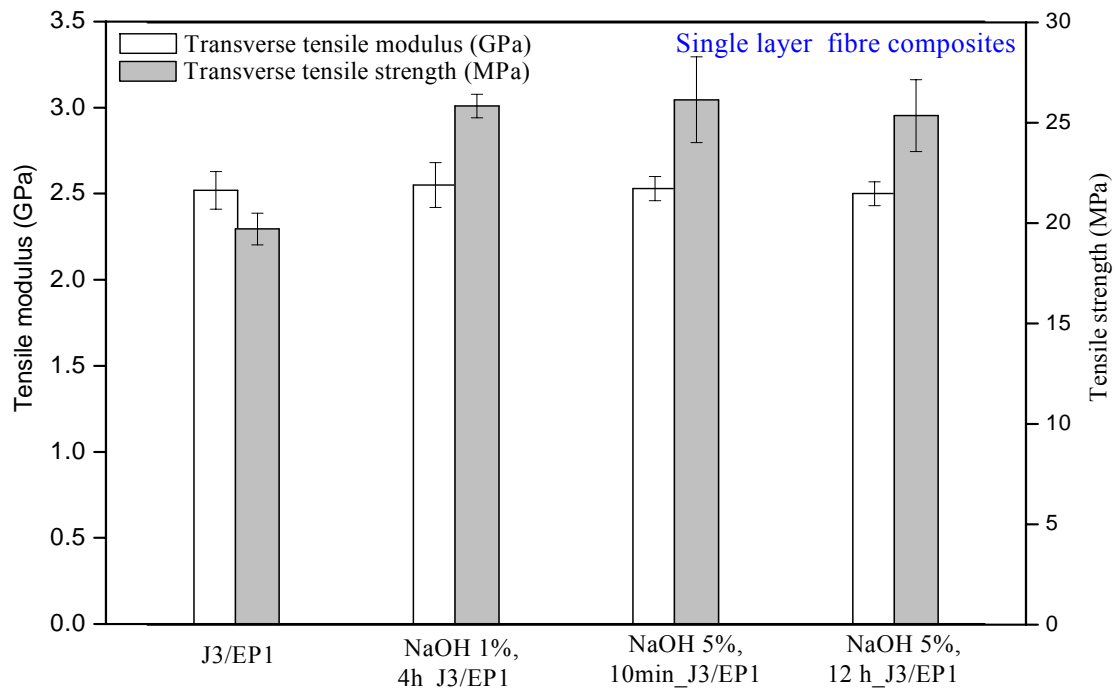


Fig. 78. Influence of the NaOH fibre treatment on the transverse tensile modulus and strength of unidirectional jute/epoxy composites

#### 5.4.1.2. Coupling agent and Sizing

The mechanical properties of unidirectional epoxy composites are given in Fig. 79 and Fig. 80. It can be clearly seen that the coupling agent and the sizing have a higher degree of influence on the strengths than on modulus in both tensile and bending tests. The transverse tensile strength of the untreated jute composite is about 23.6 MPa and increases with fibre treatments. An improvement of the transverse tensile strength was found about 32% for the sizing APS+XB and 25% for the coupling agent Y9669, reaching 31.18 MPa and 29.46 MPa, respectively. A lower transverse tensile strength of APS treated fibre than of APS+XB treated fibre was observed. It is assumed that the epoxy dispersion XB can react with APS and has a chemical structure similar to that of the epoxy matrix. Therefore, the APS+XB treated fibre may have better wetting by epoxy resin matrix and also the curing reaction with hardening catalyst similar to epoxy matrix. The better mutual diffusion as well as reaction between the epoxy dispersion and the epoxy matrix with hardener catalyst can make better adhesion at the interface. In contrast, it was observed that, the improvement of the transverse tensile strength for Y9669 treated fibre is better than for Y9669+XB treated one. It can be supposed that, the presence of phenyl group in aromatic silane Y9669 made the treated fibre surface less hydrophobic, which is suitable for epoxy matrix wetting. It is a necessary prerequisite to establish close contact and good adhesion

between the fibre and matrix [149]. The addition of XB may not contribute more wetting of the epoxy matrix. Moreover, the presence of the phenyl group in the aromatic silane Y9669 may hinder spatially the reaction between the amine group of the silane and epoxy group of epoxy dispersion. That makes the surface coating layer inhomogeneous. Therefore, the interfacial adhesion of the composites decreased slightly when the fibre is treated by the aromatic silane Y9669 in the presence of epoxy dispersion XB.

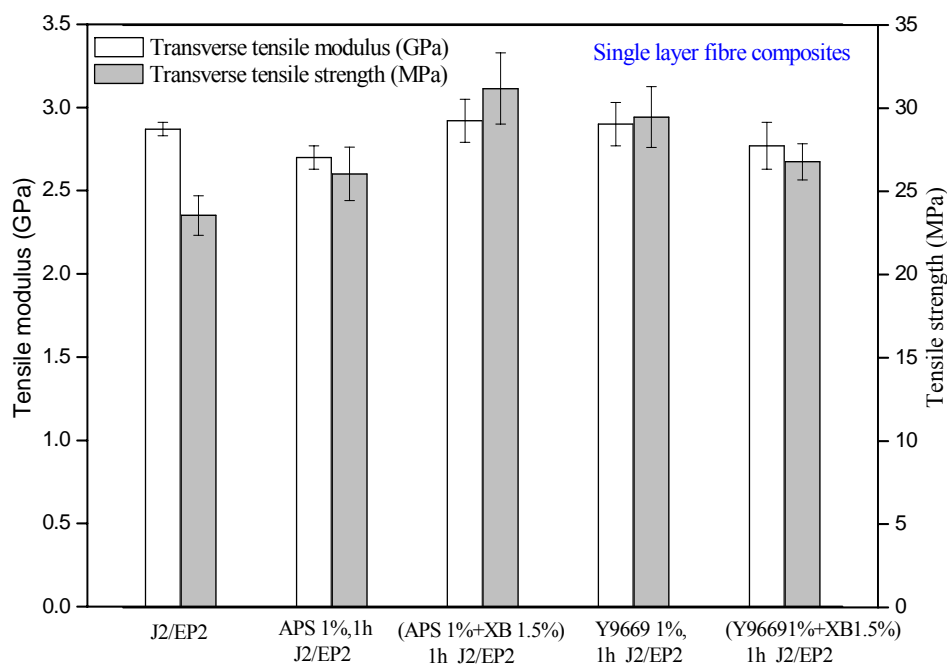


Fig. 79. Influence of the fibre sizings on the transverse tensile modulus and strength of unidirectional jute/epoxy composites

Furthermore, the fibre surface treatments showed same ranking to tensile strength but had lesser effect on the transverse bending strength. An increase by 13% for the sizing of APS+XB and by 15% for the sizing of Y9669 was evaluated. The fibre treatments by APS and Y9669+XB showed no improvement in the transverse bending strength of the composites (Fig. 80).

In general, the transverse bending strength is much greater than the transverse tensile strength which is due to the failure behaviour of the outermost resin layer much more involved in bending failure. However, in transverse tensile test the crack initiation starts at the fibre-matrix interface.

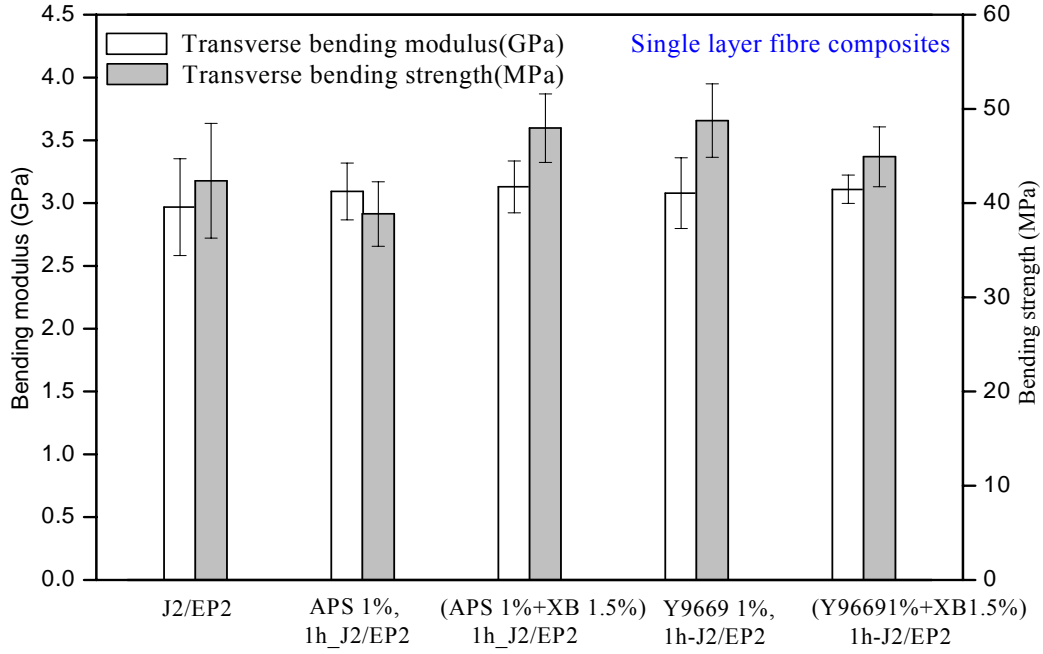


Fig. 80. Influence of the fibre sizings on the transverse bending modulus and strength of unidirectional jute/epoxy composites

#### 5.4.1.3. Combination of fibre alkali treatment with the coupling agent and the sizing

The influence of the combinations of the treatments on the mechanical properties was investigated. The sizing of APS+XB and coupling agent Y9669, which were estimated better than the others used. It is expected that the combination of alkali and silane treatment leads to slightly higher effects than the NaOH treatment at concentration of 1wt% for 4 hours only, which was chosen above to be the optimal condition for the alkali treatment. As the same alkali, coupling agent and size cases, the combinations of these treatments also did not significantly influence the tensile and bending modulus. However, both tensile and bending strengths increased with the treatments. The transverse tensile strengths of unidirectional jute/epoxy composites increased by 29%, 37% and 34% for NaOH, NaOH/(APS+XB) and NaOH/Y9669 treatments, respectively. Data is shown in Fig. 81. An improvement of transverse bending strengths of the unidirectional composites was also observed in the cases of fibre surface treatments (Fig. 82). Compared with untreated fibre composite, the transverse bending strength of NaOH treated fibre composite increased about 17% from 42.61 MPa to 49.86 MPa. A further increase of transverse bending strength was seen by 29% for NaOH/APS+XB treatment and by 27% for NaOH/Y9669 one, reaching 54.84 MPa and 53.97 MPa, respectively. That confirms the better interfacial adhesion using a combination of the treatments.

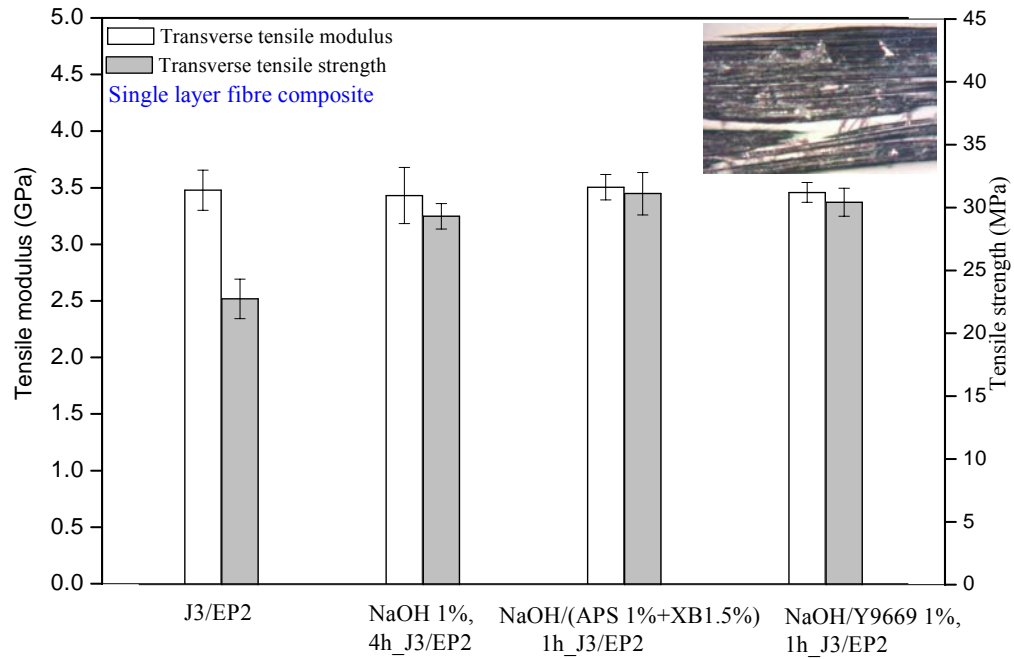


Fig. 81. Influence of the fibre treatments on the transverse tensile modulus and strength of unidirectional jute/epoxy composites (insert: optical microscopy image of a failure surface after transverse tensile test indicating the failure in weak regions at the interface)

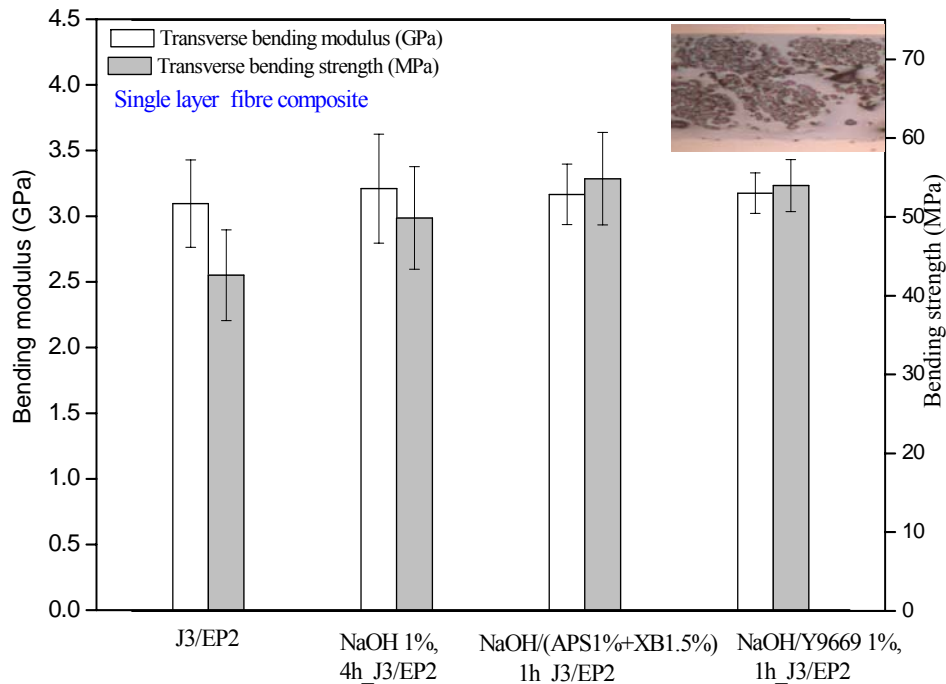


Fig. 82. Influence of the fibre treatment on the transverse bending modulus and strength of unidirectional jute/epoxy composites (insert: optical microscopy image of a polished cross section indicating the fibre/matrix distribution)

#### **5.4.2. SEM**

Microscopic images of fracture surfaces after tensile tests (A) and fibre surfaces (B) of the jute epoxy composites with and without treatments are compared in

Fig. 83. The presence of voids due to the failure of the interface was observed in the fracture surface of the untreated fibre composites. And, the untreated fibre surface after tensile test appeared relatively smooth. However, the fibre surface treatments lead to the improvement of the interfacial adhesion of the composites. The fewer breaks at the interfaces are seen. A stronger tear at the interface during the tensile test causes the high peak of resin remaining on the fibre surface. Therefore, the images of the fibre surfaces after tensile test became rougher. That can confirm better bonding between the fibre and matrix in the cases of the fibre surface treatments as was shown by bending and tensile test results in section 5.4.1.3.

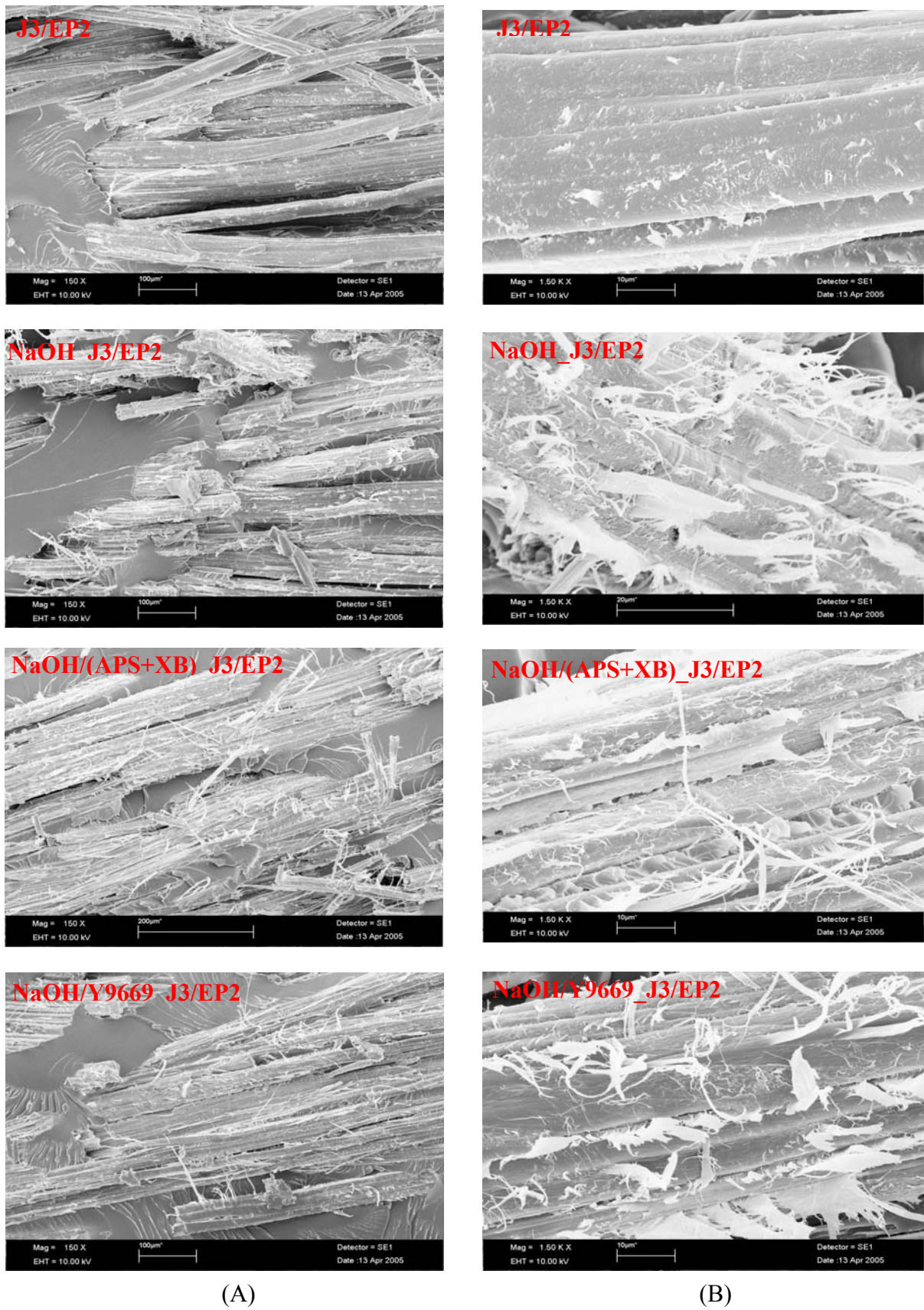


Fig. 83. SEM photographs of (A) fracture surfaces and (B) fibre surface after tensile test of unidirectional jute fibre epoxy composites

### 5.4.3. Dynamic mechanical analysis

The dynamic storage modulus curves ( $E'$ ) obtained at 1 Hz for the composite samples and non-reinforced epoxy matrix are shown in Fig. 84. It is readily apparent that the addition of the jute fibre increases the storage modulus of the epoxy matrix due to the highly stiff behaviour of the jute fibre. The NaOH treatment of the fibre increases the mechanical interlocking between the fibre and the matrix. Therefore, a stress transfer at the interface is more efficient, as reflected by a higher stiffness over the whole temperature range. In the cases of NaOH/(APS+XB) and NaOH/Y9669 composites, the interfacial adhesion was further improved due to the formation of covalent bond. Therefore, the storage moduli were found to be higher than both untreated and NaOH treated cases.

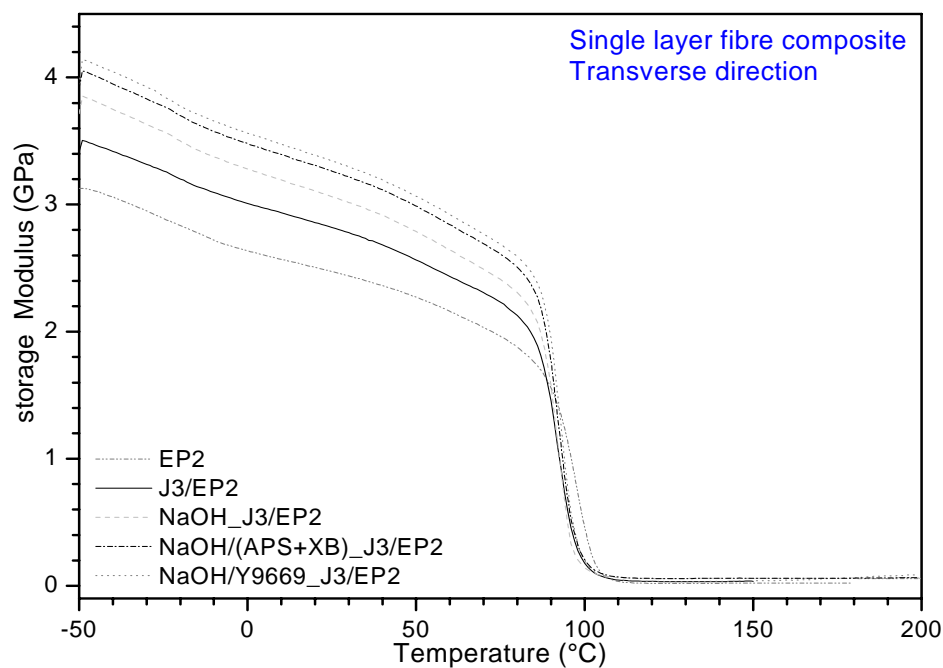


Fig. 84. storage modulus curves for epoxy sample and unidirectional jute/epoxy composites with and without fibre treatments as a function of temperature at a frequency of 1 Hz

Trends of change in the mechanical damping parameter  $\tan \delta$  of the samples with the temperature are shown in Fig. 85. The temperature corresponding to the peak for the epoxy sample and for the unidirectional jute/epoxy composites indicates the  $T_g$  for the epoxy matrix in the system [150]. The glass transition temperature is the highest for the bulk epoxy ( $T_g=106^\circ\text{C}$ ) and decreases in the presence of the fibre in both non-treated and treated cases ( $T_g \approx 100^\circ\text{C}$ ). It is expected that the proximity of the stiff fibre and preferential adsorption of readily diffusible



constituents as the amines, the low molecular weight curatives, on the fibre surface may impose a relatively high crosslink density due to notable depletion of the amine curative. Therefore, that causes the development of a more than expected stiffness level at the fibre-matrix interface and less complete curing in the bulk matrix close to interface. The matrix in the zone next to the interface becomes softer and hence the glass transition temperature of the fibre reinforced epoxy is lower than that of non-reinforced epoxy [150, 151].

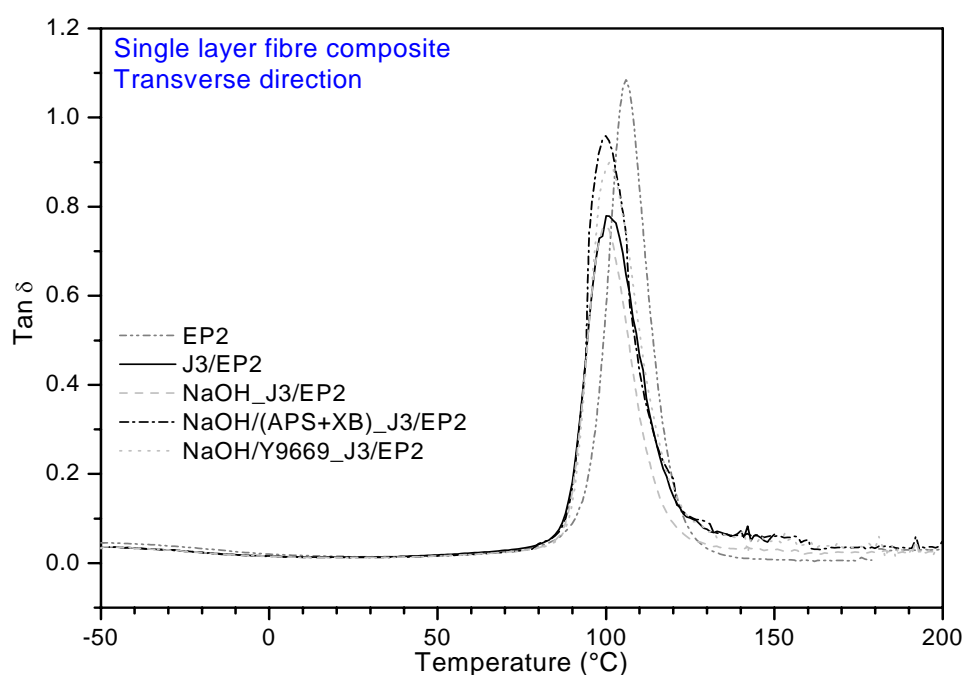


Fig. 85. Tan  $\delta$  curves for epoxy sample and unidirectional jute/epoxy composites with and without treatments versus temperature

Moreover, the peak height of the glass transition point ( $\tan \delta$ ) indicates the damping character of the sample. The relatively high viscoelastic damping parameter for the cured epoxy resin observed becomes substantially lowered while reinforcing with the jute fibre. It can be assumed that the interaction at the interface between the jute fibre and epoxy matrix would remarkably reduce the number of chain units engaged in the glass transition, causing a decrease in the peak amplitude compared with neat epoxy. For the composites, it is said that the damping peak height is related to the internal energy dissipation of the interphase, the matrix and the fibre [152, 153, 154]. The fibre volume fraction, fibre orientation angle and matrix type are assumed identical in the composites, the changes in the glass transition peak intensity can be contributed to the interfacial effect [151]. In the case of untreated and NaOH treated fibre composites, the secondary bond and mechanical interlocking between the fibre and the matrix play the



predominant role. However, besides the interfacial interaction mechanism resembled the above cases, the composites based on the fibres treated by coupling agent and sizing showed the presence of covalent bonds at the interface due to the reaction of functional groups in the coupling agent and sizing with hydroxyl group of the fibre and functional groups of epoxy matrix. The covalent bond is sparse enough to form the relative flexibility, resulting in a higher damping peak.

#### 5.4.4. Water absorption

The Fig. 86 shows the relationship between weight gain of the epoxy plate and the unidirectional jute epoxy composites in transverse direction versus the immersing time in water. The water absorption of the samples follow Fickian laws as characterized by a linear relationship between the weight gain and square root of time until reaching saturated status. In principle, the water uptake by a composite is mainly due to the sorption via fibre, matrix and fibre/matrix interface. Due to hydrophilic behaviour of the jute fibre, the epoxy composite contained the jute fibre has much higher water absorption than neat epoxy. It is clearly seen that the equilibrium water uptake by neat epoxy is only about 1.3 wt%, while the saturation value of the epoxy reinforced untreated jute fibre reaches 7.95 wt%. It is interesting to note that the fibre surface treatments lower the water diffusivity of the jute fibre composites. The improvement of the interfacial adhesion by NaOH treatment leads to lower water uptake of the composites, reaching 6.13 wt% at the saturated status. Moreover, the combinations of NaOH treatment with coupling agent and sizing further improved the water resistance of the samples. The NaOH/(APS+XB) and NaOH/Y9669 treated fibre composites were found to absorb the water up to 4.95 wt% and 5.04 wt%, respectively, at the saturated status. It can be explained by the building of chemical bonds as well as hydrogen bonds leading to stronger adhesion, which reduces the water uptake. The diffusion constants of the neat epoxy and jute epoxy composites were calculated using the Fickian diffusion equation and shown in Fig. 87. The diffusion constant of neat epoxy is about  $1.7 \times 10^{-7} \text{ mm}^2/\text{s}$  and increases significantly with the presence of the untreated jute fibre, reaching  $4.9 \times 10^{-7} \text{ mm}^2/\text{s}$ . However, the fibre surface treatments decrease the diffusivity of the composites compared to untreated case. The diffusion constants of the composites based on jute fibres treated by NaOH, NaOH/(APS+XB) and NaOH/Y9669 were determined to be  $3.69 \times 10^{-7}$ ,  $3.17 \times 10^{-7}$  and  $3.20 \times 10^{-7} \text{ mm}^2/\text{s}$ , respectively.

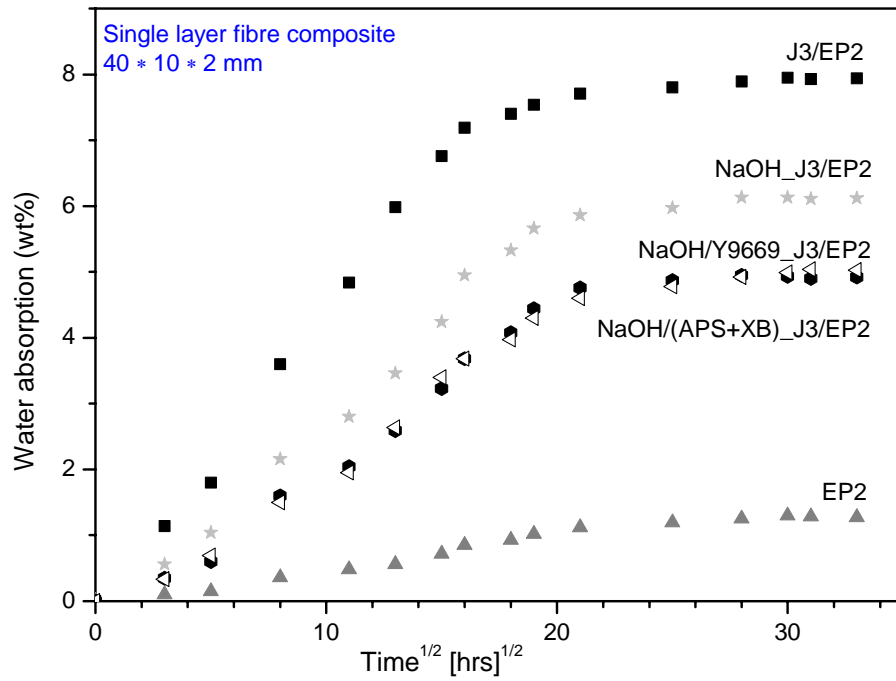


Fig. 86. Water absorption behaviour of epoxy plate and unidirectional jute/epoxy composite with and without treatments

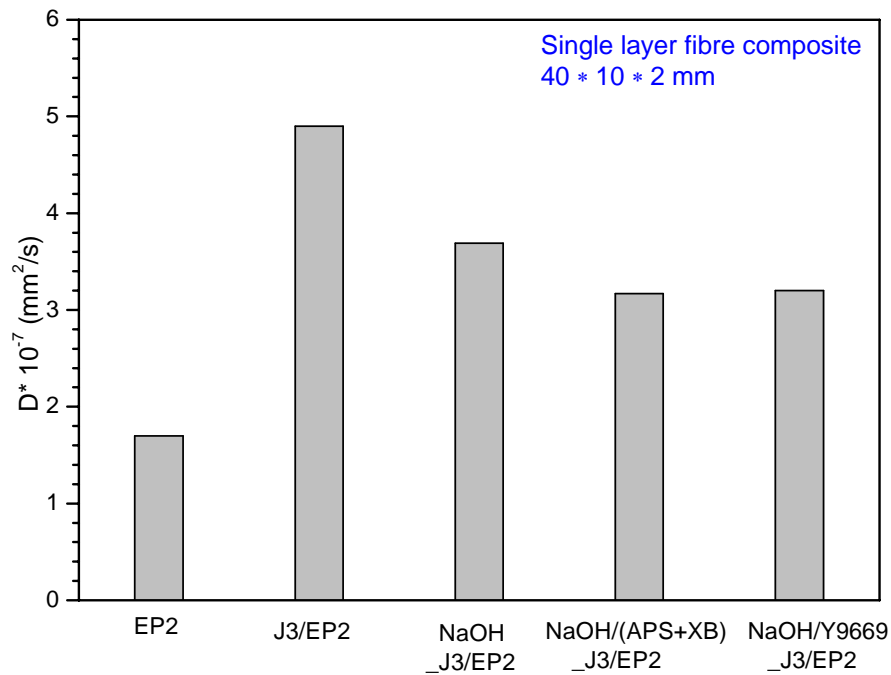


Fig. 87. The diffusion coefficient of epoxy plate and unidirectional jute/epoxy composite with and without treatments

## 6. Summary

This work comprises three main topics

- i) investigation of mechanical, thermal and wetting behaviour of jute fibres in the reference state, after dewaxing and after surface modification aimed at using as reinforcement fibres in composites.
- ii) investigation of mechanical, thermal and hygrothermal performance of jute/polypropylene composites influenced by polypropylene type, matrix modification by maleic anhydride grafted polypropylene and fibre volume fraction.
- iii) investigation of interfacial interaction and resulting mechanical properties in jute/epoxy composites influenced by alkali treatment and surface modification of jute fibres.

### 6.1. Fibres

- Jute fibres have a wide scatter of tensile strengths, which decreased with increasing gauge length from 5mm to 20mm and increased with jute fibre cross-sectional area at a constant gauge length.
- The measured fibre tensile strength actually increases with jute fibre cross-sectional area at a constant gauge length, which is inconsistent with the statistic failure behaviour of other brittle reinforcement fibres where the probability of critical defects causing fracture increases with increasing volume. The intrinsic tensile properties of jute fibres were found to be proportional to fibre cross-sectional area associated with its perfect circle shape. The previous commonly used Weibull model does not describe the tensile strength of the natural fibre when the cross-sectional area is considered.
- The fibre tensile strength increases slightly with a 4 hour alkali treatment by a 1wt % aqueous solution of NaOH. At more extreme conditions (NaOH 5%, 12 hours), the NaOH treatment hardly causes a further increase in tensile strength. A further surface modification by a silane coupling agent and a film former have no significant effect on the tensile strength of the fibre.
- Jute fibre has a high moisture absorption, which is different by the different resources. Fibre surface treatments by NaOH/(3-Aminopropyl-triethoxy-silane + Epoxy dispersion XB 3791) and NaOH/3-Phenylaminopropyl-trimethoxy-silane significantly reduced the moisture uptake.
- Surface treatments affect the wettability of the fibre. A higher wettability of the alkali treated fibre may be due to increasing fibre surface free energy after alkaline treatment.

However, a better wetting by resin on the fibre surface in the composites in the cases of coupling agent/film former may be obtained by the chemical similarity between the polymer matrix and the coupling agent/film former.

- The thermal stability of the fibre is improved in the cases of NaOH/(3-Aminopropyltriethoxy-silane + Epoxy dispersion XB 3791) and NaOH/3-Phenylaminopropyltrimethoxy-silane treatments.

## **6.2. Jute/polypropylene composites**

- The work has identified the effect of coupling agents on both interfacial and bulk mechanical properties of jute fibre/polypropylene composites, which is essential for the understanding of the macro-mechanical response to interfacial fracture.
- Three kinds of maleic anhydride grafted polypropylene (MAHgPP), namely Exxelor PO 1020 (Ex), Polybond 3200 (PO) and TPPP 8012 (TP) were used as matrix modifier. Ex was found to achieve the best mechanical properties at a content of 2 wt%.
- The addition of 2 wt% Ex to polypropylene matrices significantly improved the adhesion strength with jute fibres and in turn the mechanical properties of composites. The PP-grade also significantly affected the improvement of jute/PP composite by MAHgPP coupling agents. Higher molecular weight PP1 with less melt flow rates improved the mechanical properties to a greater extent than lower molecular weight PP2. The tensile modulus of jute/PP composites increased with increasing fibre content and showed less sensitive the variation of interfacial adhesion. Taking into account the interfacial properties, a modified rule of mixture (ROM) theory was formulated which fits well to the experimental tensile strength results.
- Thermal behaviour of the jute, PP and composites was determined different under nitrogen and air flows. The thermal resistance of PP1 composites decreased with increasing fibre content in nitrogen atmosphere. However, the TG curves of these composites in air shift towards a lower temperature region and the thermal resistance of composites was found to increase with increasing fibre content. Using 2 wt% Ex as a coupling agent has a positive effect on the thermal resistance of the composites.
- The diffusion process of water in jute/polypropylene composites followed Fickian model. An increase in moisture absorption was observed with increasing fibre content. At the same fibre content, the modified polypropylene composites have lower moisture absorption than that of unmodified ones.

- The jute fibre's saturation moisture absorption of 10 to ~26 wt% could be reached after humidity aging at different relative humidities.
- An increase of the tensile strength occurred for jute/PP composites after humidity aging, which is attributed to the improved both polymer and interfacial adhesion strength.
- Using jute fibre as the reinforcement increased the storage modulus, with increasing fibre content. However, the moisture uptake caused a decrease in the storage modulus for most temperatures and also in glass-transition temperature at the same fibre content.

### **6.3. Jute/epoxy composites**

- For the epoxy matrix, fibre surface treatment by alkali, organosilane, epoxy dispersions and the combinations lead to better interfacial adhesion. Especially the presence of coupling agent or epoxy film former, incorporated into the composites to tailor the chemical structure, lead to improved interfacial adhesion, through chemical bonds between the fibre and coupling agent/film former and the coupling agent/ film former and matrix.
- 1 wt% NaOH for 4 hours was found to be the optimal condition for the fibre surface treatment. Higher concentrations of NaOH did not further improve the interfacial adhesion. The combination of the silane with epoxy dispersion is efficient with an aliphatic silane (3-Aminopropyl-triethoxy-silane), but not with an aromatic silane (Phenylaminopropyl-trimethoxy-silane).
- The combination of alkali treatment and coupling agent (Y9669) or sizing (APS+XB) lead to slightly improved interfacial interaction than the NaOH treatment only. Therefore, the storage modulus of the NaOH/(APS+XB) and NaOH/Y9669 treated fibre composites were higher than both untreated and NaOH treated ones.
- The transverse tensile strengths of unidirectional jute/epoxy composites (J3/EP2) increased by 29%, 37% and 34% and the transverse bending strength increased by 17%, 29%, 27% for NaOH, NaOH/(APS+XB) and NaOH/Y9669 treatments, respectively. However, the fibre surface treatment did not significantly influence the tensile and bending modulus because of same fibre volume contents.
- The water absorption of the jute/epoxy composites also follows a Fickian model. The fibre surface treatments decrease the water uptake and the diffusivity of the composites compared to the untreated state.

The properties of jute/epoxy composites were investigated by using samples reinforced by single jute yarn layer, in transverse direction. Further research should focus on a variation of fibre content. Macro-mechanical parameters of longitudinal fibre composites should be measured and the “rule of mixture” should be used to estimate the experimental data of this system.

## References

- /1/ Mohanty A K, Misra M, Drzal L T. Sustainable Bio-Composites From Renewable Resources: Opportunities and Challenges in the Green Materials World. *Journal of Polymers and the Environment* 2002. Accepted June 30, Vol 10, Issue 1,19-26.
- /2/ Thomas GS. Renewable Materials for Automotive Applications.Daimler-Chrysler AG, Stuttgart.
- /3/ Bledzki AK, Sperber VE. and Faruk O. Natural and Wood Fibre Reinforcement in Polymers. *Rapra Review Reports*, Vol.13, No. 8, Report 152, 2002. University of Kassel.
- /4/ Karus M, Ortmann S, Vogt G D. Use of natural fibres in composites in the German automotive production 1996 till 2003. Nova-Institute, September 2004.
- /5/ Eckert C. Opportunities for natural fibres in plastic composites, presented at 3 rd Annual Ag Fibre Technology Showcase 2000, Memphis, TN, USA.
- /6/ Karus M, Kaup M and Lohmeyer D. Study on Markets and Prices for Natural Fibres (Germany and EU). FNR-FKZ: 99NR163, nova Institute, 2000.
- /7/ Beckmann A and Kleinholz R. Proceedings 2. Internationales Symposium “Werkstoffe aus Nachwachsenden Rohstoffen”, Erfurt, Germany 1999.
- /8/ Ishak Z A M, Yow B N, Ng B L, Khalil H P S A, Rozman H D. J. *Applied Polymer Science* 2001, 81, 742-753.
- /9/ Lin Q, Zhou X, Dai G. *Journal of Applied Polymer Science* 2002, 85, 2824-2832.
- /10/ Joseph P V, Rabello M S, Mattoso L H C, Joseph K, Thomas S. *composites science and technology* 2002, 62, 1357-1372.
- /11/ Stamboulis A, Baillie C A, Garkhail S K, Van Melick H G H and Peijs T. Environmental durability of flax fibers and their composites based on polypropylene matrix. *Applied Composite Materials* 2000, 7, 273-294.
- /12/ Stamboulis A, Baillie C A, Peijs T. Effects of environmental conditions on mechanical and physical properties of flax fibres. *Composites Part A* 2001, 32, 1105-1115.
- /13/ Tajvidi M, Ebrahimi G. *Journal of Applied Polymer Science* 2003, 88, 941-946.
- /14/ Bledzki A K, Gassan J. Composites reinforced with cellulose based fibres. *Progress in Polymer Science* 1999, 24, 221-274.
- /15/ Fung K L, Li R K Y., Tjong S C. Interface modification on the properties of sisal fiber-reinforced polypropylene composites. *Journal Applied Polymer Science* 2002; 85: 169-176.

- /16/ Mohanty A K, Drzal L T, Misra M. Journal of Materials Science Letters 2002, 21, 1885-1888.
- /17/ Joseph P V, Joseph K, Thomas S, Pillai C K S, Prasad V S, Groeninckx G, Sarkissova M. The thermal and crystallisation studies of short sisal fibre reinforced polypropylene composites. Composites Part A 2003, 34, 253-266.
- /18/ Feng D, Caulfield D F, Sanadi A R. Effect of compatibilizer on the structure-property relationships of kenaf-fiber/polypropylene composites. Polymer Composites 2001, 22, 4, 506-517.
- /19/ Sanadi A R, Caulfield D F. Transcrystalline interphases in natural fibre-PP composites: effect of coupling agent. Composite Interfaces 2000, 7 (1), 31-43.
- /20/ Qiu W, Zhang F, Endo T, Hirotsu T. Preparation and characteristics of composites of high-crystalline cellulose with polypropylene: effects of maleated polypropylene and cellulose content. Journal of applied Polymer Science 2003, 87, 337-345.
- /21/ Rana A K, Mandal A, Bandyopadhyay S. Short jute fibre reinforced polypropylene composites: effect of compatibiliser, impact modifier and fibre loading. Composites Science Technology 2003, 63, 801-806.
- /22/ Karmaker, A C, Hoffmann A, Hinrichsen G. Influence of water uptake on the mechanical properties of jute fiber-reinforced polypropylene. Journal Applied Polymer Science 1994, 54, 1803-1807.
- /23/ Karmaker A C, Youngquist J A. Injection molding of polypropylene reinforced with short jute fibres. Journal Applied Polymer Science 1996, 62, 1147-1151.
- /24/ Kamaker A C. Effect of water absorption on dimensional stability and impact energy of jute fibre reinforced polypropylene. Journal of Material Science Letters 1997, 16, 462-464.
- /25/ Gassan J, Bledzki A K. The influence of fiber-surface treatment on the mechanical properties of jute-polypropylene composites. Composites Part A 1997; 28A (12), 1001-1005.
- /26/ Gassan J, Bledzki A K. Influence of fiber surface treatment on the creep behavior of jute fiber-reinforced polypropylene. J of Thermoplastic Composite Materials Sep 1999; 12 (5), 388-398.
- /27/ Paunikallio T, Kasanen J, Suvanto M, Pakkanen T T. Influence of maleated polypropylene on mechanical properties of composite made of viscose fiber and polypropylene. Journal Applied Polymer Science 2003, 87, 1895-1900.



- /28/ Snijder M.H.B., E.J.M. Reinerink and H.L. Bos, Proceeding. 2nd International Symposium. On Natural Polymers and Composites 1998, Brazil.
- /29/ Ray D, Sarkar B K, Rana A K and Bose N R. Effect of alkali treated jute fibres on composite properties. Bulletin of Materials Science 2001, 24,2:129-135.
- /30/ Mishar S, Misra M, Tripathy S S, Nayak S K and Mohanty A K. Graft copolymerization of acrylonitrile on chemically modified sisal fibers. Macromolecular Material and Engineering 2001 b, 286, 2:107-113.
- /31/ Ray D, Sarkar B K, Das S, Rana A K. Dynamic mechanical and thermal analysis of vinylester-resin-matrix composites reinforced with untreated and alkali-treated jute fibres. Comp Sci and Tech 2002, 62, 911-917.
- /32/ Ray D, Sarkar B K, Basak R K, Rana A K. Study of thermal behaviour of alkali-treated jute fibres. J Appl Polym Sci 2002, 85, 2594-2599.
- /33/ Ray D, Sarkar B K, Rana A K. Fracture behavior of vinylester resin matrix composites reinforced with alkali-treated jute fibres. Journal Applied Polymer Science 2002, 85, 2588-2593.
- /34/ Mwaikambo L Y, Ansell M P. Hemp fibre reinforced cashew nut shell liquid composites. Composite Science and Technology 2003, 63, 1297-1305.
- /35/ Gassan J, Bledzki A K. Possibilities for improving the mechanical properties of jute/epoxy composites by alkali treatment of fibres. Composites Science Technology 1999, 59, 1303-1309.
- /36/ Prasad S V, Pavithan C, Rohatgi P K. Alkali treatment of coir fibres for coir–polyester composites. Journal Material science 1983, 18, 1443-1454.
- /37/ Sydenstricker T H D, Mochnaz S, Amico S C. Pull-out and other evaluations in sisal-reinforced polyester biocomposites. Polymer Testing 2003, 22, 375-380.
- /38/ Culler SR, Ishida H and Koenig J L. The silane interphase of composites: effects of process conditions on  $\gamma$ -aminopropyltriethoxysilane. Polymer Composites 1986, 7(4), 231-238.
- /39/ Ghatge N D and Khisti R S. Performance of new silane coupling agents along with phenolic no-bake binder for sand core. Journal of Polymer Materials 1989, 6,145-149.
- /40/ George J, Bhagawan S S. and Thomas S. Improved interactions in chemically modified pineapple leaf fibre reinforced polyethylene composites. Composite Interfaces 1998, 5(3), 201-223.

- /41/ George J, Ivens J and Verpoest I. Die Angewandte Makromolekulare Chemie 1999, 272, 17.
- /42/ Gassan J, Bledzki A J. Effect of moisture content on the properties of silanized jute-epoxy. Polym Composites 1997, 18, 2, 179-184.
- /43/ Yan Li, Yiu-Wing Mai and Lin Ye. Effects of fibre surface treatment on fracture-mechanical properties of sisal-fibre composites. Composite Interfaces 2005, 12, 1-2, 141–163.
- /44/ Mäder E. and Gliesche K. Langfaserverstärkte Kunststoffe auf der Basis von Naturfasern. 7<sup>th</sup> International Techtexil-Symposium, Frankfurt, Germany, 20-22. 6. 1995.
- /45/ Booth and C. Price. Fibre, vegetable. Comprehensive polymer science Vol 7, pp 22. ed. by C., Pergamon, Oxford, 1989.
- /46/ Per Ole Olesen. Perspectives on the performance of natural plant fibres. The Royal Veterinary and Agricultural University, Taastrup, Denmark. Conference 27 – 28 May 1999, Copenhagen, Denmark.
- /47/ Eichhorn S J, Baillie C A, Zafeiropoulos N, Mwaikambo L Y, Ansell M P, Dufresne A, Entwistle K M, Herrera-Franco P J, Escamilla G C, Groom L, Hughes M, Hill C, Rials T G, Wild P M. Review current international research into cellulosic fibres and composites. Journal of Material Science and technology 2001, 36, 2107-2131.
- /48/ Martin H B Snijder. Reinforcement of commodity plastic by hemp and flax fibres- Extending the market opportunity. Canada, bio-based products mission, march-2004.
- /49/ Hon D N S, Shiraishi N. Wood and cellulosic chemistry, 2 ed.. Marcel Dekker: New York, 2001.
- /50/ Farabee M J. The Online Biology Book. Estrella Mountain Community College, in sunny Avondale, Arizona.
- /51/ Mohanty A K, Misra M and Hinrichsen G. Biofibers, biodegradable polymers and bio-composites: An overview. Macromolecular Materials and Engineering 2000 a, 276/277, 1-24.
- /52/ Bei Wang. Pre-treatment of flax fibers for use in rotationally molded bio-composites, Master thesis 2004. Department of agricultural and bio-resource engineering, university of Saskatchewan, Canada.
- /53/ Mohanty A K, Misra M, Drzal L T. Surface modifications of natural fibers and performance of the resulting biocomposites: An overview. Composite Interfaces, Volume 8, Number 5, 1 October 2001, 31, 313-343.

- /54/ Polymerwerkstoffe- lecture from Prof. Heindrich, IPF Dresden, Germany.
- /55/ Concise encyclopedia of Composite Materials, Pergamon Press, Oxford New York, Beijing, Frankfurt, 1989. Editor Anthony Kelly CBE, FRS.
- /56/ Jacob M, Joseph S, Pothan L A and Thomas S. A study of advances in characterization of interfaces and fiber surfaces in lignocellulosic fiber-reinforced composites. *Composite Interfaces* 2005, 12, 1-2, 95–124.
- /57/ Bump M M B. The effect of chemistry and network structure on morphological and mechanical properties of diepoxide precursors and poly(hydroxyethers). Doctor thesis 2001, Blacksburg, Virginia.
- /58/ Mäder E, Pisanova E. Interfacial design in fibre reinforced polymers. *Macromol. Symp.* 2001, 163, 189-212.
- /59/ George J, Ivens J, Verpoest I. Mechanical properties of flax fibre reinforced epoxy composites. *Die Angewandte Makromolekulare Chemie* 1999, 272, 41-45, Nr. 4747.
- /60/ Anon. Silane coupling agents. Dow Corning Corporation, Form No.23-0120-90.
- /61/ Löwenstein K L. The manufacturing technology of continuous glass fibres. Elsevier Science publishers B.V. Netherlands, 1993.
- /62/ Doan T-T-Loan, Mäder E. Performance of jute fibre reinforced polypropylenes. Poster of 5<sup>th</sup> Global Wood and Natural Fibre Composites Symposium, April 27-28, 2004, Kassel, Germany.
- /63/ Mali J, S P, Leena S L, Sini M K, Jouko P, Markku V, Tuula K, Stella T. Woodfibre-plastic composites. Report on 31.12.2003
- /64/ Introduction to composites. Reference handbook. Editor: Tara E. Miller. New York: Composites Institute, 1998, 47-48.
- /65/ Amico S C, Mochnaz S and Costa T H S. Tensile strength of the sisal fibres II: Influence of chemical treatment from the point of view of a Weibull distribution. IX international macromolecular Colloquium.
- 66/ Arnold N T, Martin P A, Marie-laetitia P and David E P. Weibull analysis of microbond shear strength at sisal fibre–polyester resin interfaces. *Composite Interfaces* 2005, 12, 1-2, 77–93.
- /67/ David M Wilson. Statistical tensile strength of Nextel™ 610 and Nextel™ 720 fibres. 3M Metal matrix composites department, St. Paul, Minnesota 55144-1000.

- /68/ Pickering K L, Abdalla A, Ji C, McDonald A G, Franich R A. The effect of silane coupling agents on radiata pine fibre for use in thermoplastic matrix composites. *Composites Part A* 2003, 34, 915-926.
- /69/ Briggs D, Hearn M J, Hodge D J, Middlemiss B, Peacock J A. Correlation between fibre surface energetics and fibre-matrix adhesion in carbon fibre reinforced PEEK composites. The R&D solution to surface wettability analysis, a primer on dynamic contact angle technology, Seminar Thermal Analysis, Ankersmit-Cahn, December 4, 1996, Groot-Bijgaarden.
- /70/ Drzal L T, Mescher J A, Hall D T, *Carbon* 1979, 17, 375.
- /71/ Bascom W D. *Modern Approaches to Wettability: Theory and Applications*. M E Schrader, G. Loeb (Eds.), Plenum Press, New York, 1992, p. 366.
- /72/ Miller B. *Surface Characteristics of Fibres and Textiles, Part II*. M. J. Schick (Ed.), Marcel Dekker Inc., New York 1977, p. 417.
- /73/ Van de Velde K, Kiekens P. Wettability of natural fibres used as reinforcement for composites. *Die Angewandte Makromolekulare Chemie* 1999, 272, 87–93, Nr. 4761.
- /74/ Liu F P, Gardner D J, Wolcott M P. 1994. A model for the prediction of polymer surface dynamic behavior Part I. Contact angle vs. polymer surface properties. 208<sup>th</sup> National ACS Meeting, Warhington, DC.
- /75/ Gassan J, Gutowski V S, Bledzki A K. About the surface characteristics of natural fibres. *Macromolecular Material Eng* 2000, 283, 132-139.
- /76/ Van De Velde K and Kiekens P. Influence of fibre surface characteristics on the flax/polypropylene interface. *Journal of Thermoplastic Composite Materials* 2001, 14, 244 - 260.
- /77/ Cantero G, Arbelaiz A, Llano-Ponte R, Mondragon I. Effects of fibre treatment on wettability and mechanical behaviour of flax/polypropylene composites. *Composites Science Technology* 2003, 63, 1247-1254.
- /78/ Akita K, Kase M. *Journal of Polymer Science and technology* 1967, A-1 5:833
- /79/ Wielage B, Lampke Th, Marx G, Nestler K, Starke D. Thermogravimetric and differential scanning calorimetric analysis of natural fibres and polypropylene. *Thermochimica Acta* 1999, 337, 169-177.

- /80/ Paunikallio T, Suvanto M, Pakkanen T T. Composition, tensile properties, and dispersion of polypropylene composites reinforced with viscose fiber. *Journal Applied Polymer Science* 2004, 91, 2676 - 2684.
- /81/ Mohanty A K, Drzal L T and Misra M. Engineered natural fibre reinforced polypropylene composites: influence of surface modifications and novel powder impregnation processing. *J Adhe Science and technology* 2002, 16, 8, 999-1015.
- /82/ Rana A K, Basak R K, Mitra B C, Mark Lawther A N. Banerjee. Studies of acetylation of jute using simplified procedure and its characterization. *Journal of Applied Polymer Science* 1997, 64, 1517.
- /83/ Mitra B C, Basak R K, Sarkar M. Studies on jute-reinforced composites, its limitations, and some solutions through chemical modifications of fibres. *Journal of Applied Polymer Science* 1998, 67, 1093–1100.
- /84/ Digital Instruments. Dimension<sup>TM</sup> 3100 Instruction Manual Version 4.31, 25.08.1997, NanoScope Command Reference Manual Version 5.12 Revision B. 03.04.2001.
- /85/ Gao S-L, Mäder E, Zhandarov S. Carbon fibres and composites with epoxy resins: Topography, fractography and interphases. *Carbon* 2004, 42, 515-529.
- /86/ Gao S-L, Mäder E. Characterisation of interphase nanoscale property variations in glass fibre reinforced polypropylene and epoxy resin composites. *Composite part A* 2002, 33, 559-576.
- /87/ Thornton J et al. Training book. Digital Instruments. Digital. Instruments NanoScope<sup>TM</sup> Scanning Probe Microscopes 1999.
- /88/ George J, Ivens J, Verpoest I. Mechanical properties of flax fibre reinforced epoxy composites. *Die Angewandte Makromolekulare Chemie* 2000, 272, 1, 41 – 45.
- /89/ Piggott M R. In *Interfacial Phenomena in Composite Materials* 91, ed. I. Verpoest and F.R. Jones, Butterworth- Heinemann, Oxford, 1991, 3.
- /90/ Kelly A, Tyson W R. Tensile properties of fibre reinforced metals-copper/tungsten and copper/molybdenum. *J Mechanical Physics. Solids* 1965, 13, 329-50.
- /91/ Madell J F, Chen J H & Mc Garry FJ. A micro-debonding test for in situ assessment of fibre/ matrix bond strength in composite materials. *Int Journal Adhesion Adhesives* 1980, 1, 40-4.
- /92/ Penn L. S., Bowler E. R. A new approach to surface energy characterization for adhesive performance prediction. *Surf. Interfac. Ana.* 1981, 3, 161-4.

- /93/ Miller B, Muri P, Rebenfeld L. A microbond method for determination of the shear strength of a fibre-resin interface. *Composite Science and Technology* 1987, 28,17-32.
- /94/ Wang C. Fracture mechanics of single fibre pull-out test. *Journal of materials science* 1997, 32, 483-490.
- /95/ Kerans RJ, Parthasarathy TA. Theoretical analysis of the fibre pull-out and push-out test. *J. Am Ceram Soc* 1991, 74,1585-96.
- /96/ Liu CH, Nairn JA. Analytical fracture mechanics of the micro-bond test including the effect of friction and thermal stresses. *Int J Adhesion Adhesive* 1999, 19, 59-70.
- /97/ Zhandarov S, Mäder E. Characterization of fibre/matrix interface strength: applicability of different tests, approaches and parameters. *Composites Science and Technology* 2005, 65, 149-160.
- /98/ Jenschke W. Bedienungsanleitung und technische Programmbeschreibung zum Programm Pullout 2, Version 2.0. Leibniz-Institut für Polymerforschung Dresden e. V., Abt. FK. September 2003.
- /99/ Mäder E. Grenzflächen, Grenzschichten und mechanische Eigenschaften faserverstärkter Polymerwerkstoffe. Habilitationsschrift, Technische Universität Dresden, Dresden 2001.
- /100/ Jenschke W. Bedienungsanleitung und technische Programmbeschreibung zum Programm PullOut2 Version 2.0. IPF Abt. FK 2003.
- /101/ Stamboulis A , Baillie C, Schulz E. Interfacial characterisation of flax fibre-thermoplastic polymer composites by the pull-out test. *Die Angewandte Makromolekulare Chemie* 1999, 272, 117-120. Nr. 4759.
- /102/ Manchado M A, Lopez Arroyo M, Biagiotti J, Kenny J M. Enhancement of mechanical properties and interfacial adhesion of PP/EPDM/flax fibre composites using maleic anhydride as a compatibilizer. *Journal of Applied Polymer Science* 2003, 90, 8, 2170-2178.
- /103/ Joseph K,Varghese S, Kalaprasad G, Thomas S, Prasannakumari L, Koshy P, Pavithran C. Influence of interfacial adhesion on the mechanical properties and fracture behaviour of short sisal fibre reinforced polymer composites.*European Polymer Journal* 1996, 32, 10, 1243-1250.
- /104/ Garcia-Hernandez E, Licea- Claverie A, Zizumbo A, Alvarez- Castillo A, Herrera-Franco P J. Improvement of the interfacial compatibility between sugar cane bagasse fibres and polystyrene for composites. *Polymer Composites* 2004, 25, 2.

- /105/ Mäder E, Grundke K, Jacobasch HJ, Panzer U. Interphase characterization in reinforced polymers. In: Proceedings of 31<sup>st</sup> international man-made fibre congress, Dornbirn, Austria: 1989.
- /106/ Rao R M, Balasubramanian N and Chanda M. Factors Affecting Moisture Absorption in Polymer Composites. Part-1: Influence of Internal Factors. Environmental effects on Composite Materials 1988, 3, 75-87.
- /107/ Rong M Z, Zhang M Q, Liu Y, Zhang Z W, Yang G C, Zeng H M. Mechanical properties of sisal reinforced composites in response to water absorption. Polymers & Polymer Composites 2002, 10, 6, 407- 426.
- /108/ Bledzki A K, Faruk O. Creep and impact properties of wood fibre-polypropylene composites: influence of temperature and moisture content. Composite Science and Technology 2004, 64, 693-700.
- /109/ Aurich T, Mennig G. Determination of interfacial shear strength and critical fibre length in injection moulded flax fibre reinforced polypropylene. Advanced Composite Letters 2001, 10, 6, 299-303.
- /110/ Cabral H, Cisneros M, Kenny J M., Vazquez A and Bernal C R. Structure properties relationship of short jute fibre-reinforced polypropylene composites. Journal of Composite Materials 2005, 39, 1, 51-65.
- /111/ Keller A, Compounding and mechanical properties of biodegradable fibre composites. Composites Science Technology 2003, 63, 1307-1316.
- /112/ Biagotti J, Lopez-Manchado M A, Moreschi G, Kenny J. M. Effects of vegetal fibers on the processing and properties of polypropylene matrix composites:a comparative study. 22. Int. SAMPE Europe Conference, 27.-29.03.2001, Paris.
- /113/ Hornsby P R, Hinrichsen E, Tarverdi K. Preparation and properties of polypropylene composites reinforced with wheat and flax straw fibres. Part II Analysis of composites microstructure and mechanical properties. Journal of Materials Science 1997, 32, 1009-1015.
- /114/ Jayaraman K. Manufacturing sisal-polypropylene composites with minimum fibre degradation. Composites Science Technology 2003, 367-374.
- /115/ Massimo Baiardo, Elisa Zini, Mariastella Scandola. Flax fibre-polyester composites. Composites part A 2004, 35, 703-710.

- /116/ Gao S-L, Mäder E, Plonka R. Surface flaw sensitivity of glass fibres with carbon nanotube/polymer coating. Int. Conf. On Composite Materials (ICCM-15) 2005, Durban, South Africa.
- /117/ Hirsch T J. Journal of the American Ceramics Institute 1962, 59, 427–452.
- /118/ Springer G S and Shen C H. Moisture absorption and desorption of composite materials. Environmental effects on composite materials 1988, 3, 15-33.
- /119/ Gopalan R, Rao R M, Murthy M V and Dattaguru B. Diffusion studies on advanced fibre hybrid composites. Environmental effects on composite materials 1988, 3, 96-105.
- /120/ Rangaraj S. Durability assessment and modelling of wood–thermoplastic composites. Master thesis of science in mechanical engineering 1999, Washington state university.
- /121/ Springer G S. Environmental effects. Environmental effects on composite materials 1988, 3, 1-34.
- /122/ Crank J. The Mathematics of Diffusion 1956 (1st Ed.). Oxford University Press.
- /123/ Rao R M, Balasubramanian N and Chanda M. Factors Affecting Moisture Absorption in Polymer Composites. Part-2: Influence of External Factors. Environmental effects on Composite Materials 1988, 3, 89-95.
- /124/ Peters S T. Handbook of composites. Process Research, Mountain View, California, 1998.
- /125/ Espert A, Vilaplana F, Karlsson S. Comparison of water absorption in natural cellulosic fibres from wood and one- year crops in polypropylene composites and its influence on their mechanical properties. Composites part A 2004, 35, 1267-1276.
- /126/ Yuan X, Jayaraman K and Bhattacharyya D. Plasma treatment of sisal fibres and its effects on tensile strength and interfacial bonding. In Proceedings the Third International Symposium on Polymer Surface Modification: Relevance to Adhesion, Journal of Adhesion Science and Technology 2002. Special Publication 00(0):1-25. Newark, NJ: MST Conferences, LLC.
- /127/ Joseph P V, Matew G, Joseph K, Groeninckx G, Thomas S. Dynamic mechanical properties of short sisal fibre reinforced polypropylene composites. Composite Part A 2003, 34, 275-290.
- /128/ Rana A K, Mitra B C, Banerjee A N. Short jute fibre reinforced polypropylene composites: Dynamic mechanical study. Journal of Apply polymer science 1999, 71, 531-539.
- /129/ Gassan J, Bledzki AK. Composites processing and microstructure. Proceedings of ICCM-II 1997, 4, Gold Coast, Australia, 762-70.



- /130/ Aziz S H, Ansell M P. The effect of alkalization and fibre alignment on the mechanical and thermal properties of kenaf and hemp bast fibre composites: part 2-cashew nut shell liquid matrix. *Composites Science Technology* 2004, 64, 1231-1238.
- /131/ Rials T G and Wolcott M P. *Physical and Mechanical Properties of Agro-Based Fibres in Paper and Composites from Agro-Based Resources*. CRC Press, Boca Raton, 1996.
- /132/ Doan T T L, Gao S-L, Mäder E. Jute/polypropylene composites I. Effect of matrix modification. *Composites Science and Technology*. Article in press. Accepted 20 august 2005. Available online 4 october 2005.
- /133/ Mwaikambo L Y, Ansell M P. Chemical Modification of Hemp, Sisal, Jute and Kapok Fibres by Alkalization, *Journal of applied Polymer Science* 2002, vol 84, 2222-2234.
- /134/ Drzal L T, Mohanty A K, Burgueno R, and Misra M. *Biobased Structural composite Materials for Housing and Infrastructure Applications: Opportunities and Challenges*. The NSF- PATH Housing Research Agenda Workshop. February 12-14, 2004.
- /135/ Li X, Panigrahi S A, Tabil LG WJ. Flax Fiber-reinforced Composites and the Effect of Chemical Treatments on their Properties. North Central ASAE/CSAE Conference in Winnipeg, Manitoba, Canada. September 24-25, 2004.
- /136/ Gassan J and Bledzki A K. Effect of cyclic moisture absorption Desorption on the mechanical properties of silanized jute-epoxy composites. *Polymer composites* 1999, 20, 4.
- /137/ Pisanova E and Mäder E. Acid-base interactions and covalent bonding at a fibre-matrix interface: contribution to the work of adhesion and measured adhesion strength. *Journal Adhesion Science Technology* 2000, 14, 3, 415-436
- /138/ Zhandarov S F, Mäder E and Yurkevich O R. Indirect estimation of fibre/polymer bond strength and interfacial friction from maximum load values recorded in the microbond and pull-out test. Part 1: local bond strength. *Journal Adhesion Science Technology* 2002, 16, 9, 1171-1200.
- /139/ Wuttke B. *Flachsfaserverstärktes Polypropylene-Mikromechanik und Warseraufnahmeverhalten*. Berlin 1996, D83, 30-32
- /140/ Krenchel H. *Fibre Reinforcement*. Akadmisk Forlag, Copenhagen, 1964.
- /141/ Fukuda H, Kawada K. On Young's modulus of short fibre composites. *Fibre Science Technology* 1974, 7, 207-222.
- /142/ Madorsky S L. *Thermal Degradation of Organic Polymers*. Interscience Publication, New York 1964, Chap.4.

- /143/ Zanetti M, Camino G, Reichert P, Mülhaupt R. Thermal behaviour of poly(propylene) Layered Silicate Nanocomposites. *Macro-mol. Rapid Commun*: 2001; 22: 176.
- /144/ Liang J Z, Li R K Y, Tjong S C. Dynamic mechanical analysis of low- density polyethylene with glass beads. *Journal of Thermoplastic Composite* 2000,13, 12-20.
- /145/ Wunderlich B. The nature of glass transition and its determination by thermal analysis. In *Assignment of the glass transition*. Seyler R. J editor, ASTM STP 1994, 1249, 17-31, Philadelphia.
- /146/ Chartoff R P. The application of Dynamic mechanical methods to Tg determination by thermal analysis, in *assignment of the glass transition*. Seyler R J editor. ASTM STP 1994, 1249, 88-107. Philadelphia.
- /147/ Eherenstein G W, Riedel G, Trawiel P. *Praxis der thermischen Analyse von Kunststoffen* 1998, Wien, Hanser, p.164.
- /148/ Espert A, Vilaplana F, Karlsson S. Comparison of water absorption in natural cellulosic fibres from wood and one-year crops in polypropylene composites and its influence on their mechanical properties. *Composite Part A* 2004, 35, 1267-1276.
- /149/ Aranberri- Askargorta I, Lampke T and Bismarck A. Wetting behaviour of flax fibres as reinforcement for polypropylene. *Journal of Colloid and interface science* 2003, 263, 580-589.
- /150/ Ghosh P, Bose N R, Mitra B C, Das S. Dynamic mechanical analysis of FRP composites based on different fiber reinforcements and epoxy resin as the matrix material. *Journal of applied Polymer Science* 1997, 64, 2467-2472.
- /151/ Rong M Z, Zhang M Q, Liu Y, Yan H M, Yang G C, and Zeng H M. Interfacial interaction in sisal/epoxy composites and its influence on impact performance. *Polymer composites*, April 2002, 23, 2.
- /152/ Thomason J L, *Investigation of Composite Interphase Using Dynamic Mechanical Analysis: Artifacts and Reality*. *Polymer Composite* 1990, 11, 105.
- /153/ Dong S and Gauvin R. Application of dynamic mechanical analysis in carbon fiber/epoxy composite materials. *Polymer Composite* 1993, 14, 414.
- /154/ Thomason J L. The interface region in glass fibre-reinforced epoxy resin composites: 3. Characterization of fibre surface coatings and the interphase. *Composites* 1995, 26, 487.